PORE PRESSURE CHARACTERISTICS OF AN EXTRASENSITIVE CLAY

by

THOMAS EDWARD GLYNN

B. E., UNIVERSITY COLLEGE OF GALWAY, IRELAND, 1948

A THESIS SUBMITTED IN PARTIAL FULFILMENT OF

THE REQUIREMENTS FOR THE DEGREE OF

M. A. Sc.

IN THE DEPARTMENT

of

CIVIL ENGINEERING

WE ACCEPT THIS THESIS AS CONFORMING TO THE REQUIRED STANDARDS.

THE UNIVERSITY OF BRITISH COLUMBIA

APRIL 1960

In presenting this thesis in partial fulfilment of the requirements for an advanced degree at the University of British Columbia, I agree that the Library shall make it freely available for reference and study. I further agree that permission for extensive copying of this thesis for scholarly purposes may be granted by the Head of my Department or by his representatives. It is understood that copying or publication of this thesis for financial gain shall not be allowed without my written permission.

Department of Civil Engineering

The University of British Columbia,
Vancouver 8, Canada.

Date April 13th 1960

ABSTRACT

The results of a laboratory investigation into the pore pressure characteristics of an extrasensitive marine clay are presented. The soil samples were obtained from the Port Mann area of British Columbia. Experimental work consisted of the performance of long-duration triaxial shear tests with pore-pressure measurements. A stress-controlled triaxial machine equipped with a null-indicating type pore-pressure device was employed for all shear tests.

The observed data show that for this soil a slow build-up of pore pressure occurs for both increases in cell pressure and axial stresses in the triaxial test. Even in saturated specimens the slow build-up effect prevailed. The rates of build-up observed for changes in axial stress were slower than those recorded for changes in cell pressure. Measurements at the upper end of some specimens, and at the centre of others, indicated that the pore pressure required more time to reach equilibrium, at the ends of cylindrical specimens. The hypothesis is put forward that the observations can be explained by plastic deformations of the adsorbed layers surrounding the particles.

Strength and pore pressure parameters have been obtained for the soil.

An automatic control has been developed to assist in the performance of long-duration tests. The apparatus employs the photo-electric effect to control movements of pore water. A detailed description of this device is presented.

CONTENTS

GRAPHS

ILLUSTRATIONS

LIST OF TABLES

ACKNOWLEDGMENT

The writer wishes to express his appreciation and indebtedness to his supervisor, Mr. R. A. Spence, for assistance in all stages of this undertaking. He also wishes to thank Professor J. F. Muir, of the Department of Civil Engineering, for making arrangements to procure equipment required for the experimental work of this thesis.

NOTATIONS

A	pore pressure parameter:axial.
Å	Angstrom unit
a	area
a_r	contact area of particles
B	pore pressure parameter:all round
γ	surface tension
γ_w	density of water
C_w	compressibility of water
C_c	compressibility of soil skeleton
C_v	coefficient of consolidation
c	cohesion
c'	apparent cohesion:effective stresses
c_u	cohesion undrained:total stresses
c_r	true cohesion
Δ	incremental change:prefix
E	Young's modulus
ϵ	unit strain
f	at/to failure: suffix
η	porosity
θ	angle of failure plane to plane of major principal stress
k	coefficient of permeability
L	Length
μ	Poisson's ratio
σ	stress

NOTATIONS (Cont'd.)

σ_1	major principal stress:total
σ_3	minor principal stress:total
$\bar{\sigma}_1$	major principal stress:effective
$\bar{\sigma}_3$	minor principal stress:effective
τ	shearing stress
t	time
u	pore pressure
V	volume

CHAPTER I.

PHYSICAL PROPERTIES OF SOILS

A. Introduction

In the course of a laboratory investigation carried out by R. A. Spence, Consulting Engineers, on the mechanical properties of Port Mann marine clay, anomalies were observed in the pore pressure vs. applied stress relationships, obtained from triaxial tests. The results of these tests indicated that the behavior of the soil departed from accepted theory concerning pore pressures of clays from submerged strata, with consequent effect on shear strength. In particular, it was noted that a time lag existed in attainment of equilibrium between pore pressure and the applied total stresses in undrained triaxial shear tests. The research reported in this thesis was undertaken to investigate further the pore pressure vs. applied stress relationship, by concentrating on long duration tests. Special apparatus and testing procedures were developed for the long duration triaxial tests reported in this thesis.

By way of abstracts from the literature, background information is presented in this, and the following Chapter. Although part of the discussion in Chapters I and II applies to soils in general, particular emphasis is placed on topics pertinent to marine clay. Chapter III and subsequent Chapters deal with the present investigation.

B. Soils - General

1. Geological Aspects.

Inorganic soils may be broadly separated into two major groups, residual and transported. Residual soils are found in close proximity to the parent rock. Physical and chemical weathering are the main factors governing their formation and characteristics. Detrital accumulations remote from the source of origin constitute the transported soils, irrespective of the transporting agency. Thus glacial, alluvial, colluvial, lacustrine, eolian and marine deposits are examples of transported soils.

Usually, the history of a transported soil has a marked effect on its characteristics. Parent material, erosion and transportation agencies, depositional conditions, time and geographic factors may all contribute to the observed properties. Organic soils are not included in the above simplified classification. The organic component in most soils develops in-situ as a result of the growth and decay of plants and organisms. In contrast to residual and transported deposits, organic accumulations are commonly confined to comparatively thin strata.

Organic matter, however, may be a constituent of either residual or transported soils.

The foundation engineer is usually most interested in the strength and/or load-carrying ability of the soil. Except in rare instances, residual soils have high strength and stability, especially in temperate climatic zones. On the other hand, transported soils show considerable variations from place to place, even within the same stratum. Loose or soft deposits commonly occur for considerable depths. Organic soils must be carefully considered for foundations, because of the high compressibility associated with organic deposits. Research on the engineering properties has been focussed mainly on soils of the transported type.

Deposits which have been subjected to stresses greater than the present overburden pressure are termed preconsolidated or precompressed. Unlike normally consolidated deposits which have not been subjected to excess pressures in the past, the properties of precompressed soils are greatly influenced by the extent of the preloading. The effect is most pronounced on the strength and settlement characteristics, Terzaghi and Peck (1948). The temporary excess pressure may have been caused by the weight of soil strata which was later removed by erosional agencies. Glacial recession has a similar action and is often responsible for precompression. Geological evidence is of much assistance in ascertaining whether a soil is normal or preconsolidated.

2. Size and Shape of Soil Particles.

Grain size and shape largely determine the behavior of soils as an engineering material. Coarse grained soils, such as gravels, sands and silts, are usually cohesionless; there is little or no tendency for the grains to adhere to one another. Primarily, their strength depends on frictional properties. Packing density, particle size and shape largely determine their frictional resistance to applied loads. As the grain size diminishes, the action of inter-particle forces becomes more pronounced; these forces are manifested in the property known as cohesion. Tentatively, cohesion will be considered as that property which enables a soil mass to retain its shape in the absence of external confining stresses. If cementation of individual particles is excluded, cohesive soils are predominantly fine grained. By virtue of cohesion, such soils are often capable of carrying considerable external loads, in the absence of lateral support.

It has been observed that cohesive soils are composed mainly of flake-like particles, whereas granular soils tend to have mostly cubical or bulky fragments. The flaky particles result from the weathering of the least stable minerals of the parent rock. Evidently, cohesion is related to the mineralogical composition of the particle. Thus, quartz for example, independent of the fineness of the grains, behaves as a cohesionless material whether dry or fully saturated.

Other things being equal, the Atterberg limits increase

with decrease in grain size. Skempton reports that a linear proportionality practically exists between the plasticity index and the clay fraction of colloidal size[1]. The ratio plasticity index/clay fraction is termed the "activity" of the soil, Skempton (1954).

3. Mineralogical Composition of Fine-Grained Soils.

The principal clay-forming minerals are montmorillonite, illite and kaolinite. Chemically, they are all crystalline arrangements of silicon, aluminum, potassium, oxygen and water molecules, Terzaghi and Peck (1948). Clay minerals have a laminated structure. Recent work reported by R. E. Grim indicates that the laminae are composed of two fundamental building blocks; a tetrahedral unit and an octohedral lattice, Fig. 1 (a), (b). Similar elemental blocks combine to form a sheet-like structure as shown in Fig. 1 (c), (d). The particular atoms present and the arrangement of the sheets determine the mineral type. The sheets adhere to one another, thus forming the individual particles. The flakiness characteristics of clay particles can be traced to the mineral structure.

Montmorillonite is composed of two silica tetrahedral sheets separated by one octohedral unit. The thickness of the layer is about 9.5 Å, while the dimensions in the other two directions are indefinite, Grim (1959). The 9.5 Å layers are stacked one above the other to form the montmorillonite particle.

---

(1) Equivalent diameter less than 0.002 millimeters.

To follow page 5

Crystalline Components of Clay Minerals.

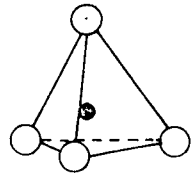

(a)

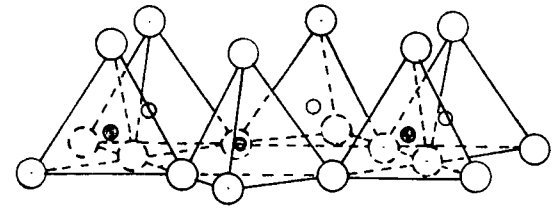

(c)

○ and ◌ Oxygens. ○ and ● Silicons.

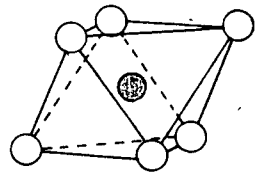

(b)

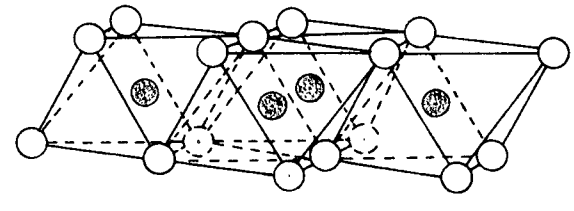

(d)

○ and ◌ Hydroxyls ◉ Aluminums, magnesiums etc.

FIG 1. CLAY MINERALS.

(After R.E. Grim. 1959)

There is little bonding force between layers of montmorillonite. The high swelling capacity of soils formed of this mineral, is believed to be evidence of the weak bonding. Apparently water can penetrate between the layers, enter the crystal lattice and promote swelling, Terzaghi and Peck (1948). Illite has a similar structure to montmorillonite, but there is a substantial replacement of the silicon by aluminum in the tetrahedral layers. Potassium is present between layers where it serves as a bonding link. Clays with a predominance of illite are not nearly so subject to swelling as those formed of montmorillonite. Kaolinite is the least active of the three minerals. Its structure consists of an alumina octohedral sheet interlocked with a parallel silica tetrahedral sheet to form a layer about 7 Å thick[2]. The layers are stacked like the leaves of a book to form the kaolinite crystal, Grim (1959). Consequently, all clay particles tend to have cleavage planes in the direction of the larger dimensions.

Forces of the type that bind the mineral layers, also act at the boundaries of the particles. T. W. Lambe (1958) attributes the boundary forces in soils to "the nonsymmetrical distribution of electrons in the silicate crystals (arising from heterpolar bonds), the crystals act as a large number of dipoles." This gives the particle magnet-like properties which are reflected in surface activity.

4. Surface Activity and Absorbed Layers.

The chemical and physical manifestations of the surface charge constitute the surface activity of the mineral. Surface

---

(2) Angstrom Unit 1 Å = 10^{-8}cms.

activity is dependent on both the mineralogical composition and fineness of the particles. Bulky particles such as quartz, exhibit little surface activity. Montmorillonite, on the other hand, is most active among the clay minerals. It can be shown experimentally[3] that clay particles carry a surface charge. The electrical charge results from the unsatisfied bonds of the mineral matrix, Baver (1956), Lambe (1958). Generally, clay particles are negatively charged. To neutralize this charge, substances possessing positive potentials are attracted to the particle. This results in an envelope of net positive charge enclosing the negatively charged particle. In colloidal chemistry this electrical arrangement is known as the Helmholtz double layer. Fig. 2 (a).

In natural soils the positive charges are supplied by ions of electrolytes in aqueous solution, and by the water molecules themselves. Water is attracted because of its permanent polar properties, and also the fact that it is a weak electrolyte, Baver (1956), Terzaghi and Peck (1948). The attraction between the particles and the surrounding medium results in an ion-water complex bonded to the soil particles. Fig. 2 (b). That part of the complex closer to the surface of the particle than 10 Å is termed the <u>adsorbed layer</u>. Further afield, but still under the influence of the surface charge, is the <u>double layer</u> water. Outside the double layer is the <u>free fluid</u>, which is

---

(3) Experiments on the electrophoresis effect show that clays are attracted to the anode if a potential gradient is applied to a disperse suspension.

To follow page 7.

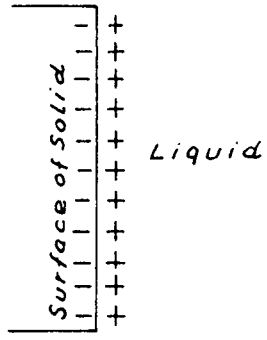

(a) Helmholtz Double Layer

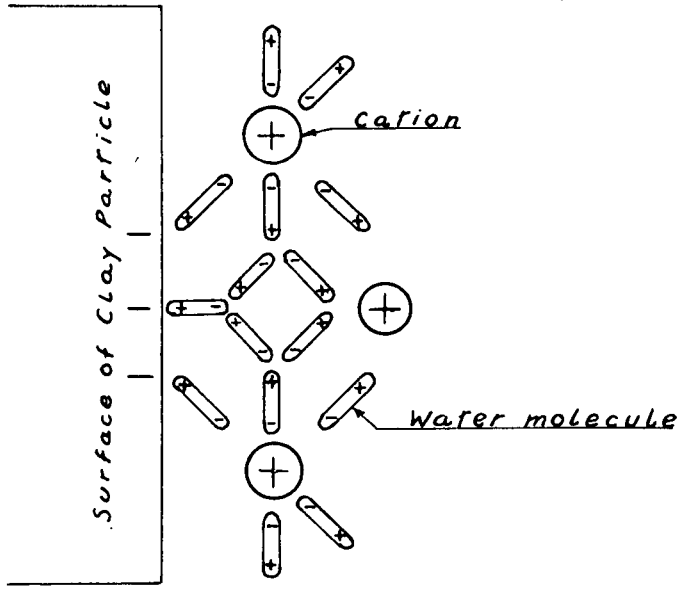

(b) Ion-water complex.

FIG 2. HELMHOLTZ AND DIFFUSE LAYERS

not affected by the presence of the soil particle. There being no definite physical boundary between the three, the water in a soil mass is more or less arbitrarily divided into adsorbed water and free water. The strength of the bond between the adsorbed layer and the particle is believed to be so great that it produces a solid or a highly viscous substance in the vicinity of the interface.

As the distance from the particle surface increases, the held water reverts to normal water. According to Lambe (1958) practically all the pure water in a clay under normal field conditions is within the double layer. An idea of the dimensions involved may be obtained from Fig. 3.

The adsorbed layers (including the double layer) have a marked influence on the behavior of fine-grained soils. Properties such as cohesion, plasticity, sensitivity(4) and trixotropy(5) are believed to depend on the nature of the adsorption complex. For instance, the cohesion of a clay may be removed by replacing the water by a non-polar liquid such as carbon tetrachloride. The thickness of the adsorbed layers has thus a considerable effect on the properties.

The dimensions of the layer are influenced by the nature of the adsorbed ions. According to Baver (1956), both the valence

---

(4) Sensitivity $= \frac{\text{Unconfined compressive strength undisturbed}}{\text{Unconfined compressive strength remoulded}}$

(5) Trixotropy - Reversible sol-gel transformation.

To follow page 8

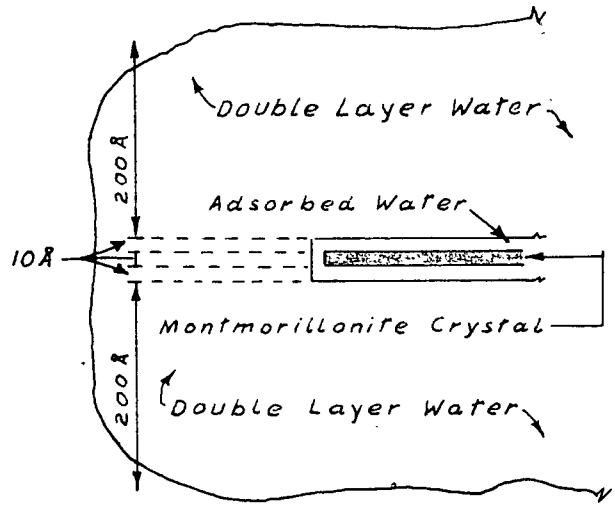

Montmorillonite Sheet

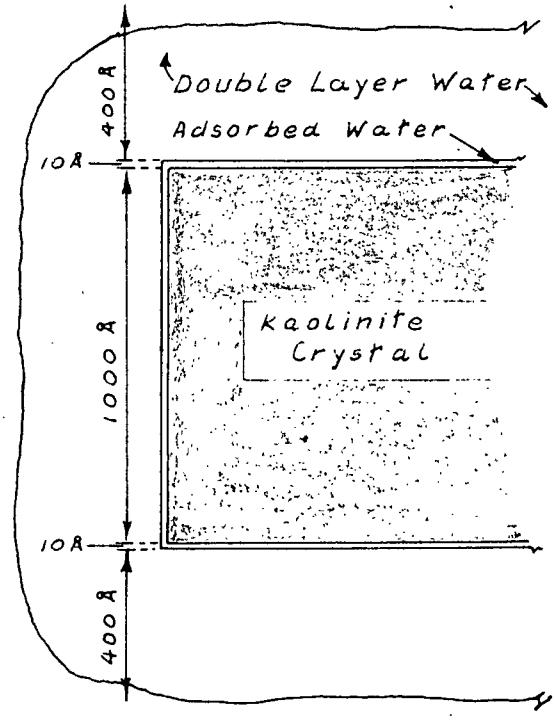

Kaolinite Sheet

FIG 3. CLAY-WATER SYSTEM.

(After T.W. Lambe. 1958)

and size of the ion is important. The electric-field intensity of an ion is known to increase directly with the charge and inversely with the radius squared. In other words, some ions attract more water molecules towards the adsorbed layer than others, thereby increasing its thickness. Sodium, calcium, hydrogen and potassium are the principal adsorbed ions in natural clays. Sodium tends to produce thick layers, while on the other hand, hydrogen ions are adsorbed in comparatively thin layers, Tschebotarioff (1951). If a particular ion predominates, the clay is sometimes given the name of this element, for example, Na-clay or Ca-clay. Ions of one element may be removed and replaced by those of another; the process is known as base exchange. Generally, exchange of ions leads to change in properties. To quote one example, Winterkorn (1941) found the liquid limit of a sample of Putnam clay to vary with the adsorbed cation as follows:

	Natural	Na	Ca	Al	H	Mg	K
Liquid limit	64.5	88	61.9	60.2	56.4	56.3	52.8

TABLE I.

LIQUID LIMIT OF PUTNAM CLAY.

The percolation of pure water through a soil reduces the salt content. Adsorbed ions can be largely exchanged by this means; complete exchange producing an H-clay. Certain marine clays have been subjected to leaching by fresh water. Attempts

are being made to account for the unusual properties of such clays in terms of the degree of leaching, Bjerrum (1954) and Rosenquist (1959).

5. Flocculation.

Flocculation is another topic connected with the adsorbed layers. Marine clay largely owes its structure to this phenomenon. When a neutral electrolyte is introduced into a dispersed suspension of soil particles in water, the negative charges which hitherto tended to separate the particles, are neutralized. The mass attraction, or Van der Waal's forces are then capable of collecting the particles into a floc large enough to settle under the action of gravity. The flocculent action is not very selective regarding size; silts as well as clay being taken up by the flocs. Hence, the origin of the uniform texture observed in some marine deposits.

6. Structure of Marine Clay.

In Soil Mechanics literature the term "structure" is used to denote the arrangement of the particles in a soil mass. Thus the soil skeleton may be referred to as having a single-grained, honeycomb, or a flocculent structure, depending on the prevailing grain assemblage, Taylor (1948). With fine-grained soils in mind, T. W. Lambe (1958) has extended the definition to read: "Structure means the arrangement of the soil particles and the electrical forces acting between adjacent particles." The importance of the electrical forces in promoting and maintaining structure is thus emphasized.

As noted earlier, marine clays are sedimentary deposits resulting from the settlement of flocs on to the sea floor. Their formation in a saline environment gave ready access to the dissociated ions contained in sea water. Consequently, the finer particles were enveloped in relatively thick adsorbed layers. Burial under further depths of sediment "tightened up" the flocculent structure. With sufficient overburden pressure and time, the particles may be virtually brought into contact with one another, over at least part of their surfaces, Skempton and Northerley (1952). The strength characteristics of such a deposit are determined by the degree of consolidation in the normal manner, Taylor (1948). The sensitivity is not abnormal; it may be anywhere in the range one to eight.

A different situation arises however, if for any reason the original salt content of a marine deposit is lowered. Leaching reduces the thicknesses of the adsorbed layers, while the water content remains almost unchanged; the volume of the free pore fluid increases at the expense of the adsorption complex, Skempton and Northey (1952). This has a two-fold effect on the engineering properties: it lowers the undisturbed strength, but more important, it greatly increases the sensitivity. At the same time, it has been observed that the Atterberg limits are reduced, Bjerrum (1954).

Leaching of natural deposits is accomplished by percolation of fresh water through the pores. In most cases, leaching is the result of the uplift of marine deposits to above sea level. In Europe and North America, geological evidence indicates that

uplift took place following the retreat of Pleistocene glaciation. The classical example of this type of development is along the coast of Norway. Investigation of the Norwegian clays by Bjerrum, indicates that the loss of shear strength mentioned above, does not take place in linear proportion to the reduction in salt concentration. Bjerrum reports that even a decrease in salt concentration from the original 35 grams down to 10 - 15 grams per litre, results only in a negligible reduction in shear strength. Further leaching, however, resulting in salt concentrations below 10 grams, produces a considerable decrease in strength. The reduction in undisturbed strength has taken place over a long period of time; therefore, except in cases where further leaching is possible, this reduction in shear strength is mainly of academic interest.

Of greater significance, is the increase in sensitivity following leaching. "Quick" clays, as they are called, are among the most difficult soils encountered by engineering projects. The explanation for the sensitivity can be found, in part at least, from the structure. Rosenquist has investigated the structure of Norwegian "quick" clays. With the aid of electron microscopy, he has shown that the structure corresponds remarkably close to a configuration proposed earlier by W. T. Tan. The essence of the structure is that the edges of some particles are virtually in contact with the flat surfaces of others to give a sort of card-house framework. Fig. 4.

The meta-stable structure, illustrated in Fig. 4, breaks down if subjected to repeated stresses or shock. Undisturbed samples of some marine deposits are so sensitive that they can

To follow page 12

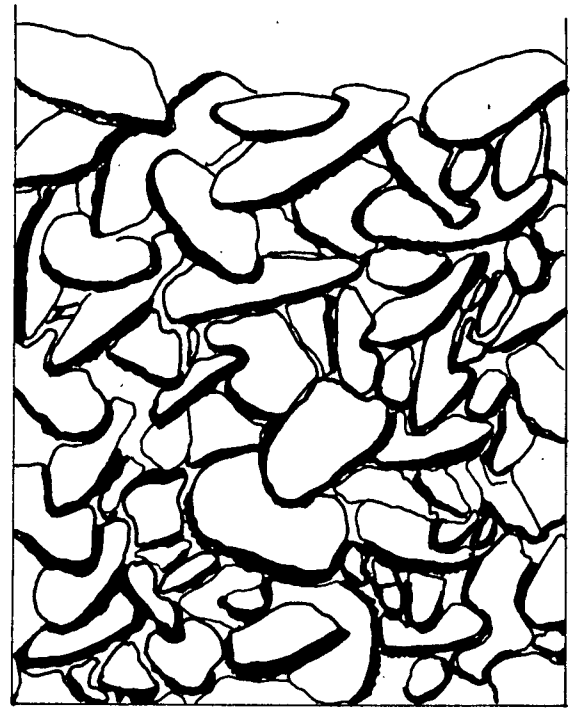

FIG 4. STRUCTURE OF MARINE CLAY.

(After T.K. Tan. 1957.)

be transformed by remoulding alone, from a firm clay, to one with the consistency of a viscous fluid.

The current investigation is concerned with the properties of a "quick" clay. As the investigation is mainly concerned with shear strength characteristics, a brief discussion on strength theory follows.

CHAPTER II.

STRENGTH THEORY

A. Introduction

Foundation and earthwork engineering often require a knowledge of the behavior of soils located below the water table. When external loads are applied to a submerged stratum, internal stresses result. Part of the internal stresses is taken by the solid constituents, or soil structure, while the interstitial medium (for the most part water) absorbs the remainder. The stresses taken by the soil skeleton are known as effective stresses. Pore pressure, or neutral stress, is applied to the portion taken by the "free fluids"[1] occupying the pores. Thus pore pressures are peculiar to the interstitial water only, while effective stress pertains to the particle and its adsorbed layer.

---

(1) "Free fluids" refers to the water, gases, etc., which are not intimately held to the surface of the particles. It is considered here to include the double layer water.

B. Effects of Pore Pressure

1. Relationship Between Pore Pressure and Shear Strength.

The question arises as to how the pore pressure effects the strength properties. For the purpose of this discussion, no distinction will be made between the various types of structure and textures which may be found in natural soils. Generally, positive pore pressures reduce the contact stresses, whereas negative pressure leads to an increase in the contact or effective stress between particles. The interstitial water is capable of taking either compression or tensile stresses, but all shearing stresses must be taken by the soil skeleton, Bishop and Henkel (1957). If an external load is to produce failure, it must overcome the shearing resistance of the soil mass. Moreover, the load must be capable of maintaining the deformation. Hence, there is a distinction between the appreciable amount of deformation that may occur without causing failure, and the prolonged deformation known as creep which may ultimately lead to failure over a period of time. Elementary mechanics shows that the relationship between the force necessary to produce relative motion of two surfaces in contact, is a function of the normal load and the friction angle. The relationship is expressed by the formula $F = N \tan \alpha$ where F denotes the force required to produce sliding. N corresponds to the normal force and α denotes the friction angle peculiar to the materials in contact. In Soil Mechanics these concepts are

embodied in the well-known Coulomb-Terzaghi equation:

$$s = c' + (p - u) \tan \phi' \qquad \text{Eqn. } (2 - 1)$$

where s denotes the maximum resistance to sheer on any place

c' denotes the apparent cohesion) In terms of effective stress

ϕ' denotes the angle of shearing resistance)

p denotes the total pressure normal to the plane considered,

and u denotes the pore pressure.

The above equation is used in most problems involving the shear strength of soils. However, an analysis of the terms appearing in the formula, is of interest in order to gain an understanding of its validity.

The stresses[2] (equation 2-1) are defined in respect to a plane (in the geometrical sense) passing through the pore space and the points of contact of the soil particles. Stresses, and areas, are then considered as projected on to this plane. The effective stress on the plane is assumed to be represented by the term $(p - u)$. A more exact expression for the effective stress would be $p - u(1 - a_r)$, where a_r denotes the contact area of the particles per unit area of the plane. A precise evaluation of the effective stress therefore, requires a knowledge of contact areas. In practice, direct measurement of the contact areas of all particles on a slip plane, is an extremely difficult problem. Indirect methods however, indicate that $(1 - a_r)$ is in fact

(2) Compression stresses considered positive, and tensile negative.

close to unity for both sands and clays, Bishop and Eldin (1950). The validity of the assumption that the friction component of shear strength is $(p - u) \tan \phi'$ is based on this this observation.

The friction angle (ϕ') is known to depend primarily on the size, shape, packing density, interlocking and mineralogical composition of the particles. Bishop and Henkel (1957) report that ϕ' also depends somewhat on the rate of strain; high rates tend to increase ϕ'. In clays, the decrease in the value of $\tan \phi'$ is about 5% for each tenfold increase in the duration of a shear test.

The cohesion appears in equation 2-1 as the component of the shear strength independent of the normal stress. For any one cohesive soil the apparent cohesion depends on the water content, stress history and rate of deformation under load. Generally, the cohesion increases as the moisture content is lowered. Preconsolidation leads to an increase in cohesion because the soil is in equilibrium with a lower stress than the original consolidation pressures. High rates of deformation tend to increase the observed cohesion, Taylor (1943). This is due to the mobilization of the viscous component of the interstitial water. Consequently, the prefix 'apparent' is used, in connection with friction angles and cohesion, in order to signify the dependence of these parameters on factors which are not necessarily basic soil properties. Later, the more fundamental properties of true friction angle and true cohesion will be considered.

2. Relationship Between Compressive Strength and Pore Pressure.

The shearing resistance on any plane may be obtained from the Coulomb-Terzaghi equation provided the pore pressure, strength parameters and normal stress on the plane are known. However, the total stresses on the principal planes are more readily accessed in practice, therefore equation 2-1 will be derived in terms of the total principal stresses. One purpose of this is to emphasize the role played by pore water pressure in the engineering performance of the soil. The relationship can be conveniently derived from the Mohr diagram, Fig. 5.

In Fig. 5 the total principal stresses at failure are represented by σ_1 and σ_3 (3) The compressive strength is then $(\sigma_1 - \sigma_3)$; FGH represents the corresponding Mohr circle. For this system of total stresses, let the effective stresses be represented by $\bar{\sigma}_1$ and $\bar{\sigma}_3$. The Mohr circle F'G'H' associated with the latter will be located to the left by a distance corresponding to the pore pressure (u). Assuming the failure envelope for effective stress is represented by the line AB, then the circle F'G'H' will touch AB at failure. The shear stress at failure (τ_f) is represented by OL.

It is required to express the compressive stress $(\sigma_1 - \sigma_3)$ in terms of the strength parameters (c', ϕ') and the pore pressure u.

---

(3) In triaxial test σ_1 is total axial stress and σ_3 represents the cell pressure or the confining stress. In a natural soil deposit σ_1 represents vertical stress on an element, and $\sigma_3 = K.\sigma_1$ where K = coefficient of lateral earth pressure.

From the geometry of the diagram it follows that

$$\tau_f = \frac{(\sigma_1 - \sigma_3)}{2} \cos \phi'$$

Also $\tau_f = \left\{(\sigma_3 - u) + \frac{\sigma_1 - \sigma_3}{2} - \frac{\sigma_1 - \sigma_3}{2} \sin \phi'\right\} \tan \phi' + c'.$

$$\frac{(\sigma_1 - \sigma_3)}{2} \cos \phi' = (\sigma_3 - u) \tan \phi' +$$

$$\frac{(\sigma_1 - \sigma_3)}{2} \tan \phi' - \frac{(\sigma_1 - \sigma_3)}{2} \sin \phi' \tan \phi' + c'.$$

$$\frac{(\sigma_1 - \sigma_3)}{2} (\cos \phi' - \tan \phi' + \sin \phi' \tan \phi') = c' + (\sigma_3 - u) \tan \phi'$$

or $$\frac{(\sigma_1 - \sigma_3)}{2} = \frac{c' + (\sigma_3 - u) \tan \phi'}{\cos \phi' - \tan \phi' + \sin \phi' \tan \phi'} \times \frac{\cos \phi'}{\cos \phi'}$$

$$= \frac{c' \cos \phi' + (\sigma_3 - u) \sin \phi'}{\cos^2 \phi' - \sin \phi' (1 - \sin \phi')}$$

Since $\sin^2 \phi' + \cos^2 \phi' = 1$

$$(\sigma_1 - \sigma_3) = 2\left\{\frac{c' \cos \phi' + (\sigma_3 - u) \sin \phi'}{1 - \sin \phi'}\right\} \qquad \text{Eqn. 2-2}$$

Furthermore $$(\sigma_1 - \sigma_3) = \frac{2 c' \cos \phi'}{1 - \sin \phi'} + \frac{2\sigma_3 \sin \phi'}{1 - \sin \phi'} - \frac{2 \sin \phi'}{1 - \sin \phi'} u$$

$$= 2\left\{\frac{c' \cos \phi' + \sigma_3 \sin \phi'}{1 - \sin \phi'}\right\} - 2\left(\frac{\sin \phi'}{1 - \sin \phi'}\right)u$$

$$(\sigma_1 - \sigma_3) = Y - Zu$$

where Y and Z are constants for any one value of σ_3

Equation 2-2 et sequo shows that the compressive strength comprises a constant term minus a function of the pore water pressure. The measured compressive strength is therefore largely determined by the pore pressure.

To follow page 19

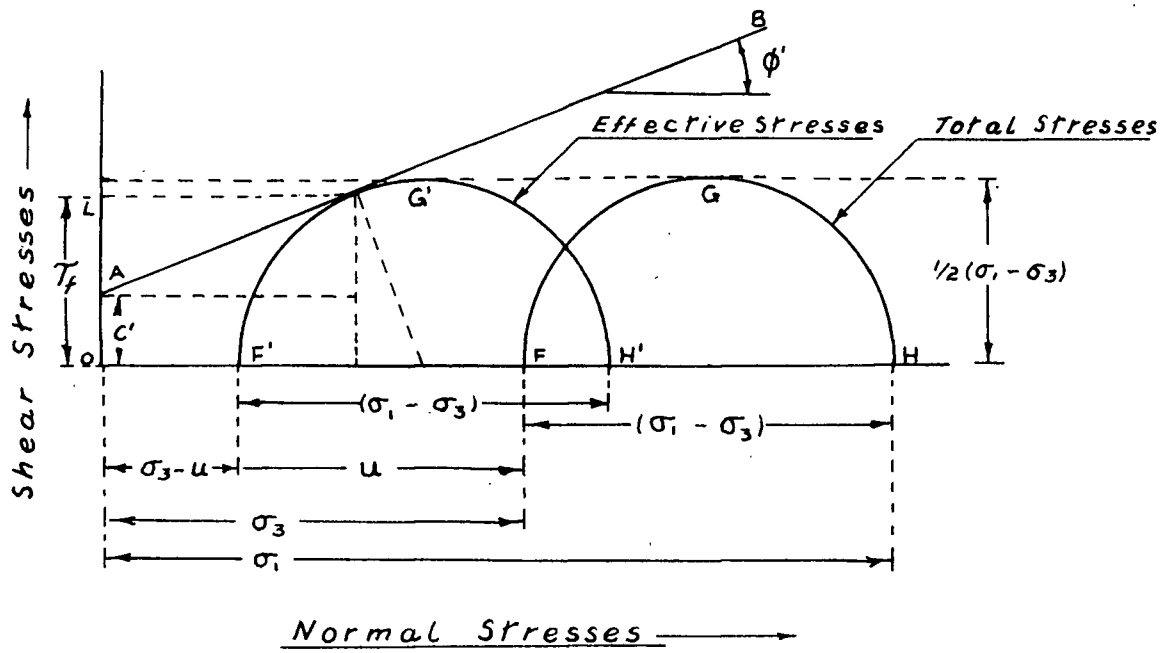

Fig 5. Mohr Diagram : Total and Effective Stresses

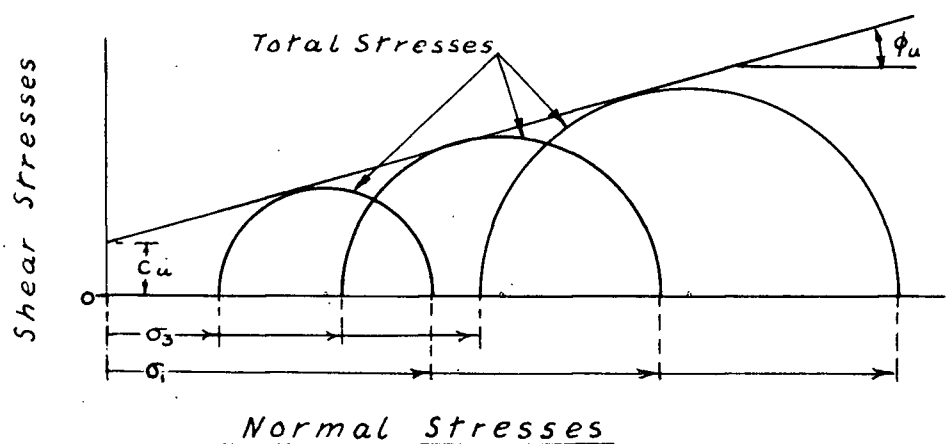

Fig 6. Mohr Diagram : Total Stresses

FIGS. 5 and 6

The 'apparent' strength parameters c' and ϕ' are obtained in the laboratory, from a series of triaxial tests with pore pressure measurements. Individual specimens are first consolidated at different cell pressures (corresponding to σ_3). Shear tests are then performed on the specimens, which in general will have different moisture contents due to the differences in consolidation pressures. The higher shear strengths will normally be obtained from the specimens with low moisture contents and high confining pressure. By plotting the effective stress circles on a Mohr diagram similar to Fig. 5, the failure envelope can be established. The slope of the envelope yields the 'apparent' friction angle (ϕ'), while the intercept of the envelope on the Y axis gives the 'apparent' cohesion (c').

3. Total Stress Parameters.

Two other 'apparent' parameters, c_u and ϕ_u are sometimes quoted. These are obtained from the envelope of the Mohr circles for total stresses at failure. An example of this type of plot is shown in Fig. 6.

As remarked earlier, the magnitude of the 'apparent' parameters depends on the stress history and the rate of deformation. Consequently, in an effort to obviate this dependence, the idea of true friction angle and true cohesion made its appearance in Soil Mechanics literature.

4. True Friction Angle and True Cohesion.

So far, the strength properties have been expressed in terms of the 'apparent' cohesion and friction angle. For most

purposes these are sufficient, but a more fundamental approach is desirable if the basic soil properties are to be elucidated. It has been suggested, Shempton and Bishop (1954) that the true friction angle and true cohesion can be obtained under certain conditions which will be discussed presently. The discussion applies to cohesive soils only.

The concept of true friction and true cohesion is based on Hvorslev's contention that the cohesion should be a function of the water content only, and that the friction angle is a function of any increase in strength with increase in effective stress at constant water content. It is possible to have two samples of a soil at identical water contents (void ratios the same if saturated) but in equilibrium with different effective stresses. This can be seen by referring to the results of a conventional consolidation test on a normally consolidated clay. Fig. 7.

It is evident from Fig. 7 that the state corresponding to point X on the loading curve is in equilibrium with consolidation pressure p_1 and that the void ratio is e_1. At point Y on the unloading curve the sample has been preconsolidated to the extent of pressure p_2 but is in equilibrium with p_3. (p_1 p_2 p_3 are effective stresses). The void ratio corresponding to pressure p_3 is e_1 also, therefore, the void ratios are identical but the effective stresses dissimilar. Assuming saturation, the cohesion will then have the same magnitude for states represented by X and Y.

If shear tests with pore pressure measurements are carried out on two samples, whose consolidation histories correspond to

To follow page 21

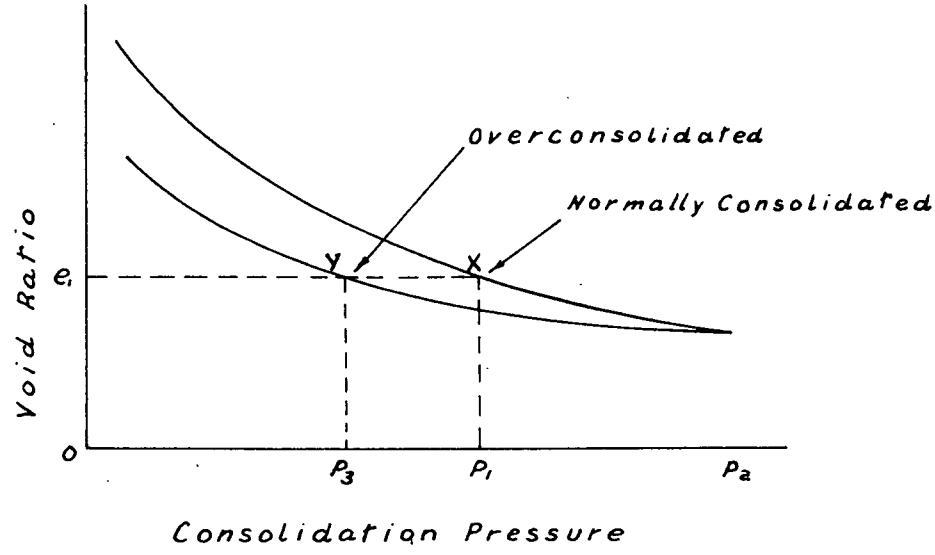

FIG 7. CONSOLIDATION HISTORIES

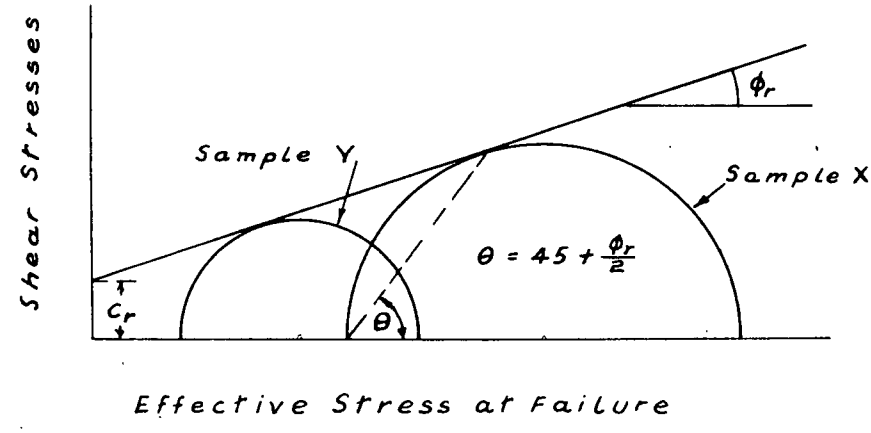

FIG 8. MOHR DIAGRAM : TRUE PARAMETERS

FIGS 7 and 8

conditions represented by points X and Y. Fig. 7, the Mohr diagram of effective stresses would resemble Fig. 8. Provided that a rate of strain is chosen which is slow enough to minimize viscous effects, the true friction angle ϕ_r and true cohesion c_r are obtained by the method indicated in Fig. 8.

The failure envelope of the two Mohr circles can be represented by the equation:

$$\tau_f = c_r + (\sigma - u) \tan \phi_r$$

where τ_f - shear stress on the plane of failure

σ - total normal stress on the same plane

u - pore pressure

c_r - true cohesion

ϕ_r - angle of true internal friction } At the water content at failure

By analogy with equation 2-1 the compressive strength is given by:

$$(\sigma_1 - \sigma_3)^{(4)} = 2 \left\{ \frac{c_r \cos \phi_r + (\sigma_3 - u) \sin}{1 - \sin \phi_r} \right\}$$

where σ_1 and σ_3 are the major and minor total principal stresses at failure respectively.

The performance of such tests presents experimental difficulties, due to the requirement that the specimens have identical moisture contents but different stress histories. An alternative procedure for obtaining ϕ_r is to measure the inclination of the shear plane at failure. The angle of inclination

---

(4) $(\sigma_1 - \sigma)$ is equivalent to $(\bar{\sigma}_1 - \bar{\sigma}_3)$ — deviator stress.

of the shear plane to the plane of major principal stress is given by $\theta = 45 + \frac{\phi_r}{2}$

Not all samples, however, fail on a single shear plane. Therefore, this approach is not feasible in all cases. End restraint produced by loading caps also affects the angle

The true parameters have a significant correlation with the plasticity index and mineralogical composition of clays. Test results reported by Skempton (1954) indicate the order of magnitude of the true and apparent friction angles. Table II.

C. Factors Affecting Pore Pressure: The Pore-Pressure Parameters, A and B.

The magnitude of the pore pressure developed in a stressed soil mass depends primarily on two factors:

(a) The compressibility of the soil skeleton.

(b) The consituents of the fluid occupying the pore space.

In order to illustrate the dependence on the above factors, the soil is assumed to behave as an elastic isotropic material. The validity of such an assumption for the case of real soils is discussed later.

Consider a small cube AB of elastic material stressed in the manner indicated in the following sketch: where σ_x, σ_y and σ_z are compressive stresses of equal magnitude.

SOIL TYPE	LIQUID LIMIT	PLASTIC INDEX	ACTIVITY PI / % CLAY	MOISTURE CONTENT RANGE	TRUE FRICTION	APPARENT FRICTION ANGLE
Shellhaven Clay undisturbed.	123	87	1.42	52-60%	18°	23°

TABLE II.

PROPERTIES OF SHELLHAVEN CLAY.

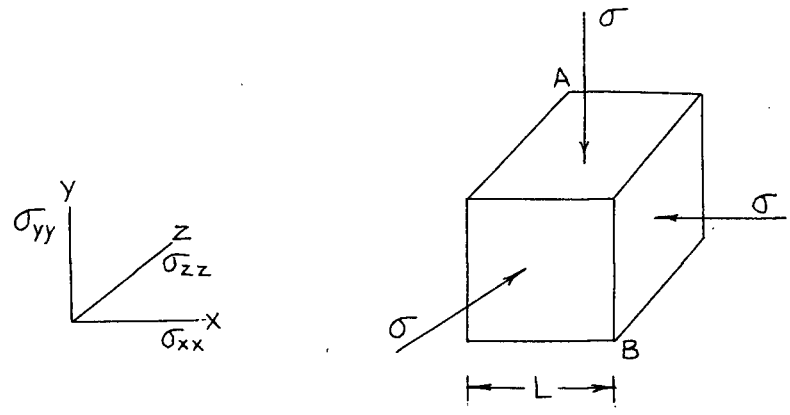

From elastic theory and the principal strains ϵ_{xx}, ϵ_{yy} and ϵ_{zz} are related by:

$$\epsilon_{zz} = \epsilon_{yy} = \epsilon_{zz} = \frac{\sigma}{E}(1 - 2\mu)$$

where μ - Poisson's ratio

E - Young's Modulus.

If L is the original length of a side of the cube and $(L - \Delta L)$ the strained length, then the strain parallel to any one axis of the co-ordinates is:

$$-\frac{\Delta L}{L} = \epsilon_{xx} = -\frac{\sigma}{E}(1 - 2\mu)$$

Hence: $$\Delta L = L\frac{\sigma}{E}(1 - 2\mu)$$

The volume of the compressed cube is then:

$$(L - \Delta L)^3 = \left\{1 - \frac{\sigma}{E}(1 - 2\mu)\right\}^3$$

$$= L^3\left\{1 - \frac{3\sigma}{E}(1 - 2\mu)\right\}$$ for small value of ΔL.

Since the original volume of the cube is $V = L^3$, the change in the volume $(-\Delta V)$ is given by:

$$-\Delta V = L^3 - (L - \Delta L)^3$$

$$-\Delta V \simeq L^3 \left\{ \frac{3\sigma}{E} (1 - 2\mu) \right\}$$

$$\text{or} \quad -\Delta V \simeq V \left\{ \frac{3\sigma}{E} (1 - 2\mu) \right\}$$

Similarly if $\sigma_{xx} \neq \sigma_{yy} \neq \sigma_{zz}$

Volume change: $$-\Delta V = V \left\{ \frac{1 - 2\mu}{E} (\sigma_{xx} + \sigma_{yy} + \sigma_{zz}) \right\} \qquad (1)$$

Turning now to a soil mass subjected to incremental changes in the total stresses on principal planes - equivalent to $\Delta\sigma_1$ $\Delta\sigma_2$ and $\Delta\sigma_3$ the relationships between the changes in total and effective stresses are given by:

$$\overline{\Delta\sigma_1} = \Delta\sigma_1 - \Delta u \quad ; \qquad (a)$$

$$\overline{\Delta\sigma_2} = \Delta\sigma_2 - \Delta u \quad ; \qquad (b)$$

$$\overline{\Delta\sigma_3} = \Delta\sigma_3 - \Delta u \quad ; \qquad (c)$$

Where $\overline{\Delta\sigma_1}$, $\overline{\Delta\sigma_2}$ and $\overline{\Delta\sigma_3}$ represent the change in effective stresses on the principal planes $-\Delta u$ denotes the pore pressure change.

Then from expression (1) the decrease in volume (ΔV) of

the soil skeleton is approximated by:

$$-\Delta V = \frac{V(1 - 2\mu)}{E}\left(\overline{\Delta\sigma_1} + \overline{\Delta\sigma_2} + \overline{\Delta\sigma_3}\right) \qquad (2)$$

where and E are Poisson's ratio and Young's modulus respectively for the soil skeleton.

The decrease in the volume of the soil skeleton is almost entirely due to a decrease in the volume of the voids.(5) If the initial porosity is denoted by η,(6) and C_w the compressibility of the pore fluid, the volume change (assuming no drainage occurs) is given by:

$$-\Delta V = V \eta C_w \Delta u \qquad (3)$$

Combining equations (2) and (3)

$$\eta C_w \Delta u = \frac{1 - 2\mu}{E}\left(\Delta\sigma_1 + \Delta\sigma_2 + \Delta\sigma_3\right) \qquad (4)$$

For the case where $\Delta\sigma_2 = \Delta\sigma_3$(7) expression (a) (b) (c) can be written:

$$\overline{\Delta\sigma_1} + \Delta u = \Delta\sigma_3 + (\Delta\sigma_1 - \Delta\sigma_3)$$

$$\overline{\Delta\sigma_2} + \Delta u = \Delta\sigma_3$$

$$\overline{\Delta\sigma_3} + \Delta u = \Delta\sigma_3$$

---

(5) Compressibility of the soil grains is negligible.

(6) Porosity $\eta = \dfrac{\text{Volume of Voids}}{\text{Total Volume}}$

(7) Triaxial test and most practical problems $\Delta\sigma_2 = \Delta\sigma_3$

By addition:

$$(\Delta\sigma_1 + \Delta\sigma_2 + \Delta\sigma_3) + 3\Delta u = 3\Delta\sigma_3 + (\Delta\sigma_1 - \Delta\sigma_3)$$

From (4) $\eta C_w \Delta u \quad \frac{1 - 2\mu}{E}\left\{3\Delta\sigma_3 + (\Delta\sigma_1 - \Delta\sigma_3) - 3\Delta u\right\}$

If the compressibility of the soil skeleton for unit stress change is denoted by C_c, then:

$$C_c = 3\left(\frac{1 - 2\mu}{E}\right)$$

Introducing C_c, rearranging the terms and dividing by 3, the change in pore pressure for an all-round change in stress is given by the expression:

$$\Delta u = \frac{1}{1 + \eta \frac{C_w}{C_c}} \left\{ \Delta\sigma_3 + \frac{1}{3}(\Delta\sigma_1 - \Delta\sigma_3)\right\} \qquad (5)$$

The term outside the bracket $\frac{1}{1 - \eta \frac{C_w}{C_c}}$ is known as the pore pressure parameter B, Bishop and Henkel (1957).

The coefficient $\frac{1}{3}$ in Exp. (5) only applies, of course, in the case of an idealized elastic soil. Real soils are not even approximately elastic, therefore, it is necessary to replace the coefficient of the deviator stress by a parameter A. Equation (5) then becomes:

$$\Delta u = B\left\{\Delta\sigma_3 + A(\Delta\sigma_1 - \Delta\sigma_3)\right\} \qquad \text{(Eqn. 2-3)}$$

The value of the parameter A at failure ranges from about -0.1 for normally consolidated soils to about 1.3 for pre-consolidated clays, Bishop and Henkel (1957).

For fully saturated soils the value of C_w - that of water alone - is so small that B = 1. When the pore water contains air and other gases, the value of B is less than unity, but depends on the stress range; B approaches unity as the total stresses increase. Where $\Delta\sigma_1 = \Delta\sigma_3$ as is the case in build-up of pore pressure at the initial stages of a triaxial shear test, B is given by the expression $B = \frac{\Delta u}{\Delta\sigma_3}$ where Δu denotes the <u>change</u> in pore pressure, and $\Delta\sigma_3$ denotes the <u>change</u> in cell pressure.

CHAPTER III.

APPARATUS: DEVELOPMENT AND OPERATION

A. Triaxial Shear Tests with Pore Pressure Measurements.

1. General.

The triaxial apparatus used in the investigation was designed to accommodate specimens of $2\frac{1}{2}$" diameter with a length up to 6". Previous research[1] indicates that best results are obtained with a length to diameter ratio of 2:1. All results reported here are for specimens $2\frac{1}{2}$" diameter and 5" long. Excessive buckling of the specimen during test is thus avoided.

Direct loading was used because the stress remains virtually constant for any load increment. This enables the development of pore pressure to be compared with the incremental change in axial stress. Also this test set-up closely corresponds to the loading of soils in practice, where the soil is normally allowed to deform at will under an almost uniform stress. Changes in cross sectional area, in the course of a test, will tend to reduce the axial stresses, but the magnitude of such changes will not

---

(1) Bishop and Henkel (1957).

be very great, if the specimen fails at small strain.

It is more convenient to measure the pore pressure at the top, or at the base of a specimen, than at intermediate points in its length. It was felt, however, that end restraint may have a bearing on the observed rate of pore pressure development. Therefore, some tests were run with pore pressure measurements at or about the centre of the specimen.

2. Stress-Controlled Triaxial Apparatus

The loading apparatus is shown in Fig. 9. The frame is made of 2" x 2" aluminum box section, bolted down to a 30" x 1" x ½" thick aluminum base. A wooden bench supports the frame. Provision is made for levelling the frame, by the incorporation of adjustable screws in the bench legs. The loading yoke is constrained to move in a vertical plane by guide tracks fixed to the frame uprights. A counter-balance system keeps the yoke and proving ring in a "floating" position, thereby reducing to a minimum the initial load on the specimen. The triaxial cell is mounted on a centering column. With the cell in position, the unit was aligned by means of a surveyor's theodolite. Axial loading or as nearly so as possible, is thus obtained. Although the loading yoke is fitted with roller bearings and the counter-balance weights are suspended from low friction pulleys, the proving ring is incorporated for the purpose of eliminating friction errors from the estimated load. The loads are applied to the yoke via the shackle and pan, located beneath the bench.

To follow page 31

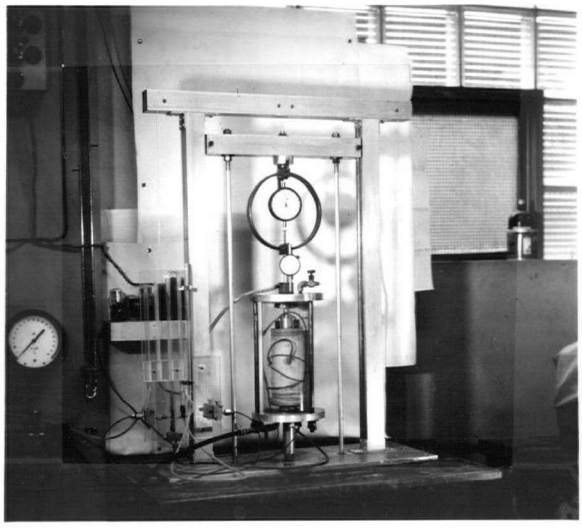

FIG 9. STRESS-CONTROLLED TRIAXIAL MACHINE

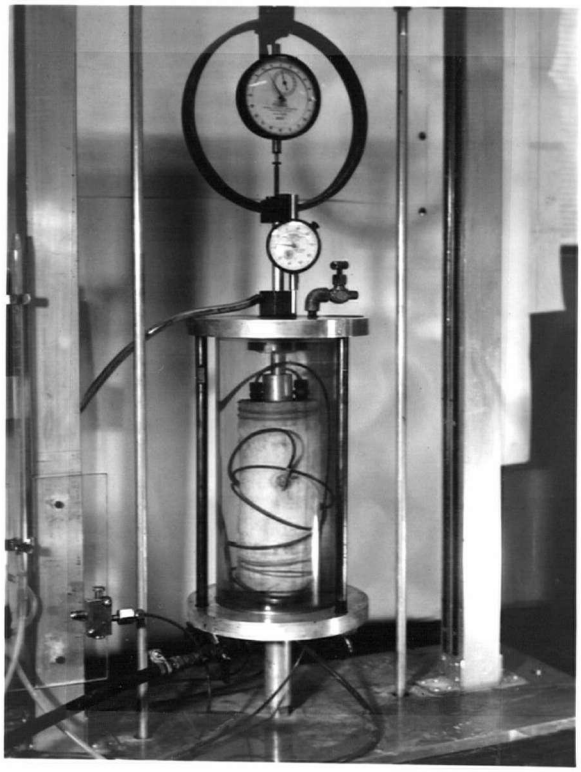

FIG 10. TRIAXIAL CELL

3. The Triaxial Cell

The pressure chamber of the triaxial cell consists of a "lucite" cylinder ($\frac{1}{4}$" wall thickness) capped top and bottom by 3/4" thick plates, Fig. 10. The cylinder is seated on grooves in the plates and is sealed by synthetic rubber washers. Clamping down bolts are fitted with wing nuts for easy assembly. The loading plunger is inserted through a brass bushing in the upper plate. In order to minimize friction, and at the same time prevent excessive leakage, the stainless steel plunger is finished to give a clearance of 0.0003 inches. External loads for the plunger are transmitted to the specimen by the loading cap. The lower end of the plunger is machined to a hemispherical shape which registers in a central coned seating in the cap. The cap is free to tilt through angles up to 10 degrees to the horizontal. Greater tendency to tilt is prevented by a guide which forms an integral part of the cap. A pedestal, which can be slipped over the centering column of the loading frame, protrudes through the lower plate of the chamber. The base for the specimen is screw-fitted to the top of the pedestal.

Both cap and base have shallow radial grooves, on the specimen side, which lead to drainage outlets. Two outlets are provided in the top cap and there is one central outlet in the base. One outlet in the cap may be connected to either the pore pressure apparatus or to a vacuum pump, depending on the requirements of the test. The other lead in the cap and the lead from the base are intended for drainage purposes. "Saran"

tubing is used for all leads. Flow in the tubing is controlled by piston valves located outside the cell. The operation of this type of valve does not introduce undesirable volume changes anywhere in the drainage system.

Drainage from the specimen is measured by means of two burettes. Air expelled from unsaturated samples is measured in an inverted U-tube fitted in the line to the base burette.

4. Lateral Pressure Control

The control of chamber pressure to the degree of precision demanded in triaxial testing, is not an easy matter. This is particularly true in the case of long duration tests. Commercial pressure regulators usually employ a spring-loaded diaphragm. This mechanism is prone to instability, and in the absence of auxiliary equipment cannot be used for precise pressure control over long periods of time.

A number of systems have been devised to meet the problem. Most, however, require elaborate instrumentation. Two systems commonly used, one developed at Imperial College, London, and the other at the Norwegian Geotechnical Institute, Oslo, have proved satisfactory under certain conditions. The method used at Imperial College employs a self-compensating mercury manometer, one limb of which can be raised, to provide the required pressure head. A drawback to this equipment is that it requires considerable head-room in the laboratory, if sufficiently high pressures are to be obtained. If head-room is limited, the apparatus must

be duplicated, which adds to the cost of the installation. The Norwegian apparatus is essentially a hydraulic system. A ram loaded by means of dead weights maintains the pressure in an oil filled cylinder. The cylinder must be carefully aligned otherwise friction errors arise. Leakage of oil past the ram and the limited weight capacity are the main disadvantages. Both the above systems are, therefore, most convenient for low cell pressures.

For investigations, like the one reported here, pressures up to 100 pounds per square inch are desirable. To obtain pressures of this magnitude, a diaphragm-type regulator was used for the main control. A method of counteracting pressure fluctuations was devised. The modification consists of allowing a continuous bleeding of air to the atmosphere from the main regulator. This bleeding is controlled by a fine adjustment auxiliary regulator. The latter is fitted downstream of the main control. Using this method, regulation better than 0.15 pounds per square inch was obtained for the medium and high cell pressures. At pressures below 15 pounds per square inch, the system is less efficient; presumably this is due to the lowered momentum of the air, rendering the auxiliary regulator ineffective.

A reservoir, fed from an air compressor, maintains the desired pressure. The capacity of the reservoir is large, compared with possible volume changes in the specimen, or leakage from the cell. Deaired water was used as the chamber fluid for all tests reported in this thesis, in order to minimize flow through

protective membranes. A Bourdon gauge (total range 0-100 lb./sq.in.) indicates the pressure. A deduction of 2.5 lb./sq.in. from the gauge reading is necessary to allow for the loss of head between the reservoir and cell. The Bourdon gauge was checked against a standard gauge tester. A random discrepancy of not greater than 0.3 lb./sq.in. was observed in this guage. The cell pressure may be relieved by opening the needle valve located in the upper plate of the chamber.

The cell pressure, acting on the plunger, decreases the load on the specimen to values lower than those registered by the proving ring. The correction to be applied to the ring deflection, in order to obtain the actual load, is shown in Fig. 15.

5. Load and Deformation Measuring Devices.

A dial gauge, reading to 0.0001" is used for indicating the proving ring deflection. For loads in the range 5-220 lbs. the ring constant K = 0.444 lbs./0.0001" deflection.

The deformation of the specimen is measured by another dial gauge (0.001"/div) set between the lower clamp on the proving ring and the upper plate of the chamber.

6. Apparatus for Measuring Pore Pressure.

In undrained triaxial tests, it is essential that moisture changes in the specimen be prevented during the loading stage. Consequently, any apparatus used for measuring pore pressures must be capable of operating on a minimum of pore water movement. The usual laboratory methods of measuring pressure - the mercury

manometer and the Bourdon gauge - cannot be applied directly to the measurement of pore pressure, owing to the volume of pore water which would have to flow from the specimen to cause the instrument to register.

For large specimens, a transducer-type apparatus may be used. This device measures the deflection of a metal diaphragm by means of electrical strain gauges. Changes in hydrostatic pressure produce deflections of the diaphragm which lends itself to pore pressure applications, Plantima (1953). This method departs somewhat from the no-flow condition. Permanent moisture changes can be entirely avoided, however, by the use of the null method of pressure measurement originally devised by Rendulic (1937). The apparatus used in the present investigation employs the latter system.

The method adopted for the measurement of pore pressure is essentially that developed at Imperial College, London. It is equally efficient for all specimen sizes. The apparatus and procedure are described in detail by Bishop and Henkel in their book "The Triaxial Test". Therefore, only a brief description will be given here.

Main features of the apparatus are a null indicator, a control cylinder, and a Bourdon gauge coupled to a manometer, Fig. 13. The null indicator employs a mercury column in a glass capillary tube. This column is maintained throughout the duration of the test at a predetermined level (the null position) in the capillary tube. Any pore pressure developed in the specimen

is brought to act on the upper surface of the mercury. Changes in pore pressure tend to dislocate the mercury maniscus from the null position. The control cylinder is used to restore the mercury column to the initial position, and at the same time provide fluid to actuate the Bourdon gauge - manometer unit. In this manner, drainage from the specimen is prevented, and the pore pressure is registered on the Bourdon gauge or the manometer.

The Bourdon gauge is used for indicating pressures higher than atmospheric pressure (considered positive). Before it was put into service, the gauge was checked against a standard gauge tester with which it agreed, within the limits of accuracy of reading the dials. Pore pressures below atmospheric pressure (negative) are indicated by the manometer. The manometer may be used also for cell pressures up to 20 lb./sq.in. Pore pressures within the range -15 to + 100 lb./sq.in. can be measured with this installation. Changes in pressure of 0.1 lb./sq.in. can be detected.

It is of the utmost importance that the system be completely filled with water and free from leaks. To facilitate the removal of air from the various tubes and fittings, a vacuum is applied. Freshly boiled water is then flushed through the apparatus, until all trapped air is taken into solution by the water as it cools. Finally, deaired water is pumped into the system. The mercury trough (a part of the null indicator unit) can be lowered, thereby allowing water to be pumped from the control cylinder to the location in the specimen, where the measurement of pore pressure is desired. The latter feature is,

To follow page 37.

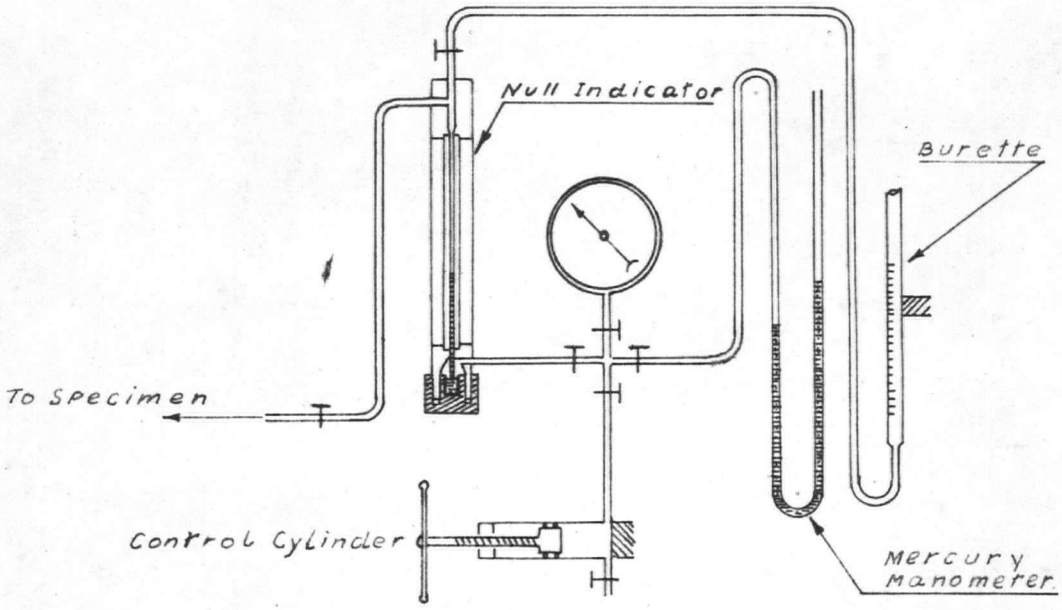

Layout of Apparatus for Measuring Pore Pressure.

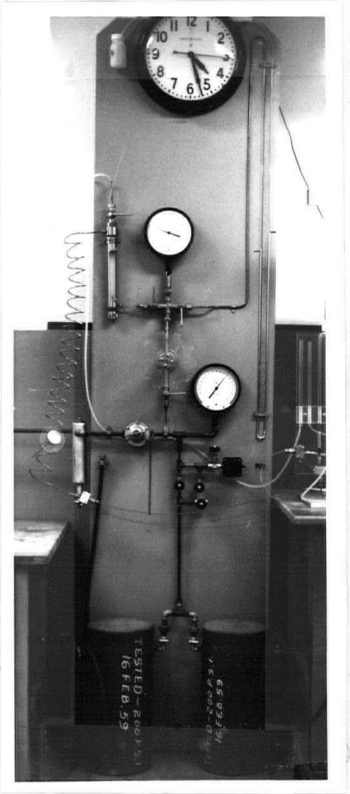

FIG 13. PORE-PRESSURE APPARATUS.

perhaps, the greatest single advantage of this apparatus; it ensures liquid to liquid continuity between the pore water and the measuring gauges.

The apparatus, as used at Imperial College, measures the pore pressure at the upper, or lower, ends of the specimen. In the latter stages of the present investigation, this method was modified in order that measurements may be obtained anywhere on the longitudinal axis of the specimen. The only alteration to the apparatus, consists of the incorporation of a porous probe (sometimes called a pilot) of the type developed at the Massachusetts' Institute of Technology, Lambe (1951). The probe is inserted in the specimen, pore pressure being measured in the region of the tip.

7. Automatic Control.

The pore pressure apparatus, discussed in the preceding paragraphs, requires the full time attention of an operator. The main duty of the operator is to maintain the mercury column at the null position - by manually adjusting the control cylinder. On long duration tests this can be tedious and time-consuming. Consequently, the development of an automatic control was undertaken. The system of automatic control finally adopted operates in conjunction with the existing pore pressure apparatus. Details of the new device are presented in Chapter VI of this thesis.

8. Fabrication of Membranes.

The specimen in a triaxial test must be protected against the ingress of chamber fluid by some form of flexible membrane.

The most appropriate method of protection in long duration tests was the subject of an extensive investigation conducted by Casagrande and Wilson (1949) at Harvard University. The outcome of this research points to the desirability of sealing the specimen in a jacket comprising an inner and outer membrane with a layer of hydrophobic compound between the sheathes. In accordance with these recommendations special membranes were fabricated for the present testing program. The membranes were formed by dipping a wooden mandril in rubber latex emulsion. The surfaces of the mandril were pretreated with silicone grease and castor oil; in order to seal the wood and facilitate removal of the finished membrane. Each coating of latex applied, was allowed to air dry for at least eight hours. The membranes were given about ten dips to obtain a wall thickness of 0.03 inches. Two sizes were required, the outer membrane was formed on a 2.55 inch diameter mandril, whereas the mandril for the inner membrane was 2.40 inches in diameter. The membranes are normally soaked in water before use, which has a tendency to produce stretching, hence the mandril diameters for the 2.5 inch specimen size.

Advantage can be taken, with this method of fabrication, to include sleeves which are used for the air-tight seal at the point of entrance of the pore-pressure probe. One sleeve was cast as an integral part of the inner membrane. Another sleeve used with the outer membrane was cast separately. The utilization of membranes possessing the above features, is shown in the photographic supplement to this thesis.

The measured compressive strength of the specimem must be corrected, to allow for the effects of the protective jacket. The correction to be applied can be estimated from the deformation characteristics of the membranes. A stress/strain curve for membranes formed of "Aerotex" rubber latex (used throughout the investigation) is shown in Fig. 12. Assessment of the correction is discussed in Appendix II.

9. Preliminary Testing of Apparatus

Before the performance of any soil tests, the apparatus was put through the following proving trials:

A dummy specimen, made of steel, was set up in the triaxial cell. Two membranes, with a film of castor oil between, protected the steel block from the chamber fluid (in this case, deaired water). Rubber bands were used to seal the membranes to the end fittings. A chamber pressure of 50 lb./sq.in. was applied for a period of 72 hours. At the end of this time, the block was carefully removed from the cell and examined for any evidence of leakage through the membranes or end fittings. No trace of water was observed, so it was concluded that the protective measures were adequate.

The deairing of the pore pressure apparatus passed the test prescribed by Bishop and Henkel (1957).

The functioning of the cell pressure control was also observed; it was found to be free from undesirable fluctuations.

10. Preparation of Soil Specimens.

All specimens were prepared in a humid room, in order to prevent moisture losses. The soil was trimmed from the original sample size of 2.8 inches diameter down to the required diameter of 2.5 inches. A soil lathe and wire saw were used for trimming (see photographic supplement). The surfaces were shaped to produce a cylindrical block, or as nearly so as possible, care being taken not to unduly disturb the soil structure. Before removal from the lathe, a thin plastic wrap (somewhat less than 5 inches long) was placed around the specimen. The specimen was then gripped in a split-mould and removed from the lathe. The split-mould permits trimming the ends to obtain a specimen 5 inches long. Due to the plastic wrap preventing adhesion between soil and mould, the specimen can be extracted from the mould with a minimum of disturbance.

The specimens were then weighed and a visual classification of the soil type recorded.

Filter pads(2) were placed at both upper and lower ends of the specimen. Vertical side drains made of $\frac{1}{4}$" wide filter paper strips were placed around the perimeter with a spacing of about $\frac{1}{4}$ inch between drains. This arrangement of filters is intended to facilitate drainage and distribute the pore pressure uniformly throughout the specimen.

The measured compressive strength must be corrected for the effect of the side drains as discussed in Appendix II.

---

(2) Reeve Angel No. 202 Filter Paper.

11. Setting Up Specimen in Triaxial Cell.

Prior to positioning the specimen in the testing machine, all drainage connections to the cell were freed of air by flushing with deaired water.

The pore-pressure apparatus was connected to the cell at this stage. Porous discs were placed at each end of the specimen. The drains were made to overlap the discs, thus providing uninterrupted drainage from the sides to both ends. The specimen was seated on the base and the inner membrane placed in position by means of a membrane stretcher. Air trapped between the membrane and the specimen was removed by allowing a little water to flow back from the base burette. The appropriate number of rubber bands (or rubber "O" rings) was in position while deairing. A film of castor oil was applied to the inner membrane. The second membrane was then placed over the specimen and sealed in a similar manner to the first. Any excess water which may have accumulated around the specimen during the deairing operation was withdrawn by lowering the base burette to obtain a slight negative pressure in the pore water.

The chamber was filled with deaired water and a low positive cell pressure (0.5 - 1.0 lb./sq.in.) applied. Any negative pore pressure remaining, was then relieved by allowing the pore water access to atmospheric pressure.

In tests where pore pressure measurements were obtained by means of the probe, a cavity was formed in the specimen with the aid of a drill bit. The drill was rotated into the soil by hand, producing a duct of the same diameter as the probe.

Deairing the cavity was accomplished by having the probe connected to the pressure lead from the control cylinder of the pore-pressure apparatus. By lowering the mercury trough of the null indicator, and operating the control cylinder of the pore-pressure apparatus, water was made to flow through the probe. Insertion of the probe while maintaining a steady flow of water, deaired the cavity. Finally, the stem of the probe was sealed from chamber fluid by means of rubber bands tightly stretched around the membrane sleeves. This method of insertion prevents the formation of a highly compressed zone of soil in the neighbourhood of the probe. Moreover, the small amount of water required for deairing is not likely to have deleterious effects on the specimen.

12. Temperature Control.

The temperatures in the laboratory were maintained in the range 18 - 22 degrees centigrade throughout the duration of the tests.

To follow page 43

Fig. 11. Proving-ring Correction for Cell Pressure

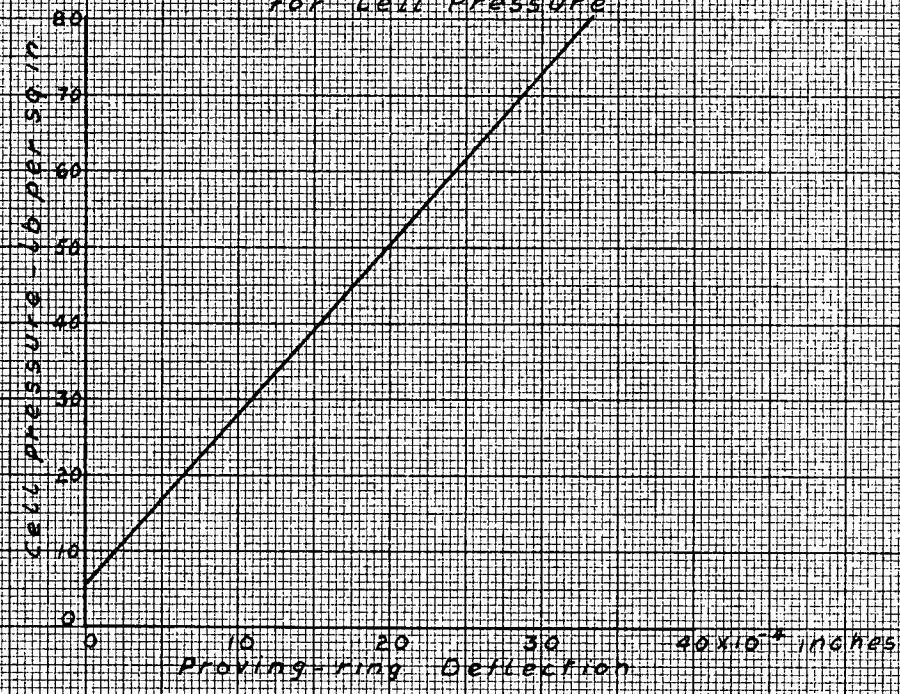

Fig 12. Rubber Membrane Stress vs Strain Curve

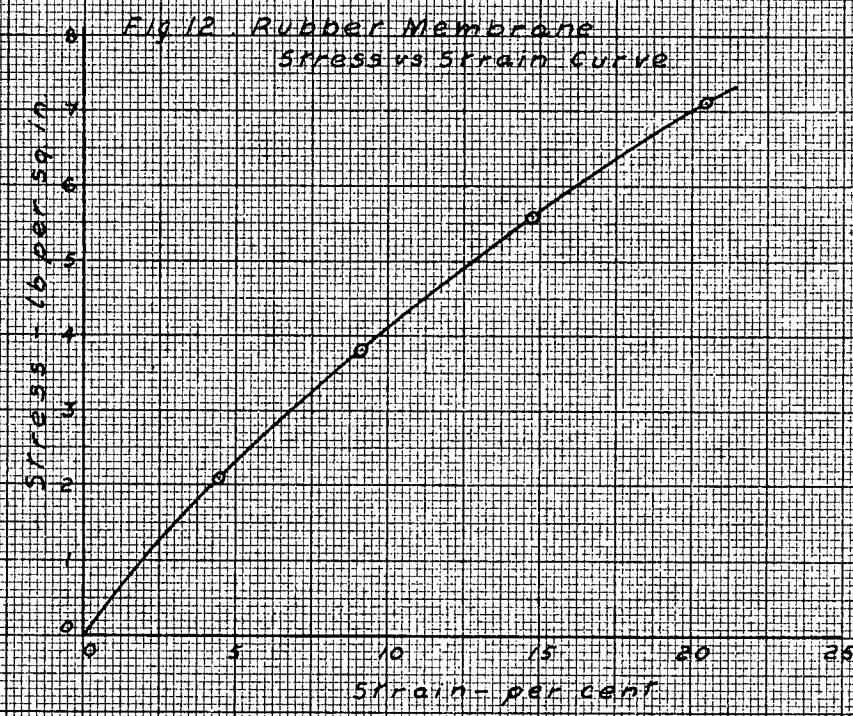

FIGS. 11 and 12

CHAPTER IV.

SHEAR TESTS WITH PORE PRESSURE MEASUREMENTS

A. Introduction

As stated at the outset of the text, the primary purpose of the investigation was to establish the pattern of pore pressure changes with applied stress and time, in long duration triaxial tests on Port Mann clay. In the course of the investigation, additional information has also been obtained on strength parameters and drainage characteristics of the soil. The report summarizes the results of all laboratory tests connected with the above assignment. The testing program extended from May, 1959 through September, 1959. All tests were performed in the Soil Mechanics Laboratory at the University of British Columbia. The soil samples required for the investigation were supplied by R. A. Spence, Consulting Engineers, Vancouver.

More specifically, the problem concerns the loss in shear strength which would result from a slow build-up of pore pressure; a phenomenon noticed in earlier rests performed

by R. A. Spence, Consulting Engineer. It was anticipated that long duration shear tests would accentuate the slow build-up effect if it were a reality. The present investigation was planned with this in mind.

B. Previous Research

Earlier works, reported by Casagrande and Wilson (1949), Taylor (1943) and others, indicate that the rate of loading in laboratory tests has a marked influence on the measured shear strength of fine-grained soils. For any one clay higher strengths are generally obtained at the faster loading rates. To cite one example, Taylor found that the strength increased by about 50% as a consequence of increasing the rate of deformation from 1% per minute to 1000% per minute. A similar change from 1% to 0.001% per minute led to a reduction of 20% in observed shear strength. Decrease in the deformation rate below 0.001% per minute had only negligible effects. Results similar to Taylor's have been obtained in tests on clay samples from widespread localities. Although the present investigation is concerned only with a particular marine clay, it is possible that the observations have a more general application to clays, in view of the findings of the above investigators.

The dependence of the measured shear strength on the rate of deformation has generally been attributed to viscous lag in the pore fluid at high deformation rates, and, to the plastic flow of the soil mass at the slower rates. Viscous effects are most significant at high deformation rates, which are outside

the scope of this investigation. Plastic flow, on the other hand, is of considerable interest. The results of the shear tests will demonstrate that plastic flow (or "creep") and pore pressure are, probably, inter-dependent, in the case of Port Mann clay, at any rate.

C. Scope of the Present Investigation

Samples obtained from two borings at the site of the New Port Mann Bridge were selected; keeping in mind that samples with as uniform a texture as possible were required. The samples were from depths ranging from 135 to 150 feet below the existing ground level. At this location, the clay stratum was found to be quite homogeneous.

Triaxial tests of this thesis extended over periods of one to twenty days. The triaxial apparatus used throughout the investigation was a controlled-stress type machine (loads applied in increments). Cell pressures up to 80 lb./sq.in. were employed.

Rates of development of pore pressure were observed throughout the duration of tests on seven specimens. Pore pressure was measured either at the top or at the centre of the specimen. Four tests were carried out with the pore pressure measurements taken at the top; in the remaining three, it was measured in the vicinity of the centre. Shear strengths, at differing degrees of consolidation, were determined for six of these specimens.

Stain tests, to obtain an indication of mineralogical

composition of the soil particles, were performed.

The sensitivity has been estimated from vane test results provided by R. A. Spence, Consulting Engineers.

Atterberg limits were determined for: (a) the clay in the natural state and (b) the clay treated with sea water. The Atterberg limits obtained in these tests are assumed to be indicative of the leaching.

D. Description of Samples

All shear tests reported in this Chapter, apply to undisturbed samples of the Port Mann clay. Swedish Foil Samplers were used to recover the 2.8 inch diameter samples from the borings. Shortly after sampling, the soil was extruded from the sampler, wrapped in polyethlene film and thoroughly waxed. This moisture seal was not removed until the samples were required for testing. This method of protection appeared to have been very effective; no discernible change in properties being observed during the period the samples were stored before testing. The sampling operation was carried out during the summer of 1958. The laboratory investigation for this thesis commenced in May, 1959.

Table III shows the order of testing, location of samples, visual description of material, etc.

E. Description of Shear Tests and Results.

In the discussion which follows, each test is treated separately. Results dependent on the correlation of a number of

tests are presented at the end of the section dealing with the individual tests. The sequence of the stages, etc., is summarized in Table IV.

SHEAR TEST NUMBER	BORING NUMBER	SAMPLE NUMBER	DEPTH BELOW GROUND LEVEL	NATURAL MOISTURE CONTENT	VISUAL DESCRIPTION OF SAMPLES
1	BN23F	22	137'-6" to 138'-4"		Dark Grey Clay with darker markings.
2	BN23F	25	139'-6" to 140'-00"	66.8%	"
3	BN23F	23	138'-4" to 139'-2"	67.6%	"
4	BN23F	27	140'-6" to 141'-4"	61.8%	"
5	BS2F	40	147'-9" to 148'-5"	68.1%	"
6	BS2F	42	148'-7" to 149'-5"	59.4%	Dark Grey Clay with Light Grey Dis-coloration on top.
7	BS2F	46	151'-3" to 152'-1"	58.1%	Dark Grey Clay with darker markings.

TABLE III - DESCRIPTION OF TEST SAMPLES.

TABLE IV -- SCHEDULE OF SHEAR TESTS

SHEAR TEST NO.	DURATION OF TEST Days	TIME ELAPSED BETWEEN PREPARATION OF SPECIMEN AND APPLICATION OF CELL PRESSURE Hours	Build-up Stages			Drainage Stages			Loading Stages		
			TOTAL NO.	CELL PRESSURES lb./sq. in.	SEQUENCE	TOTAL NO.	CELL PRESSURES lb./sq. in.	SEQUENCE	TOTAL NO.	CELL PRESSURES lb./sq. in.	TYPE OF LOADING
1	1	None	2	20 50	Consecutive	None	-	-	None	-	-
2	6	5	4	12 30 50 60	ditto	1	60	Following build-up stages	1	60	Incremental
3	9	13	1	20	-	1	20	Following build-up stages	1	20	ditto
4	10	15	4	20 40 60 80	ditto	1	80	Following build-up stages	1	80	ditto
5	10		3	20 40 60	ditto	1	60	ditto	1	60	ditto
6	17	144	2	20 40	Separated by a Drainage Stage	1	40	Intermediate between build-up stages	1	40	ditto
7	20	18	2	40 80	Separated by a Drainage Stage	2	40 80	One intermediate and one after build-up stages	1	80	ditto

LOCATION OF PORE PRESSURE MEASUREMENTS: Shear Test #1 - at top of specimen; #2 - at top of specimen; #3 - at top of specimen; #4 - at top of specimen; #5, 6 & 7 - at Centre of Specimen.

1.(a) Test 1.

Test Procedure: Test 1 was performed as a pilot test and was consequently of short duration. The pore pressure was measured at the top of the specimen. The cell pressure was raised immediately the specimen was set up for triaxial apparatus. Pore pressure changes resulting from the increase in cell pressure were recorded. The results are shown in Graph 4-1. Drainage was prevented throughout the build-up stage. The specimen was not loaded.

Results: The rate of build-up of pore pressure, and the magnitudes of the pore pressure parameter B are as follows:

INCREASE IN CELL PRESSURE σ_3 lb./sq.in From	To	TIME REQUIRED TO REACH EQUILIBRIUM MINUTES	PORE PRESSURE PARAMETER B AT EQUILIBRIUM (1)
5	20	25	0.87
20	50	20	0.92

(1) Here the values of B apply to total changes in cell and pore pressures.

(b) Test 2.

Test Procedure: The specimen was allowed to stand in the cell for a period of five hours before application of confining pressure. Pore pressure was measured at the top of the specimen throughout the duration of the test. Filter paper side drains were employed in the manner discussed earlier. Axial loading was applied in increments until the specimen failed. The moisture content was determined at three locations in the specimen after the shear test. Duration of the test was six days; the loading stage accounting for one and one-half days of this time.

Pore Pressure Build-Up Stage: A negative pore pressure of 4.8 lb./sq.in. developed during the five hour period before the cell pressure was applied. The cell pressure was raised in four increments to a maximum of 60 lb./sq.in., no drainage from specimen being permitted. Graph 4-2 shows the rate of build-up of pore pressure for each incremental change in cell pressure. The time required for the pore pressure to reach equilibrium with the cell pressures and the corresponding magnitudes of B are listed below:

INCREASE IN CELL PRESSURE σ_3 lb./sq.in. From	To	TIME REQUIRED TO REACH EQUILIBRIUM MINUTES	PORE PRESSURE PARAMETER B AT EQUILIBRIUM
0	12	110	0.57
12	30	45	0.78
30	50	40	0.87
50	60	35	0.88

The value of B however, equals unity when based on subsequent changes in cell pressures exceeding 30 lb./sq.in.; indicating that the specimen was fully saturated before the drainage stage commenced. This was the only test in which the specimen was fully saturated prior to loading.

Drainage Stage: Following the build-up stage, drainage from the specimen was allowed, while the cell pressure was maintained at 60 lb./sq.in. The flow of water was directed towards the base of the specimen. Volume changes due to expulsion of pore water were measured in the burette. A sudden drop in pore pressure was expected at the onset of drainage, but this did not materialize as is evident from the pore pressure/time curve shown in Graph 4-3. During the drainage stage the pore pressure dropped to 11.8 lb./sq.in. from the initial 51.7. Primary consolidation was 76% complete at end of drainage stage (based on dissipation of pore pressure).

Loading Stage: The cell pressure ($\sigma 3$) was maintained at 60 lb./sq. in. throughout the loading stage. Axial loading produced failure when the deviator stress ($\sigma 1 - \sigma 3$) attained a value of 31.0 lb./sq.in. During the loading stage the pore pressure gradually increased from 11.9 to 35.1 lb./sq.in. "Creep" accounted for the greater part of the deformation before failure; the instantaneous deformation being very small in comparison.

The stress vs. strain curve for the specimen is shown in Graph 4-4. The manner in which the pore pressure changed with deviator stress, time and deformation, is shown in Graph 4-5.

Time to failure t_f; 34 hours.

Type of Failure: Failure occurred on a single shear plane inclined at 60° to the plane of major principal stress, (horizontal).

Moisture Content Determinations: The following are the results of the moisture content tests performed after the shear test.

LOCATION	MOISTURE CONTENT % OF DRY WEIGHT
Top	61.0
Shear Zone	60.0
Base	55.5

(c) Test 3.

Test Procedure: The specimen was allowed to stand in the cell for a period of 13 hours before applying the cell pressure. Pore pressure was measured at the top of the specimen throughout the duration of the test. Side drains were employed to assist drainage. The specimen was tested to failure; the loads being applied in increments. Duration of test was nine days, six of which were devoted to the loading stage.

Pore Pressure Build-Up Stage: No water was allowed to escape from the specimen during the build-up stage. A negative pore pressure of 5.5 lb./sq.in. had developed before the cell pressure was applied. The cell pressure was raised in one operation to a value of 20 lb./sq.in. A period of 210 minutes elapsed before the pore pressure came to equilibrium with the increased cell pressure. The value of B at equilibrium was found to be 0.76. Pore pressure gauge readings vs. time are plotted for the build-up stage of this test in Graph 4-6.

Drainage Stage: Drainage was permitted by opening the valve to the base burette. The manner in which the pore pressure, and volume, changed during the drainage stage, is shown in Graph 4-7. There is a marked similarity between the curves obtained for the drainage stages of this test and those of Test 2. In this test, however, the volume change vs. time indicate that the average primary consolidation was complete at about 1,100 minutes(2) from the commencement of the drainage stage.

---

(2) Curve fitting to obtain t_{100} follows the method proposed by Bishop and Henkel (1957).

The curve relating decrease of pore pressure to time (Graph 4-7) shows that 70% dissipation had occurred in 1,100 minutes.

A residual pore pressure of 3.2 lb./sq.in. was recorded at the end of the drainage stage (top of specimen). Average of pore pressure would be somewhat less.

Loading Stage: The pore pressure showed a gradual increase following the application of each load increment. Failure of the specimen occurred when the deviator stress attained a value of 18.1 lb./sq.in. During the loading stage the pore pressure increased by 7.6 lb./sq.in. to 10.8 lb./sq.in. Cell pressure was maintained at 20 lb./sq.in. throughout the loading stage.

Graphs 4-8 and 4-9 pertain to the loading stage of this test.

Time to failure t_f: 114 hrs.

Type of Failure: Failure occurred on a single shear plane which was inclined at an angle of 60° to the plane of major principal stress.

Moisture Content Determinations: Moisture contents after tests were as follows:

LOCATION	MOISTURE CONTENT % OF DRY WEIGHT
Top of Specimen	61.6
Shear Zone	66.1
Base of Specimen	68.0

Water drawn into the specimen when the cell pressure was lowered may account for the high moisture content recorded at the base of the sample.

(d) Test 4.

Procedure: The specimen was allowed to stand in the triaxial cell for a period of 15 hours before cell pressure was applied. Pore pressure was measured at the top of the specimen throughout the duration of the test. Following the initial standing period, cell pressure was applied in increments; no change in the water content of the specimen being permitted. On equilibrium being beached between the pore pressure and cell pressure, drainage was permitted in order to increase the degree of consolidation. Finally the specimen was tested to failure; no drainage being allowed during the loading stage. Duration of test - 10 days.

Pore Pressure Build-Up Stage: A negative pore pressure of 5.8 lb./sq.in. developed before the cell pressure was applied. The cell pressure was raised in four increments, each 20 lb./sq. in. The manner in which the pore pressure increased, following the application of cell pressures, is shown in Graph 4-10. The pertinent data from the build-up stage are listed

INCREASE IN CELL PRESSURE σ_3 lb./sq.in From	To	TIME REQUIRED TO REACH EQUILIBRIUM MINUTES	PORE PRESSURE PARAMETER B AT EQUILIBRIUM
0	20	90	0.60
20	40	45	0.79
40	60	25	0.86
60	80	17	0.88

Drainage Stage: The specimen drained to the base burette for a period of 77 hours. During this time the pore pressure dropped from the initial value of 70 down to 10.8 lb./sq.in. The behavior of the pore pressure during the drainage stage followed a similar pattern to that observed in previous tests. The volume decrease for the drainage stage represents 11% of the original volume of specimen.

Loading Stage: The cell pressure was maintained at 80 lb./sq.in. throughout the loading stage. Incremental loading produced failure at 4.2% strain. The deviator stress at failure was 39.3 lb./sq.in. and the pore pressure 46.0 lb./sq.in. Pore pressure increases were gradual for periods up to 20 hours after the application of an increment; the rate of increase falling off sharply with time.

The stress vs strain curve is shown in Graph 4-11. Graph 4-12 shows the manner in which the pore pressure changed with deviator stress, time and deformation.

Time of failure t_f; 75 hours.

Type of Failure: The specimen failed on a single shear plane inclined at 52° to the horizontal.

Moisture contents after tests were as follows:

LOCATION	MOISTURE CONTENT % OF DRY WEIGHT
Top of Specimen	55.6
Shearing Zone	53.1
Base of Specimen	54.3

(e) Test 5.

Procedure: This test is the first of a series of three where pore pressure measurements were made in the vicinity of the centre of the specimen. For this purpose a porous probe was employed in the manner described in Chapter III. Otherwise, the procedure was similar to that of previous tests.

Unfortunately, a fault developed in a valve associated with the probe equipment. Some drainage occurred during the stage intended for the observation of pore build-up. The defect in this valve was not remedied until the loading stage was in progress. Consequently, pore pressures recorded in the build-up stage, and the initial stages of loading, were erratic. However, the trends are indicative that a similar relationship prevailed to that recorded for previous tests. In this test the only reliable information on the pore pressure is that obtained from the fourth load increment onwards. The shape of the stress-strain curve is virtually unaffected by this incident. Furthermore, the stresses at failure are appropriate when it comes to plotting Mohr diagrams.

Cell pressure was maintained at 60 lb./sq.in. throughout the loading stage. Failure occurred when the deviator stress attained a value of 34.7 lb./sq.in., at which stress the pore pressure was 35.2 lb./sq.in. The stress-strain relationship is shown in Graph 4-13.

Time to failure: t_f = 126 hours.

LOCATION	MOISTURE CONTENT % OF DRY WEIGHT
Top of Specimen	53.2
Shearing Zone	56.2
Base of Specimen	57.8

(f) Test 6.

Procedure: The specimen was allowed to stand in the triaxial cell for a period of six days before cell pressure was applied. Deaired water surrounded the specimen and its protective membranes during this time. Pore pressure measurements were made throughout the duration of the test; the probe being located at mid height of the specimen.

The procedure adopted in previous tests, that of a build-up stage followed by drainage, was slightly modified in this case. Instead, the cell pressure was raised in two increments with a drainage stage intermediate between the two build-up stages. As a result of this approach, further information was obtained on the pore pressure parameters.

The specimen was tested to failure in the usual manner. Duration of test, 17 days, included the 6 days standing time.

Pore Pressure Build-Up Stage: Although not in chronological sequence, the build-up stages will be discussed together in this paragraph; the discussion on drainage stage appearing under a separate heading. The results of the first build-up stage are similar to those reported for previous tests. No negative pore pressure, however, developed in the initial period before the specimen was subjected to cell pressures. The second stage yielded the characteristic pore pressure vs time relationship, but the value of B was considerably lower, as might be expected in view of the intervening drainage stage. The results of the build-up stages are plotted in Graph 4-14. The following tabulation shows some results for the build-up stage:

INCREASE IN CELL PRESSURE σ_3 lb./sq.in. From	To	TIME REQUIRED TO REACH EQUILIBRIUM MINUTES	PORE PRESSURE PARAMETER B AT EQUILIBRIUM
0	20	15	0.86
(Drainage Stage Between)			
20	40	12	0.51

Drainage Stage: In tests where the pore pressures are determined at the centre of the specimen, drainage may be permitted from the top and base of the specimen simultaneously. This procedure reduces the time required to obtain full dissipation of the pore pressure. Such a drainage arrangement simulates the conditions existing in the laboratory consolidation test; in fact, the results of the drainage stage of a triaxial test can be treated as if they were obtained from a consolidation test on a large specimen. The results of drainage stage may be used in determining the coefficient of consolidation (c_v), and the coefficient of permeability (k).

In the present test, drainage was permitted from the top and base of the specimen. The results for the drainage stage are plotted in Graph 4-15. At the end of the drainage stage primary consolidation was virtually complete at the centre of the specimen, as can be observed from the pore pressure dissipation vs time curve, Graph 4-15. The volume change vs time curves on the same graph indicate that on the average primary consolidation was complete at about 760 minutes from the commencement of drainage.

The coefficient of consolidation (c_v), based on the pore pressure vs time relationship, is estimated to be 0.0054 ins.^{2} per minute. (Sample calculations included in Appendix III).

Previous tests have indicated that the side drains are not effective in promoting drainage. This test afforded an opportunity of checking the efficiency of the drains. The value of c_v is computed from the volume change vs time curve on the basis of: (a) radial drainage, which takes for granted effective side drainage - and (b) drainage towards the upper and lower ends of the specimen only. By comparison with the c_v value obtained independently from pore pressure/time relationship for the same stress conditions, it is asserted that the c_v values obtained in (a) and (b) will indicate the drainage condition actually prevailing during the drainage stage. The value of c_v derived from the three considerations are listed below:

	COEFFICIENT OF CONSOLIDATION/ CU.INS.^{2}/MIN.
Based on dissipation of pore pressure	0.00540
Based on radial and end drainage	0.00026
End drainage only	0.00650

TABLE V.

DETERMINATIONS OF COEFFICIENT OF CONSOLIDATION.

Further discussion on the effects of side drains is included in the next Chapter.

The coefficient of permeability (k) is estimated to be 4.7×10^{-7} ins./min. This value applies, of course, only to the stresses corresponding to a cell press of 40 lb./sq.in.; the stress acting during the drainage stage. The pore pressure dropped from 17.2 down to 0.75 lb./sq.in. during the drainage stage.

Loading Stage: The cell pressure was maintained at 40 lb./sq.in. throughout the loading stage. Failure occurred when the deviator stress attained a value of 19.1 lb./sq.in. The pore pressure at failure was 31.0 lb./sq.in.

The value of the pore pressure parameter A is estimated at 1.01 at failure. The calculation is based on the assumption that B remained constant throughout the loading stage. In fact, the magnitude of B increases during loading, but the increase in this case would be small, because the specimen had attained a high degree of saturation prior to the loading stage.

The results of the loading stage are shown in Graph 4-16 and 4-17. It is evident from Graph 4-17 that the pore pressure showed a gradual increase for some time after the application of each load increment.

Time to failure, $t_f \approx 167$ hours.

Type of Failure: Failure occurred on at least two planes as indicated on the sketch accompanying Graph 4-16.

Moisture contents after tests were as follows:

LOCATION	MOISTURE CONTENT % OF DRY WEIGHT
Top of Specimen	62.2
Middle Zone	62.6
Base of Specimen	66.0

(g) Test 7.

Procedure: The procedure adopted was similar to that employed in Test 6. Table IV indicates the sequence of the stages. Duration of test - 20 days.

Pore Pressure Build-Up Stage: The cell pressure was raised in two increments, namely, 0 to 40 lb./sq.in. and 40 to 80 lb./sq. in. Following the build-up period for the first increase in cell pressure, drainage was permitted from the base. The second increment was applied when drainage had been in progress for a period of 4 days. The results of the build-up stages are shown in Graph 4-18. Pertinent data are listed below:

INCREASE IN CELL PRESSURE σ_3 lb./sq.in. From	To	TIME REQUIRED TO REACH EQUILIBRIUM MINUTES	PORE PRESSURE PARAMETER B AT EQUILIBRIUM
0	40	15	0.96
(Drainage Stage Between)			
40	80	25	0.65

Dissipation of pore pressure was only 63% complete at the end of the drainage stage; this may account for the rather high value of 0.65 obtained for B in the 40-80 lb./sq.in. range.

In addition to the drainage stage mentioned above, a second drainage period was permitted prior to loading. This latter stage which was conducted at a cell pressure of 80 lb./sq. in. produced a high effective stress in the specimen before

the commencement of loading. This is an advantage when Mohr diagrams are required. At the end of the second drainage stage the pore pressure was 15.7 lb./sq. in.

Loading Stage: Cell pressure was maintained at 80 lb./sq.in. throughout the loading period. The stress/strain relationship for the loading stage is shown in Graph 4-19. Failure occurred at a deviator stress of 39.4 lb./sq.in. Pore pressure at failure was 52.7 lb./sq. in.

Graph 4-20 shows the manner in which the pore pressure changed with load, deformation and time. The build-up of the pore pressure during the loading stage was somewhat erratic. This was probably due to the high cell pressure and to the high degree of consolidation at which this specimen was tested. The soil was very compact in the neighbourhood of the probe, consequently, the time required for the pore pressure to reach equilibrium showed a random variation from increment to increment. The overall trends, however, follow the pattern of previous tests.

Type of Failure: Failure occurred on a single shear plane, inclined at 60° to the horizontal.

Time to failure, t_f = 120 hours.

Moisture contents after tests were as follows:

LOCATION	MOISTURE CONTENT % OF DRY WEIGHT
Top of Specimen	43.9
Shearing Zone	43.5
Base of Specimen	46.8

2. Apparent Strength Parameters

For the purpose of deriving the 'apparent' strength parameters c and o' the tests are arbitrarily divided into two groups on the basis of the methods employed for pore pressure measurement, e.g. tests where pore pressure measurements were made at the top of the specimen, constitute one group; likewise, the tests where the pore pressure was measured at the centre, will be grouped together.

Graph 21 and Graph 22 show the Mohr circles for the effective stresses at failure. The apparent parameters, derived from the failure envelopes for the two groups, differ slightly as shown below:

POSITION OF PORE PRESSURE MEASUREMENTS	FRICTION ANGLE (APPARENT) ø' DEGREES	COHESION (APPARENT) c' lb./sq.in.
At top of Specimen. Tests 2, 3 and 4.	17	4.0
At centre of Specimen. Tests 5, 6 and 7.	21	3.0

TABLE VI.

APPARENT STRENGTH PARAMETERS - PORT MANN CLAY.

Considering the results of Test 4 as typical of the trends observed in all tests, the effects of the slow build-up of pore

pressure during the loading stage of this test will be elucidated with the aid of a Mohr diagram. The manner in which the effective stress on the failure plane changes with time is shown for two increments of axial loading Graph 4-23. It is evident from this plot that the circles representing a singular value of the deviator stress will advance towards the failure envelope with an increase in the elapsed time from the application of a load increment. In other words, the compressive strength decreases with time, even if no other effect but the slow build-up of pore pressure is taken into consideration.

The total stresses at failure are shown in the Mohr diagrams, Graph 4-24. The value of c_u and ϕ_u are estimated to be 4.5 lb./sq. in., and 9 degrees respectively.

F. Observation.

No buckling, or tilting of top cap, occurred in any of these tests.

G. Miscellaneous Tests.

1. Mineralogical Composition of Particles.

The results of stain tests shown in Table VII indicate that the soil is predominately an illite clay. Stain tests, however, provide only an indication of mineralogical composition. A more exact analysis demands the elaborate techniques of x-ray diffraction, or differential thermal analysis - which have not been attempted.

STAIN TEST (*)	COLOUR REACTION	MINERAL INDICATED
Crystal-Violet	Dark-Green	Illite predominates
Safranine y	Purple	Illite predominates
Malachite Green	Light Brown	Indefinite

(*) "Subsurface Methods" LeRoy 1949 pp. 164-166

TABLE VII.

MINERALOGICAL COMPOSITION OF PARTICLES - PORT MANN CLAY.

2. Sensitivity.

The sensitivities shown in Table VIII, have been calculated on the results of vane tests performed in boreholes BS2 and BS1B. These borings are located not more than 100 feet away from boring BS2F. It seems reasonable to assume that results of the vane tests reflect the sensitivity of the material in BS2F and BN23F.

BORING NUMBER	DEPTH BELOW GROUND LEVEL	SENSITIVITY INDEX
BS2	135' - 6"	64
BS2	136' - 3"	31
BS2	137' - 0"	77
BS1B	143' - 0"	76
BS1B	143' - 9"	39
BS1B	147' - 9"	34

TABLE VIII.

SENSITIVITY INDICES - PORT MANN CLAY.

3. Atterberg Limits.

Atterberg limits were determined for sample No. 23 - borehole BN23F. The purpose of these tests was to determine if leaching of salt from the pore water had taken place in the natural clay stratum. As stated in Chapter I, leaching is believed to reduce the values of the Atterberg limits. The index tests were therefore performed on the natural clay, and on clay which had been pretreated with sea water. The treatment consisted of mixing the clay with excess salt water and allowing it to stand for 24 hours. The flocculated soil was then separated by decanting off the superfluous liquid. Both the natural and treated soils were allowed to air dry for the purpose of obtaining the consistency of the Atterberg limit tests. The results of the tests are listed below:

BORING BN23F SAMPLE NO. 23	LIQUID LIMIT	PLASTIC LIMIT
Natural Soil	74.5	32.6
Salt-Treated Soil	89.0	31.2

TABLE IX.

ATTERBERG LIMITS - PORT MANN CLAY.

These results show that a significant change in liquid limit occurs when the soil is allowed access to the salt ions dissolved in sea water.

CHAPTER V.

DISCUSSION OF TEST RESULTS AND CONCLUSIONS

A. Effects of Overburden Pressure

At the outset of the text, attention was drawn to the effects of preconsolidation on the soil properties - notably the shear strength.

For preconsolidated clays the failure envelope of effective stresses shows a cohesion intercept on the shear stress axis, whereas for normally consolidated clays tested at cell pressures greater than the overburden pressure, the effective stress envelope passes through the origin. Geological evidence indicates that the Port Mann clay is normally consolidated, but the effective stresses at the depth of the samples tested are such that in laboratory tests, the soil would be expected to behave like a preconsolidated material until the equivalent overburden stresses of 50 - 57 lb./sq.in. have been exceeded.(1)

Due to limitation imposed by the shear test apparatus,

---

(1) Effective stresses are given in Appendix I.

only in Tests 4, 5 and 7 did the axial stress exceed the overburden pressure. Therefore, the values of 'apparent' cohesion listed in Chapter IV are to be expected.

B. Sensitivity

The results of the consolidation tests (e vs log p graphs) given in Appendix I show that the relationship between void ratio and pressure is typical of extra sensitive clays, Terzaghi and Peck (1949).

The results of the vane tests further confirm the high sensitivity of this soil deposit. (Table VIII and Appendix I). Sensitivities greater than 8 are considered high. This soil with sensitivities in the range 30 to 80, undoubtedly, belongs to the extrasensitive group of clays. The vane test results emphasize the importance of disturbance of structure on shear strength; this soil would be classified as a firm clay, in the undisturbed state, yet breaking down the structure by remoulding transforms the soil into a slurry of negligible shear strength.

In comparison with the Norwegian clays, the Atterberg limits of the samples used for these tests are high; 74 and 31 as against 26 and 18 for some Norwegian clays, Bjerrum (1954).

The sensitivity of the Norwegian clay is also higher; sensitivity indices of 300 to 500 have been reported by the same author. The natural moisture content of the Port Mann clay is close to the liquid limit.

If Atterberg limits are accepted as an indication of the degree of leaching, the process is not in an advanced stage in this deposit. The fact that the liquid limit was raised by 14.5[2] when the soil was immersed in sea water, indicated that some leaching has taken place. As the deposit is below sea level and appears to have never been subjected to subaerial leaching, the most likely source of leaching water is an artesian head[3] in the previous layer beneath the clay deposit.

It is inferred from the sensitivity that the Port Mann clay possesses a "cardhouse" structure of a similar configuration to that confirmed in the case of the Norwegian clays, Rosenquist (1959).

C. Stress-Strain Curves

All the shear tests exhibit non-linear relationship between stress and strain during the initial stages of loading e.g. Graph 4-8. Rarely have stress strain curves of this shape been reported. The cause(s) of the high initial deformation is not known. Precautions were taken during the tests to obtain a positive seating of the cell plunger on the specimen cap, before applying the axial loads. It is all the more difficult to understand in view of the drainage stages having seated the end fittings (porous discs, etc.) prior to the loading stages. Noteworthy is the fact that a considerable part of the initial de-

---

(2) See Table IX.

(3) See borehold logs, Appendix I.

formation occurred in the form of "creep"[4]. Possibly some rearrangement of structure occurs in the initial stages of loading. No peak deviator stress appears on the stress-strain curves. Membrane restraint at the higher strains may have overcome the tendency to develop the peak stress usually associated with extrasensitive clays.

D. Pore Pressure Characteristics

The results of the shear tests lead to the conslucion that in this soil, pore pressure requires considerable time to reach equilibrium with the applied stresses. Results presented in Chapter IV show that the effect is common to both the increases in allround and axial stresses produced in the triaxial test. The time lag is evident in the build-up stages, but is seen to best advantage in the loading stages, Graph 4-17, for instance.

The deformation vs time curves resemble an inverted image of the pore pressure vs time relationship in plots such as Graph 4-17. The similarity suggests that the rate of build-up of pore pressure is related to the creep of the soil skeleton (up to insipient failure). Considering the remarks made earlier (Chapter I) regarding the adsorption and structural characteristics of marine clay, it is reasonabke to assume that the cardhouse type of structure is capable of withstanding considerable effective stresses at the "edge to flat" contacts of the particles;

---

(4) Creep and plastic flow are regarded as synonymous terms.

the effective stresses resulting from a combination of the effects of interparticle forces and the external loads. Apparently, with the passing of time, the effective stresses are relieved by plastic deformations of the adsorbed layers - the particles are realigned to become more nearly parallel. It is believed that an increase in the spacing of the particles occurs in the process of realignment; regions which were initially in contact tending to separate. This hypothesis is illustrated diagramatically in Figure 14. Realignment would then permit a reduction in the effective stresses, while at the same time the stress changes would be transmitted to the pore fluid. The writer suggests that the time lag in pore pressure build-up can be attributed to realignment of the particles, resulting from plastic deformations of the adsorbed layer in the region of contact areas.

Supporting this view are investigations reported by Michel and Lambe. Michel (1956) observed that repeated stressing of a soil aligns the particles in almost parallel formation, assuming, of course, that the particles possess the characteristic flaky shapes of true clays. Moreover, Michel proved with measurements that not only remoulding, but even shear strains, arranges particles in parallel array. Lambe (1959) drew similar conclusions regarding the orientation of particles in mechanically compacted soils.

In this series the results of Test 2 substantiate the postulation concerning realignment. Although fully saturated at cell pressures higher than 30 lb./sq.in., the test yielded

To follow page 77

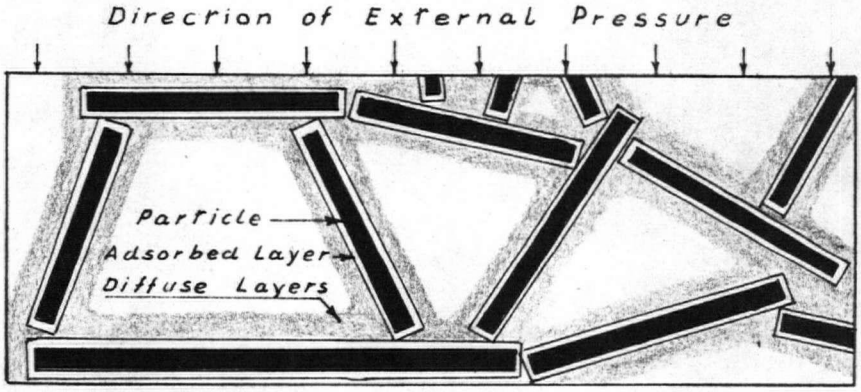

Time t_0 : External Pressure taken partly by Intergranular Stresses.

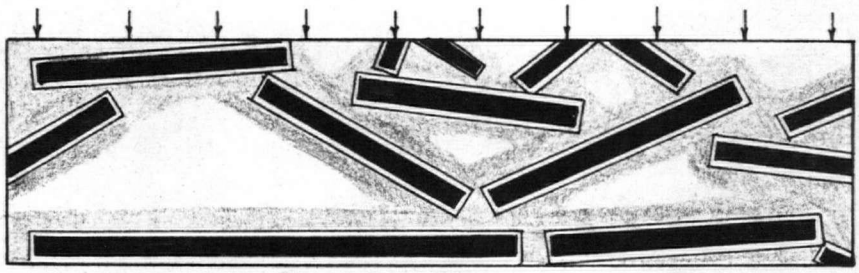

Time t_1 : External Pressure taken entirely by Pore Water.

FIG 14. CLAY- WATER SYSTEM: EFFECTS OF PLASTIC DEFORMATION OF THE ADSORBED LAYERS.

the characteristic pore pressure vs time relationship for further increases in cell pressure, and also for the loading stage, Graphs 4-2 and 4-5. The other test specimens were very close to saturation(5) prior to loading - possibly reaching saturation during the long periods devoted to the loading stages.

The rate of pore pressure build-up also depends to a large extent on degree of saturation. It has hitherto been assumed that in completely saturated soils the elastic deformation of the skeleton is sufficient to build up the pore pressure instantaneously to its final value, (due to the low compressibility of water in comparison to that of the soil skeleton). This assumption entails that the pore pressure change has the same magnitude as the applied stress provided no drainage occurs. If this assumption is valid, it does not take into consideration: (a) the interparticle stresses in colloidal materials(6), and (b) the possibility that gas bubbles may be trapped in the pore water of submerged soil strata. The relation between interparticle stresses and structure has been discussed already, so attention will now be directed to the effects of trapped gases.

Complete saturation does not seem to be a justifiable assumption in all cases of submerged strata. Transported soils may be expected to contain some air trapped at the time of deposition. Also, bacteria may be responsible for increasing the gas content of the pore fluid. Values of B slightly less

---

(5) Saturation as indicated by B values.

(6) Interparticle stresses are deemed to include both stresses arising from Van der Waal's forces and effective stresses due to external forces.

than unity have been recorded for laboratory tests on soils from submerged strata, Skempton (1954).

The values of B reported in Chapter IV, indicate that the samples of Port Mann clay were not fully saturated on receipt at the laboratory. The pore pressure developed in the shear tests are then governed by factors listed below. An evaluation of the role played by each of these factors is a complicated study; requiring a knowledge of the amount and composition of the gases, rate of deformation of adsorbed layers, etc. Only a brief discussion of the topics is presented here:

(a) Deformation of the soil skeleton.

(b) Compressibility of the pore fluid.

(c) Solubility of trapped gases.

(d) Surface tension at the gas-liquid interface.

(e) Vapour pressure of water.

(f) Temperature.

In view of earlier discussions[7], it is evident that the pressure developed in the pore fluid is a function of the deformation of the soil skeleton. The pressure developed in the gas phase will depend primarily on decrease in volume of the soil skeleton. The gases will react instantaneously to the reduced volume, building up the pore pressure in accordance with Boyle's law. From this viewpoint then, the rate of development of pore pressure is dictated by the rate of deformation of the skeleton.

---

(7) Refer to Chapter III, and earlier statements in this Chapter.

The other factors listed are of secondary importance as shall be seen presently.

An increase in the pore pressure drives an increased proportion of the trapped gases into solution in accordance with Henry's law of solubility. A time effect is introduced here, as it requires an interval for an equilibrium state to be established between the pore pressure and the concentration of gas in solution. Gases going into solution tend to lower the pore pressure, but the drop in pressure with time, due to this phenomenon, is not readily observed because the soil skeleton is deforming simultaneously. After a certain increase in pore pressure (corresponding to all gases in solution) full saturation is reached (then B will thereafter be equal to unity with respect to further stress changes). Therefore, solubility of the gases does not contribute to the gradually increasing pore pressure observed in this series of tests.

Surface tension produces a difference in pressure between the liquid and gas phases of the pore fluid. The pressure difference p is given by the expression $p = \frac{2\gamma}{r}$ where γ denotes the surface tension of water and r refers to the radius of the entrapped bubble. This effect is usually ignored - the assumption being made that the pore water and the gases are at the same pressure.

Part of the pressure in the gas phase is derived from the vapour pressure of the water. As the vapour pressure of water is about 0.35 lb./sq.in. at 20° C., pore pressures higher than this figure are not affected.

Temperature effects are inherent in all five factors discussed. In this series of tests the temperatures were restricted to the range 18-22° C., which is not likely to materially affect the results.

The slower rates of build-up recorded for those tests with pore pressure measurements at the top cap, are most likely caused by restraint imposed by the end fitting (porous discs, etc.). Shear stresses are introduced at the ends, which restricts the deformation of the soil, particularly under the action of cell pressure. The observed data provide further evidence to support the view that the rate of deformation of the soil skeleton is the prime factor determining the rate of pore pressure build-up in this soil.

The possibility of a significant time lag being inherent in the response of the measuring apparatus, is discounted by the observation that the pore pressure measurements obtained by using the probe, lead to shorter times to equilibrium than do measurements taken at the surface of the specimen. The movement of water at the tip of the probe is restricted by the small area of the perforations, which would have the effect of emphasizing any lag in the response of the pore pressure apparatus.

The tendency of the soil to expand on the relief of overburden pressure in sampling may be responsible for bringing some gas out of solution prior to testing. Negative pore pressures, however, were recorded at the surface of the specimen, despite the fact that water was used in preparing the specimens - to free the surface air. It appears that the surface tension in

the outermost pore water exceeds considerably the observed negative pressures of 5 lb./sq.in. (Tests, 2, 3, 4). Large negative pore pressures at the surface indicate that expansion has been restrained in the inner parts of the sample.

E. Strength Parameters

Although the primary objective of the investigation was to determine the pattern of pore pressure changes with applied stress, additional data has been obtained concerning the strength parameters and drainage characteristics of the soil.

The 'apparent' strength parameters (c' and o') derived from Tests 2, 3 and 4, differ from those obtained from Tests 5, 6 and 7 (Table VI). The disagreement is believed to be due to the higher rate of loading adopted in Tests 2 and 4. It is apparent from Graphs 4-5 and 4-12 that the pore pressure had not reached equilibrium with every load increment in the case of those tests. The deformation/time relationship was the only matter considered in deciding on loading rates, but it now appears that the pore pressure/time relationship is a more rational criterion; equilibrium between the pore pressure and the previous increment should be established before additional increments are applied. In the absence of information to the contrary, the values $c' = 3.0$ lbs./sq.in. and $\phi' = 21$ degrees, obtained from Tests 5, 6 and 7, are accepted as the most appropriate 'apparent' strength parameters.

On the assumption that the effective stress circles of Tests 2 and 4 should come somewhat closer to the origin in

Graph 4-21, it appears that the two systems employed for measuring pore pressure will yield results in substantial agreement with respect to strength parameters.

The true friction angle ϕ_r could not be determined from the inclination for the failure plane(s) in any test of this series. The inclinations observed appear to be influenced by the restraint developed at the end fitting, which leads to an overestimate of the true friction angle.

F. Drainage Characteristics

The coefficient of permeability $k = 4.7 \times 10^{-7}$ ins./min. determined from the data on the drainage stage of Test 6, places the clay in the category of practically impervious soils, Terzaghi and Peck, (1948).

The results shown in Table V lead to the conclusion that filter paper strips do not form effective side drains when subjected to high cell pressures. This conclusion is supported by work reported by Rowe, published about the time the testing program for this thesis terminated, Rowe (1959).

The Mohr diagram, Graph 4-23, illustrates the reduction in shear strength with time. For further investigation of this aspect, a strain-controlled triaxial machine has many advantages over the stress-controlled type used in the present test series. A strain-controlled machine, giving a wide range of test rates, has been designed, and is at present being fabricated. It is hoped to carry out further experiments on the reduction of shear strength with time to failure when the strain-controlled machine becomes available.

CHAPTER VI.

AUTOMATIC CONTROL

A. Introduction

Automatic control of pore water movements is a decided advantage where the null method of pore pressure measurement is employed. In particular, this is the case if tests are to be run over long periods of time. Adjustment of the null indicator must be made so frequently during a test that in the absence of automatic control an operator is required to devote almost his full time to the attention of this detail. In commercial laboratories this is offset somewhat by assigning one person to take charge of a number of tests. Overnight, however, the pore pressure apparatus has to be isolated from the specimen, which means that the intervening pore pressure changes must be estimated by extrapolation before the apparatus is reconnected. A disadvantage of this approach is that if a poor estimate is made, undesirable movement of the pore water results. Consequently, the development of automatic control systems has attracted considerable attention.

Ideally, an automatic control system should be capable of restricting the pore water movements to the very limited range that can be tolerated in triaxial testing. Furthermore, it should not add complications to the already difficult problem of deairing the pore-pressure apparatus. Before discussing the details of the new device, a review of existing automatic controls and remarks on their performance will be presented.

Insofar as the author is aware, only two servomechanisms have been developed for use with the null method of pore-pressure measurement. They are based on somewhat different principles, but both operate towards the same purpose; that of maintaining the mercury column of the pore pressure apparatus at a preselected level thoughout the duration of the test.

The apparatus originally designed at Delft Soil Mechanics Laboratory and later modified by Penman, employs a thermostatically controlled oil bath to maintain a back pressure on the pore water via the mercury column. A schematic of the apparatus is shown in Fig. 15. The mercury column of the null indicator makes contact with an electrode placed inside the capillary tube. An increase in pore pressure will break the contact between mercury and electrode. Breaking the contact operates a relay which switches in the heating unit installed in the oil bath. The thermal expansion of the oil restores the mercury to the null position (contact with electrode). At this point the relay cuts out the heater. In practice, a continuous make and break action (10 times per second) occurs in the vicinity

of the electrode. By this means the movement of pore water is restricted to as little as 0.1 millimeters of mercury in the 1 millimeter diameter capillary tube. The apparatus is therefore capable of very efficient control, particularly if the pore pressure is increasing. On a falling pore pressure, however, the oil bath must be cooled, which leads to mechanical complications - a pump to circulate cold water through the oil bath and some time delay switches must be installed. It is claimed that even for the case of falling pore pressure the movement of pore water can be restricted to about 0.5 millimeters, Penman (1953). When deairing the system, the presence of three liquid interfaces, namely, oil, water and mercury, seems to be a disadvantage to this method.

In 1956, Burton reported a design for an automatic control based on the application of photo-electric cells. The cells are used to monoiter the levels of a mercury column in a U-tube. The pore pressure acts on the mercury in one limb of the U-tube. To the other side of the U-tube is fitted a displacement system consisting of an actuator operating hydraulic bellows, and a pressure gauge. Any movement of the mercury causes fluctuations in the quantity of radiant energy reaching the cells from a light source. Electrical impulses received from the photo cells, control the operation of the servomechanism. The electrical circuit of this apparatus is shown in Fig. 16. Essentially, the circuit is that of an electronic bridge consisting of twin amplifiers. When the mercury is at

To follow page 86

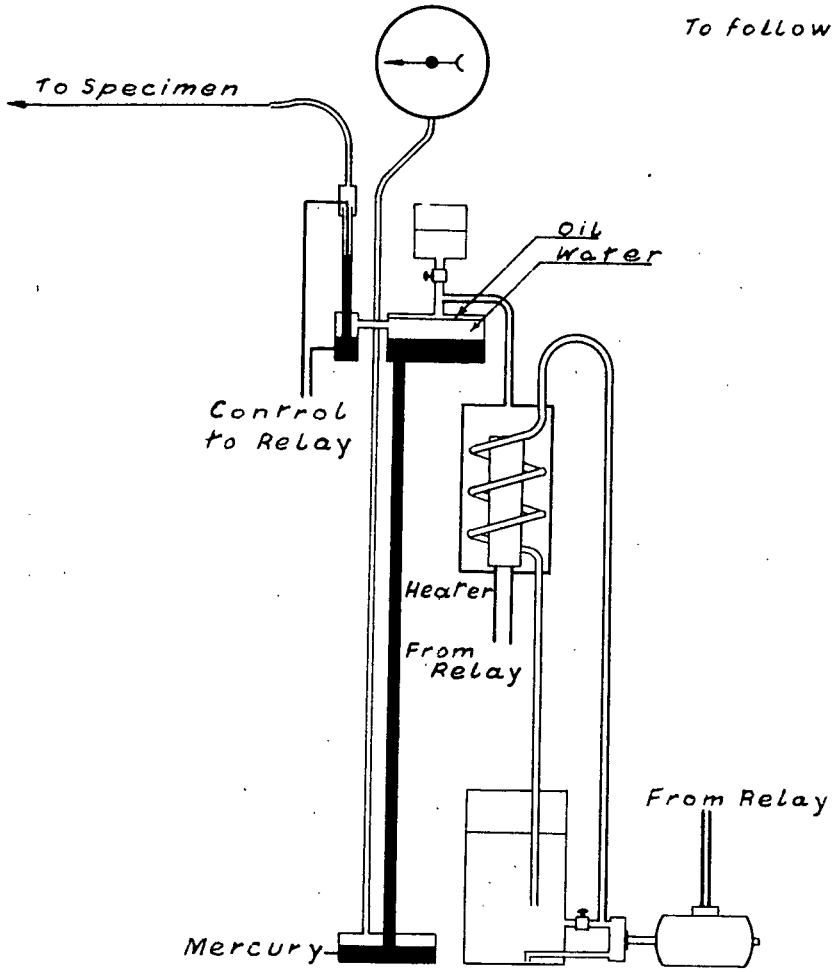

FIG 15. PORE-PRESSURE DEVICE

(After A.D. Penman 1953)

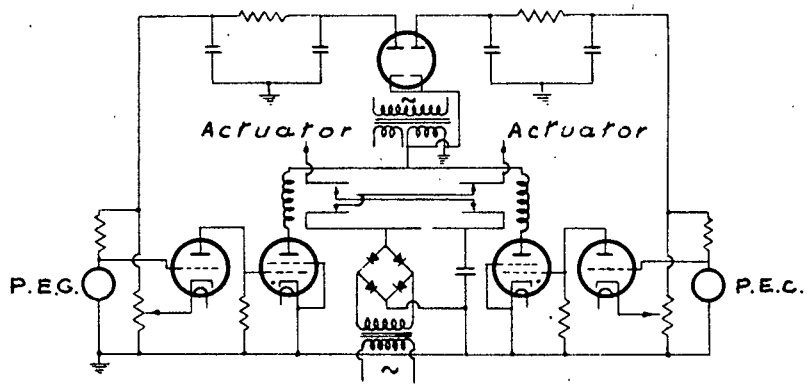

FIG 16. CIRCUIT OF AUTOMATIC CONTROL

(After L.J. Burton 1956)

FIGS 15 and 16.

same level in both limbs of the U-tube, the two amplifiers can be adjusted so that their outputs are equal and opposite. The pressure feedback unit is then idle. Any change in the mercury level unbalances the amplifiers, which closes one of the two relays in the anode circuit of the output stage. The relays control the movement of the actuator and hydraulic bellows. Direction of movement depends on which relay is closed; the hydraulic bellows works in the sense to oppose the change in mercury level. It is claimed that the device is capable of restricting the pore water movement to about 1 part in 400,000. This figure is quoted for a saturated sample 4 inches in diameter, 8 inches long and having a porosity of 20%, Burton (1956). From the soil-testing viewpoint, a drawback to the use of this apparatus is the difficulty of deairing the U-tube arrangement. Furthermore, the hydraulic bellows operates almost immediately a relay closes. This introduces the problem of "hunting" when working with soils of low permeability. Perhaps minor objections to the design is the need for two power packs and a well regulated power line voltage. Nevertheless, the apparatus provides a remarkable degree of control over pore water movements.

In order to overcome the problem of converting existing servo-controls, to work in conjunction with Bishop's pore-pressure apparatus, further possibilities were investigated, as part of the present program. The use of piezo-electric crystals was considered. At first sight, piezo-crystals, of quartz or of Rochelle salt, appear to offer an approach to the problem.

Such crystals have been effectively used for the measurement of impulse pressures, shock wave intensities, etc. Measurable potentials are developed on the crystal faces when subjected to stresses of the magnitudes occurring in pore pressure work. The deformation of the crystal would be negligible and they are available in convenient sizes. This suggested the possibility of developing a pressure cell to assist in the operation of the existing pore pressure apparatus. A study of the properties of these crystals, however, revealed that they are unsuitable for use in systems where pressure changes are gradual, as is the case in triaxial testing. In fact, the original mechanical problem becomes an electrical one of an analgous nature.

It was then decided to revert to the application of photo-electric cells, but to design a control unit that preserved, as far as possible, the advantages derived from the use of Bishop's pore pressure apparatus. The new device has proved satisfactory in achieving this objective.

B. Details of Apparatus for Automatic Control of Pore Pressure

Turning again to the null indicator of Bishop's pore-pressure apparatus, it will be recalled that it embodies a glass capillary tube which terminates in a mercury reservoir. The height to which the column of mercury will rise in the tube depends upon a state of equilibrium being attained, between the pore pressure which acts on the meniscus of the column, and the back pressure acting on the surface of the mercury in the

reservoir. At the commencement of a test, the mercury is raised to a convenient height in the capillary tube, with the pore pressure connection to the specimen isolated from the unit. Before allowing the pore water access to the mercury column, the triaxial stresses on the specimen are so arranged as to produce zero pore pressure - or as nearly so as possible. On admission of the pore water into contact with the mercury column, the initial state of equilibrium is obtained. The level of the mercury in the capillary is then taken as the null position. The null position is also made to coincide with atmospheric pressure, by opening the appropriate valves momentarily, throughout the system. An increase in pore pressure tends to drive the mercury column down - towards the reservoir, and similarly a decrease has the tendency to raise the mercury to a higher level than the null position. To maintain the mercury at the null position (no flow of pore water from specimen) the back pressure on the mercury reservoir must be adjusted. The new device automatically makes the adjustments.

The design of the automatic control centres around the characteristics of a photo-voltaic type photo cell, which is used to detect changes in the quantity of light arriving from a light source focused on the null position of the mercury column. The signals from the photo cell are interpreted by a sensitive amplifier for the purpose of regulating the back pressure on the mercury reservoir. A block diagram of the apparatus is shown in Fig. 17. Any change in the mercury level from the null position, reflects in the operation of the

To follow page 89.

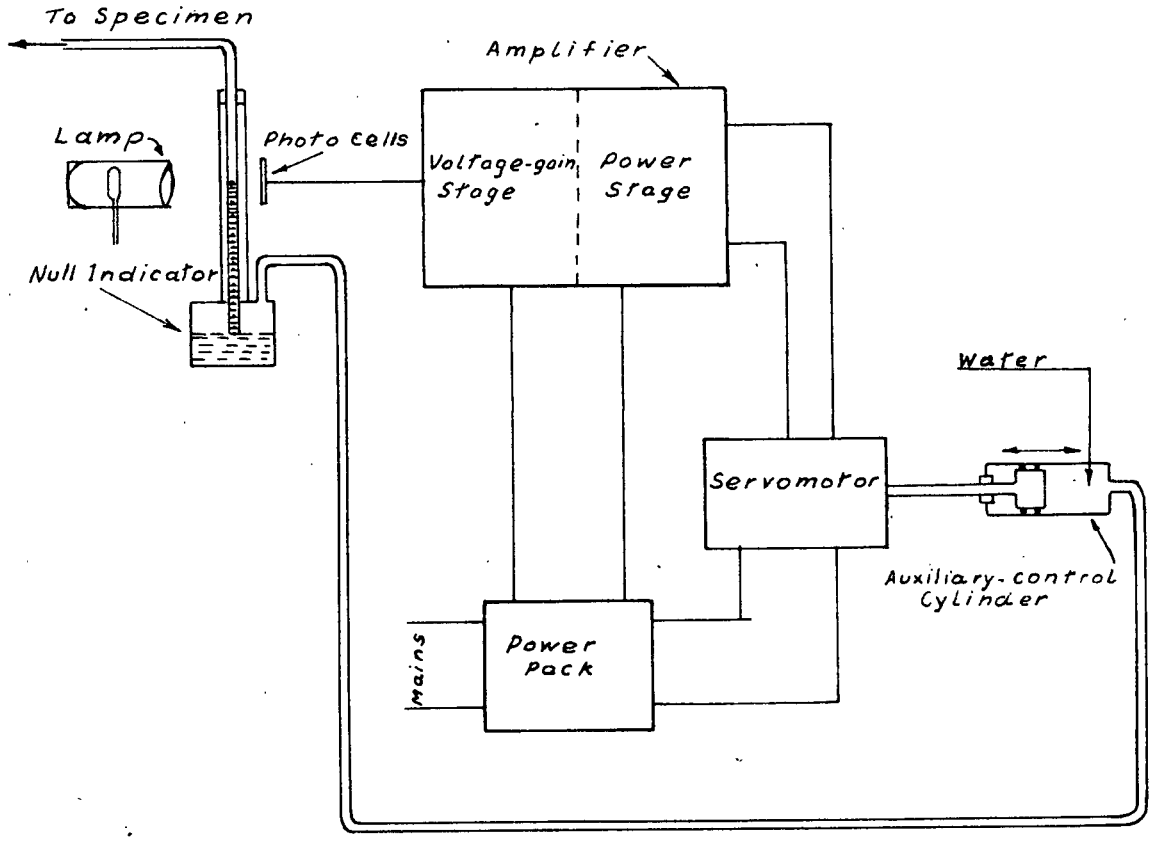

FIG 17. LAYOUT OF AUTOMATIC CONTROL

amplifier. Two relays in the output stage of the amplifier, control the course of action of the pressure feedback, so that it always reacts towards restoring the mercury column to the null position.

Exciter Lamp: The concentrated light beam required for excitation of the photo cell, is obtained from a film slide projector housing a 75 watt lamp. The condenser lens and concave mirror of the projector constitute the optical system; all other lenses are removed in order to obtain near parallel rays from the projector.

A thin metal sleeve with vertical slits cut on opposite sides, fits over the capillary tube of the null indicator. Its purpose is to minimize light scattering which would otherwise occur in the walls of the capillary tube. Due to the presence of the sleeve, light reaching the photo cell must first pass through the bore of the tube, in a direction at right angles to the longitudinal axis of the bore.

Photo Electric Cell: The light-sensitive cell is made of two identical photo-voltaic elements enclosed in a metal housing. The voltaic cells (commercially available) are formed by depositing a thin layer of selenium on an iron plate: the plate constitutes the positive electrode; the negative electrode being a transparent film of metal evaporated onto the selenium surface. Light falling on the selenium activates the cell to produce directly an E.M.F. between the electrodes. Although the amplifier is capable of operating on a single element, two photo-voltaic cells are preferable in this case. The two-cell system arises

from the requirement of an observation aperture, to enable a visual check to be made on the mercury level. It is not practicable to cut the aperture in the fragile surface coatings of the individual cell. Instead, a slit is formed by leaving a space between the upper and lower cells. Due to the small dimensions of the individual cells (0.72" x 0.44": active area 0.26 square inches) no difficulty was experienced in accommodating them in close proximity to the capillary tube. In passing, it may be of interest to note that the photo-voltaic cell is preferable to either gas-filled, or vacuum-type photo cells for this application. The cells require no external source of energy (except light), are not sensitive to infra red (heat) rays, and because of their miniature size, are easy to install.

Control Unit: For descriptive purposes the remaining parts of the control unit will be treated under two headings: (a) the electronic system and (b) the electro-mechanical system.

(a) The Electronic System: embodies the amplifier and relay switching components. An amplifier of the direct current type is employed, because a D.C. output is more readily obtainable from the photo cell. The use of a D.C. amplifier eliminates the need for a light "chopper" or other means of producing pulsating inputs from the cell The amplifier consists of a high voltage gain stage, followed by a power amplifying stage. The relays are connected in the output circuit of the power stage. The circuit of the amplifier is shown in Fig. 18(a). Conventional symbols are used to denote the various components in the circuit diagrams[1].

(1) Symbols as outlined in handbook of American Radio Relay League.

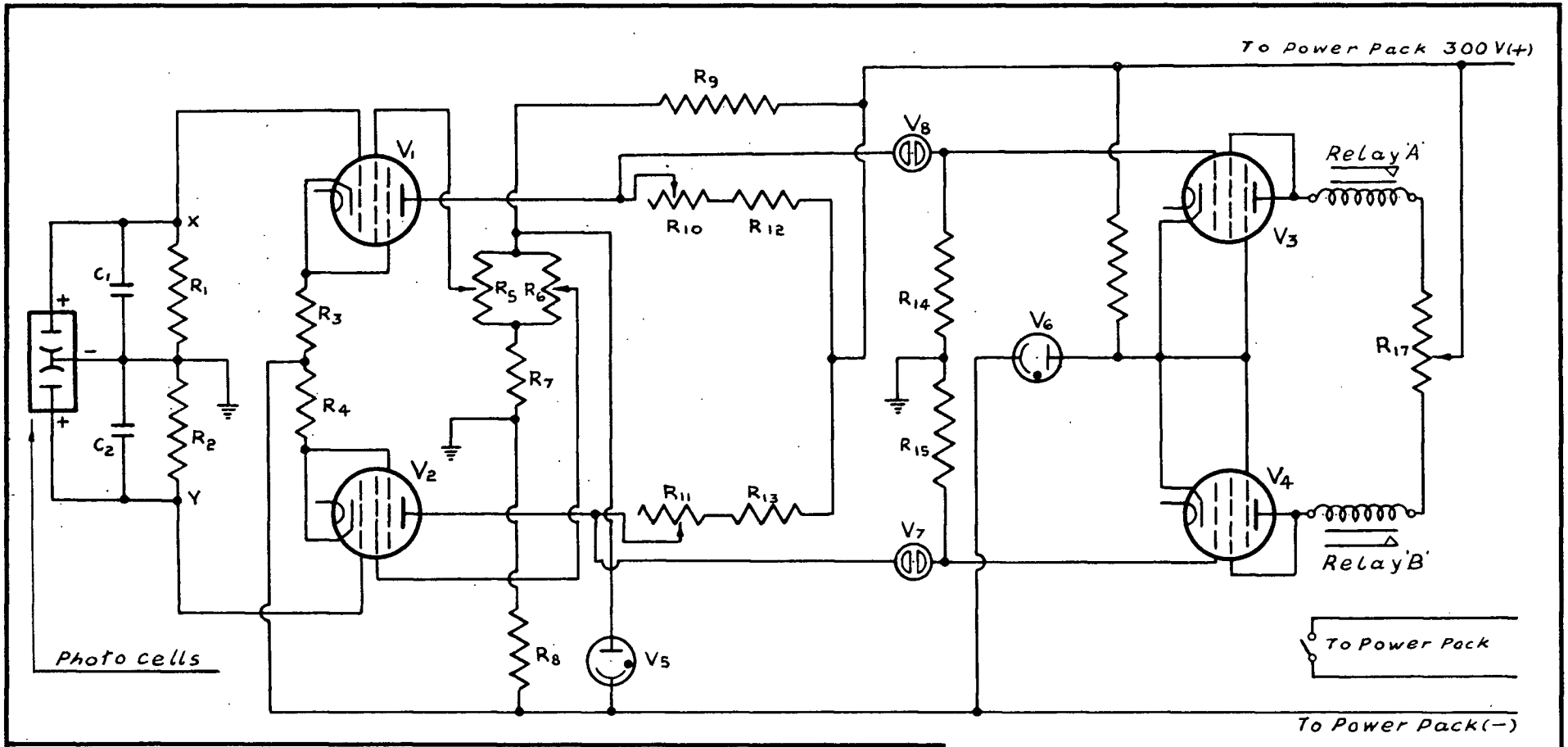

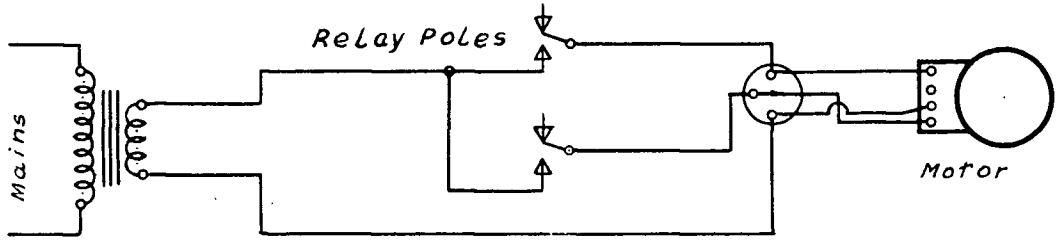

(b) CIRCUIT OF SERVOMOTOR

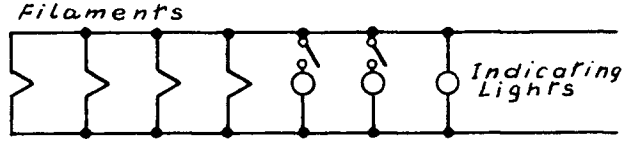

(a) CIRCUIT OF AMPLIFIER

FIG 18. AUTOMATIC CONTROL

To follow page 91.

The cells (2 No. B2M.'s) International Rectifier Corp. form part of a closed circuit which includes the resistors R_1 and R_2. The negative terminals of the cells, and the junction of R_1, R_2, are brought to a common ground, by a connection to the amplifier chassis. This, in effect, yields two independent loops, each comprising a cell with a resistance across its terminals. This arrangement provides a parallel input.

A change in flow of current from a cell to ground, produces a corresponding change in the grid potential of the thermionic tube associated with that loop. Thus, changes in the potential of X on R_1, effect the grid potential of V_1 only. Similarly, a voltage change at point Y reflects on the grid potential of V_2. Consider, for the present, the case where an equal increase has occurred in the illumination of both cells. The grids of V_1 and V_2 will then acquire a positive charge, which is proportional to the change in illumination at the cell. The positive charge will increase the conductivity of the tubes (V_1 and V_2) so that more current will flow through the load resistances (R_{10}, - R_{12}, R_{11} - R_{13}). Increase in plate current will produce a voltage drop across the load resistances in accordance with Ohm's Law. Voltage changes are tapped off R_{10} and R_{11} and applied to the grids of the power tubes (V_3 and V_4). Here a voltage drop has the effect of reducing the current flow through the relays A and B which are incorporated in the anode circuit of V_3, V_4. The relay contacts will open if the current falls below a preset value. Reducing the illumination at the

cell has the opposite effect - tends to close the contacts.

When the mercury level is at the null position relay "A" is open and "B" is closed (closed in this sense means that the contacts are pulled in towards the relay coil). The power supply to the feedback motor is connected to the poles of relay switches in such a way that the motor is idle for this condition. The motor is switched on only when both relays are either in the open or closed positions. As may be surmised, this occurs when the mercury level departs from the null position. The circuit relating to the motor and relay switches is shown in Fig. 18(b).

The functions of the other components in the amplifier will now be discussed briefly.

The condensers C_1 and C_2 are intended to smooth out ripple from the photo-cell output, caused by the alternating current supply to the exciter lamp.

The gain of the voltage amplifying stage may be regulated by setting the screen potentials of V_1 and V_2, by means of potentiometers R_5, R_6. The resistances R_3, R_4 and R_8 provide grid bias for V_1 and V_2.

Considerable difficulty was experienced in devising a means of biasing the power tubes V_3, V_4. This problem is encountered in multistage direct current amplifiers, because the grid of a following stage is at a potential close to the anode voltage of the preceding stage. The difficulty was overcome in this case, by employing neon voltage droppers (V_7, V_8) in the grid circuits; and, by introducing a voltage regulator tube (V_6) into the cathode circuit, instead of the usual cathode

resistor. In fact, it is the latter innovation that makes the operation of the amplifier possible.

"Bleeder" resistors (R_{14}, R_{15}, R_{16}) are provided in order that V_7, V_8 and V_9 remain "fired" while the amplifier is in operation. The plate potentials of V_3, V_4 may be equalized by adjusting the potentiometer R_{17}.

(b) The Electromechanical System. The electromechanical system consists of an electric motor, geared to drive a piston in an auxiliary control cylinder - the auxiliary cylinder being connected directly to the main control cylinder of the pore pressure apparatus. The motor which is reversible, gives an output speed of $1\frac{1}{4}$ r.p.m. Further reduction in speed is provided by a worm gear reduction unit. The design of the auxiliary cylinder is patterned on that of the main control cylinder. For soils of low permeability, such as the Port Mann clay, a feedback rate of 0.077 cubic inches per minute has been found satisfactory; "hunting" being eliminated entirely at this rate. A faster rate of feedback would perhaps be an advantage in more permeable soils.

The installation of the automatic control has not interfered with the manually-operated system. The only modifications to the existing pore-pressure apparatus consisted of interchanging the 1 mm bore capillary tube for a 1.5 mm tube. The larger bore capillary tube is required to provide a positive gate to the photo-cell unit. Light scattering in the walls of 1 mm. ID.(8 mm OD) tube introduced difficulties into the

adjustments of the amplifier. Provided that the mercury is maintained at the null position, increasing the bore of the tube is not a serious disadvantage. A tube with square external cross section would overcome this scatter problem and thus permit use of smaller internal bore.

Limit switches are provided for breaking the power supply to the motor in the event of exciter lamp failure, or adverse operation of the control. The test specimen is thus protected against irregularities arising in electrical system.

Performance: The control has been found to restrict the pore water movements to somewhat less than 2 mm from the null position. This represents about 1 part in 200,000 of the pore water for Port Mann clay. On a relay closing, the mercury is restored to the null position in about 45 seconds, which allows sufficient time to equalize the pressure at the tip of the probe. Pressure equalization is less critical when measuring pore pressures at the ends of the specimen.

Operation: The photo-cell unit must be positioned on the capillary tube in such a manner that the mercury at the null position appears in view at the observation slit. The controls R_5, R_6, R_{10}, R_{11}, are then adjusted to give the optimum sensitivity to movements of the mercury column. A warming-up period of 15 - 30 minutes is required to obtain stable operation of the amplifier.

Power Pack: The power pack follows conventional design, and supplies 300 volts regulated output to the amplifier. Two

voltage regulator tubes incorporated in the power pack provide a stable output voltage - independent of the load and moderate fluctuations in main's potential.

Possible Improvements: Although the sensitivity of the control unit to changes in mercury level is adequate for the present purpose, there appears to be little difficulty in modifying the apparatus to obtain even greater sensitivity. For instance, replacing the selenium cells by the new silicon type photo cells, would increase the sensitivity considerably. However, the latter cells are more expensive, and until recently were not available commercially. An optical system replacing the present observation slit would perhaps be more effective in checking the operation of the unit.

In order that the control apparatus may be of service in tests on all soil types, a variable speed gearbox is preferable to the present system of fixed gearing between motor and auxiliary control cylinder.

A smaller bore capillary would be of assistance in the deairing operation.

The complete installation is shown
in the photographic supplement.

CHAPTER VII.

SUMMARY OF CONCLUSIONS

(a) The samples were not saturated on receipt at the laboratory. B values indicate that the samples were probably saturated in the loading stage of the shear tests.

(b) The soil is an extrasensitive clay with sensitivity indices in the range 30 - 80. Some leaching of the natural deposit appears to have occurred.

(c) A slow build-up of pore pressure was observed in all triaxial tests. The rate of build-up was least for axial loading. End restraint retarded the build-up of pore pressure at top and base of specimen; a slower rate being recorded at the ends than at the centre. The pore-pressure lag in saturated specimens has been attributed to plastic deformations of the adsorbed layers surrounding the particles. Plastic deformation is assumed to lead to a realignment of the particles with time - an effect most noticeable for applications of unidirectional stresses.

(d) In triaxial tests, the specimens failed on either one or

two shear planes. The strains at failure ranged from 3 to 7%. Values of the strength parameters are as follows:

$$c' = 3 \text{ lb./sq. in.}$$
$$\phi' = 21^\circ$$
$$c_u = 4.5 \text{ lb./sq. in.}$$
$$\phi_u = 9$$

The true parameters could not be derived from the results of the shear tests.

(e) The coefficient of permeability was estimated at 4.7×10^{-7} inches per minute - a value to be expected in clays of this type.

(f) Side drains are not effective when subjected to high cell pressures.

(g) The automatic control provides satisfactory regulation of the pore water movements in triaxial tests on clayey soils.

APPENDIX I.

The following data was supplied by R. A. Spence, Consulting Engineers. Results of vane tests:

BORING NO.	DEPTH BELOW GROUND LEVEL	SHEARING RESISTANCE UNDISTURBED lb./sq.ft.	SHEARING RESISTANCE REMOULDED lb./sq.ft.
BS2	135'-6"	1930	30
"	136'-3"	1860	60
"	137'-0"	2300	30
BS1B	143'-0"	2275	30
"	143'-9"	2330	60
"	147'-9"	2045	60

BORING NO.	SAMPLE NO.	WATER CONTENT %	LIQUID LIMIT	PLASTIC LIMIT	GRAIN SIZE: MI.T SCALE SAND%	SILT %	CLAY %	DRY DENSITY lb./cu.ft.	ESTIMATED OVERBURDEN PRESSURE: EFFECTIVE lb./sq.in.	DEPTH BELOW GROUND LEVEL
BN23F	21	68.3	66.6	38.8	0	10	90	61.3		
	* 22	66.4	67.4	35.3						137'6" to 138'4"
	* 23	67.6	62.8	34.1						138'4" to 139'2"
	24	65.1						63.8	56.5	
	* 25	66.8								139'6" to 140'0"
	26	57.2	68.5	35.6	0	7	93	67.9		140'6" to 141'4"
	* 27	61.8								
BS2F	* 40	68.1						61.7		147'9" to 148'5"
	* 42	61.3						63.8		148'7" to 149'5"
	43	59.4	63.7	29.4	11	9	80		51.5	
	44	61.4								
	45	57.8								
	* 46	58.1						67.2		151'3" to 152'1"

* Samples available for the tests undertaken for this thesis.

APPENDIX I (Cont'd.)

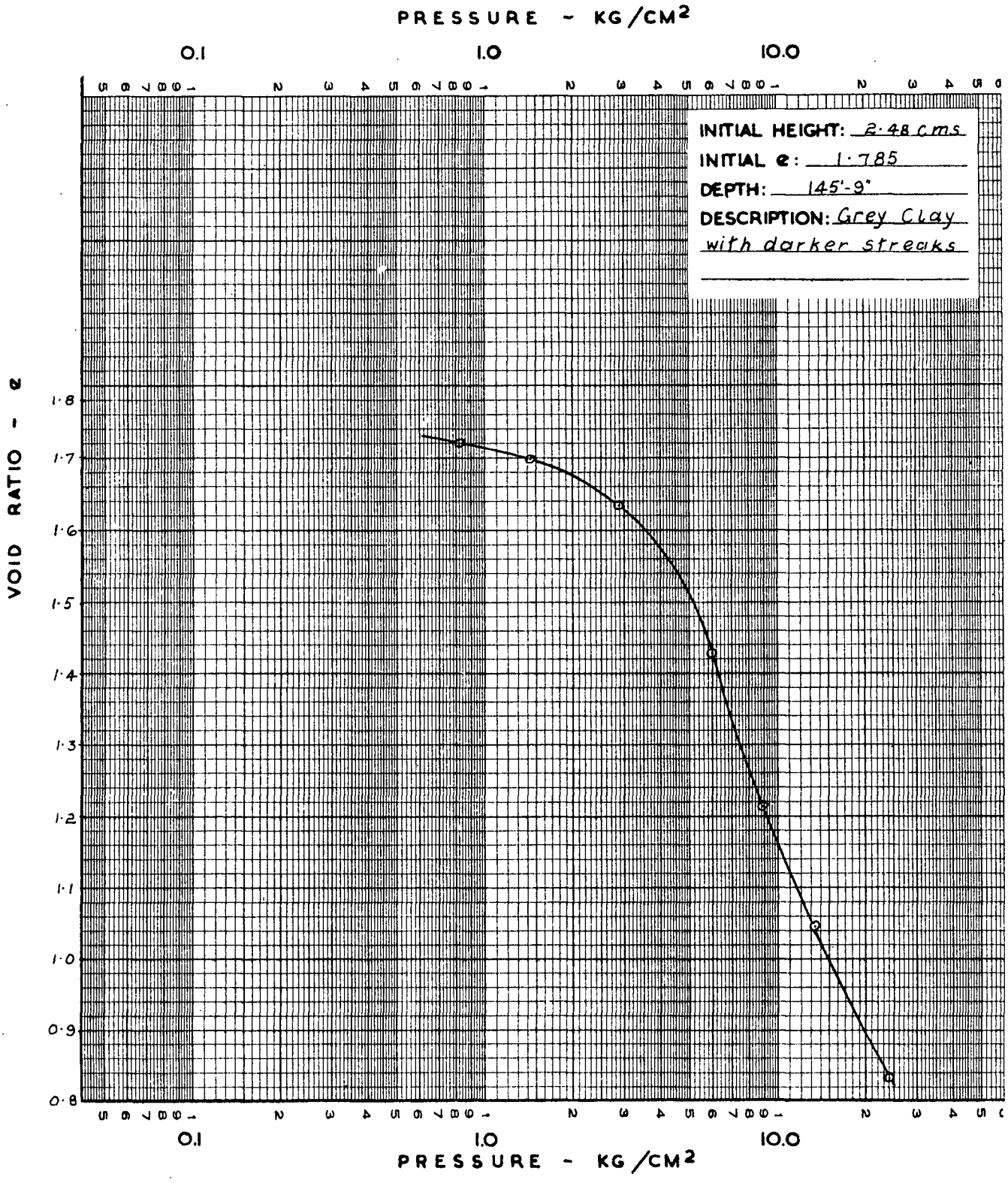

PORT MANN.	CONSOLIDATION TEST	JOB NO:
R.A. SPENCE, P.ENG.	HOLE BN23E SAMPLE 37	DATE:

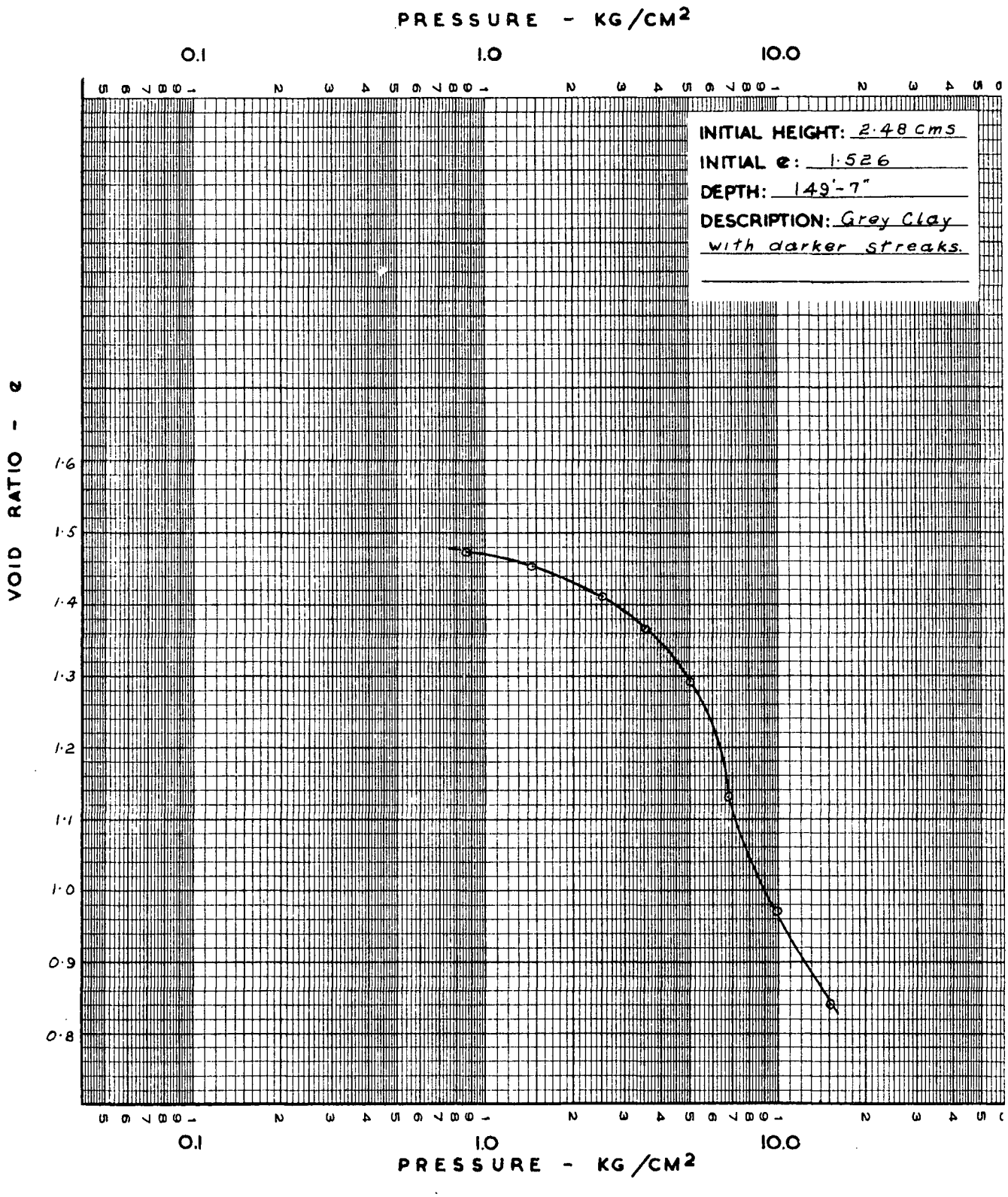

PORT MANN.	CONSOLIDATION TEST	JOB NO:
R.A. SPENCE, P.ENG.	HOLE BS2F. SAMPLE 43	DATE:

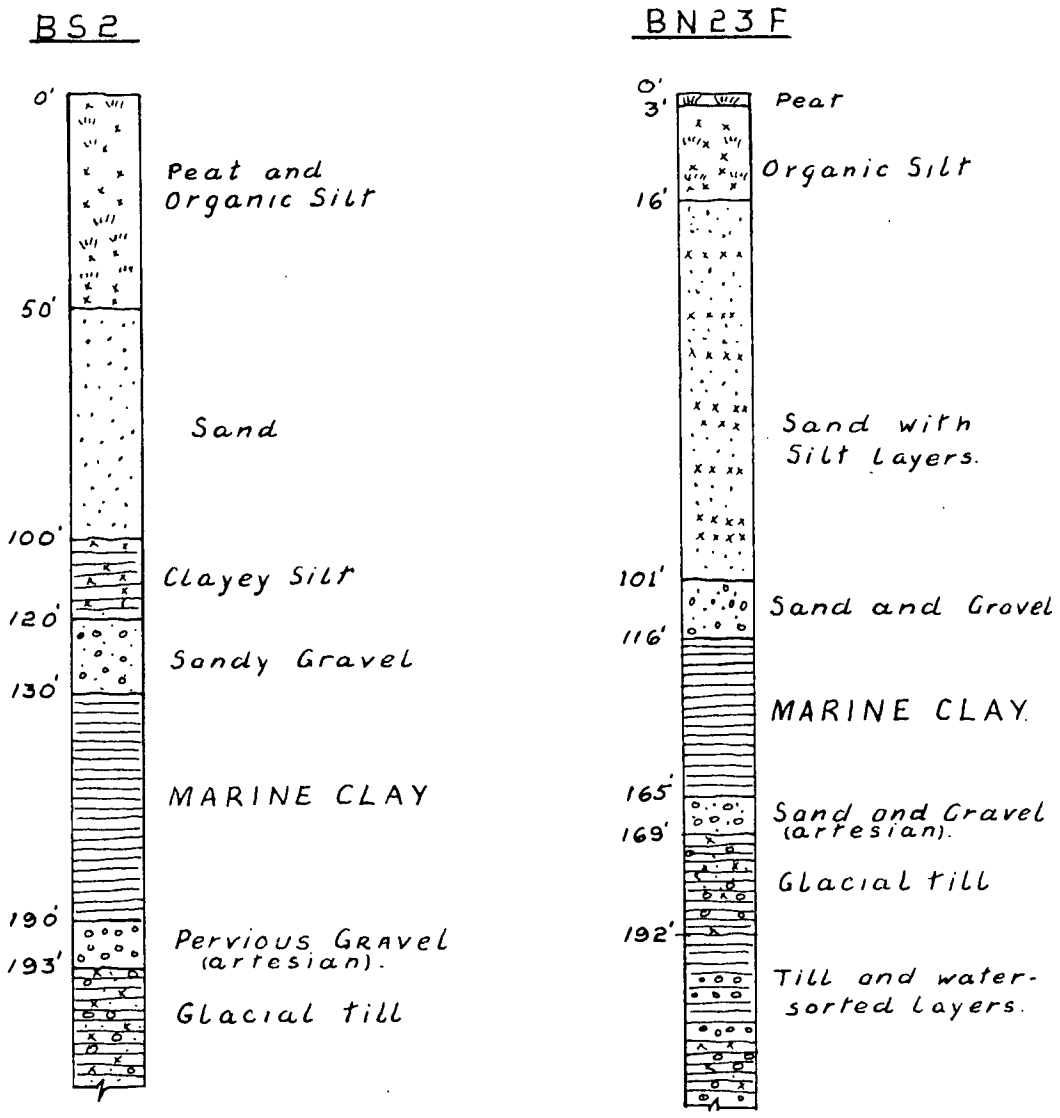

Borehole Logs (idealized).

APPENDIX II

CORRECTION OF COMPRESSIVE STRENGTHS ON BASIS OF EXPERIMENTAL FACTORS

The corrections described below were made to the apparent compressive strengths (deviator stresses) as determined by axial loading.

1. Area Correction. The cross sectional area was corrected, for both the effects of drainage and deformation of the specimen, in accordance with the expression:

$$a = \frac{a_o \left(1 - \frac{\Delta V}{V}\right)}{1 - \epsilon}$$

Where (a) denotes the area on which true deviator stress is calculated $[ins^2]$

a_o denotes the initial area $[ins^2]$

ΔV denotes volume reduction by drainage $[ins^3]$

V denotes initial volume of specimen $[ins^3]$

ϵ denotes axial strain $[ins/in]$

The area correction was ignored once a shear plane in the specimen became visible.

2. Rubber Membrane Correction. According to Bishop and Henkel (1957) only the axial stresses in the triaxial test need be corrected for membrane restraint. The correction to be applied

to cylindrical specimens is then given by the expression:

$$(\sigma_1 - \sigma_3)_m = (\sigma_1 - \sigma_3) - \frac{4wE_m}{D}\epsilon$$

Where $(\sigma_1 - \sigma_3)_m$ denotes the corrected deviation stresses

$(\sigma_1 - \sigma_3)$ denotes the apparent deviator stress

w denotes the thickness of membrane(s) [ins]

E_m denotes Young's modulus of rubber [lbs./ins.^{2}]

ϵ denotes the strain [ins./in.]

D denotes diameter of specimen at strain ϵ

Calculations based on Fig. 18 showed this correction to be in the order of 0.25 lb./sq.in. at 5% strain, for the twin membranes employed in the tests.

3. Drain Corrections. The correction for restraint arising from filter drains is also made to the axial stresses. It is not dependent on the strain however and is normally considered to be less than 1 lb./sq.in., Bishop and Henkel (1957).

A nominal correction of 1 lb./sq.in. was applied to the axial stresses to include the effects of both rubber membranes and filter drains. No correction was deemed necessary for plunger friction, but the weight of the end fittings were included in the axial loads.

APPENDIX III.

Calculations based on data obtained in Test 6.

1. Coefficient of Consolidation (C_v)

Coefficient of consolidation based on pore pressure vs. time relationship:

$$C_v = \frac{T_v H^2}{t_{50}} *$$

$$= \frac{0.38 \times 2.5)^2}{21^2}$$

$$= 0.0054 \text{ ins}^2/\text{min}$$

Where T_v – time factor of 0.38

H – length of drainage path:

2.5" neglecting initial deformations

t_{50} – time for 50% consolidation:

$(21)^2$ minutes from Graph 4-15.

---

* "Fundamentals of Soil Mechanics", Taylor (1948), pp.235.

Coefficient of consolidation based on volume change vs. time relationship, assuming radial and end drainage.

$$C_v = \frac{\pi H^2}{100 t_{100}} \quad **$$

$$= \frac{3.14 \times (2.5)^2}{100 \times (27.5)^2}$$

$$= .00026 \text{ ins}^2/\text{min}$$

Where $H = 2.5''$ as before

t_{100} – time for 100% primary consolidation, Bishop and Henkel (1957).

$t_{100} = (27.5)^2$ minutes from Graph 4-15.

** "The Triaxial Test", Bishop and Henkel (1957), pp 126.

Coefficient of consolidation based on volume change vs. time relationship, assuming end drainage only.

$$C_v = \frac{\pi H^2}{4t_{100}} \quad **$$

$$= \frac{3.14 \times (2.5)^2}{4 \times (27.5)^2}$$

$$= 0.0065 \text{ ins}^2/\text{min.}$$

Where symbols have same meaning as those on preceding page.

Calculation of pore pressure parameter A at failure.

$$A_f = \frac{\Delta u - B(\Delta\sigma_3)}{B(\Delta\sigma_1 - \Delta\sigma_3)_f}$$

$$= \frac{30.25 - 40(0.51)}{0.51 \times 19.1}$$

$$= 1.01$$

BIBLIOGRAPHY

A. Books

Baver, L. D.,1956, Soil Physics, 3rd. ed., New York, Wiley.

Bishop, A.W. and Henkel, D.J., 1957, The Triaxial Test. London: Edward Arnold.

Lambe, T.W., 1951, Soil Testing for Engineers. New York: John Wiley.

Taylor, D.W., 1948, Fundamentals of Soil Mechanics. New York: John Wiley.

Terzaghi, K. and Peck, R.B., 1948, Soil Mechanics in Engineering Practice. New York: John Wiley.

Tschebotarioff, G.P., 1951, Soil Mechanics, Foundations and Earth Structures. New York: McGraw Hill.

B. Journals and Reports

Bishop, A.W. and Eldin, G., 1950, "Undrained Triaxial Tests on Saturated Sands and their Significance in the General Theory of Shear Strength" Geotechnique, 2, 13-32.

Bjerrum, L., 1954, "Geotechnical properties of Norwegian Marine Clays" Geotechnique, 4, 49-69.

Burton, L. J., 1956, "A New Device for Automatic Pore-Water Pressure Determination" Civil Engineering and Public Works Review.

Casagrande, A. and Wilson, S.D., 1949, Report to U.S. Waterways Experimental Station.

Grim, R.E., 1959, "Physico-Chemical properties of Soils: Clay Minerals". Jour A.S.C.E. Vol.85 No. SM2. 1998; 1-16.

Lambe, T.W., 1958, "The Structure of Compacted Clay", Jour A.S.C.E. Vol. 84, No. SM2, 1654; 2-32.

Michell, J.K., 1956 "The Importance of Structure to the Engineering Behavior of Clay. Sc.D. Thesis M.I.T.

Penman, A.D.M., 1953, "Shear Characteristics of a Saturated Silt" Geotechnique III: 8, 312-328.

Plantema, G., 1953, "Electrical Pore-Water Pressure Cells: Some Designs and Experiences" Proc. 3rd. Int. Conf. Soil Mech., 1:279-282.

Rendulic, L., 1937, "Ein Grundgesetz der Tonmechanik und sein experimentaler Beweis" Bauingenieur, 18: 459-467.

Rosenquist, I.T., 1959, Physico-chemical Properties of Soils: Soil-Water Systems. Jour A.S.C.E. Vol.85, No. SM2. 2000; 31-52.

Rowe, P.W., 1959, "Measurement of the Coefficient of Consolidation of Lacustrine Clay". Geotechnique IX: 3, 107-118.

Skempton, A.W., 1954, Geotechnique 4 pp 143-147.

Skempton, A.W., and Bishop, A.W., 1950. "The Measurement of the Shear Strength of Soils". Geotechnique II: 2,90-108.

Skempton, A.W., and Bishop, A.W., 1954, "Soils" Building Materials, their Elasticity and Inelasticity. Amsterdam: North-Holland Publishing Company.

Skempton, A.W., and Northey, R.D., 1952, "The Sensitivity of Clays". Geotechnique 3, 30-54.

Taylor, D.W., 1943, Ninth Progress Report on Shear Research to U.S. Engineers, M.I.T. Publication.

Winterkorn, H.F., 1941, "Study of Changes in Physical Properties of Putnam Soil Induced by Ionic Substitution". Proc. Highway Res. Bd. 21, 415-434.

SPECIMEN PREPARATION

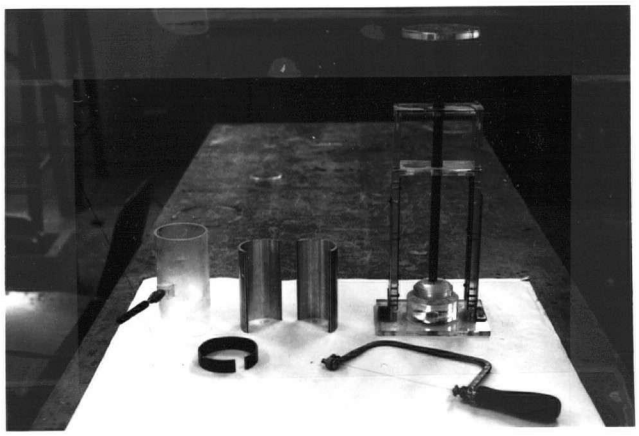

Equipment for
Preparing Specimen.

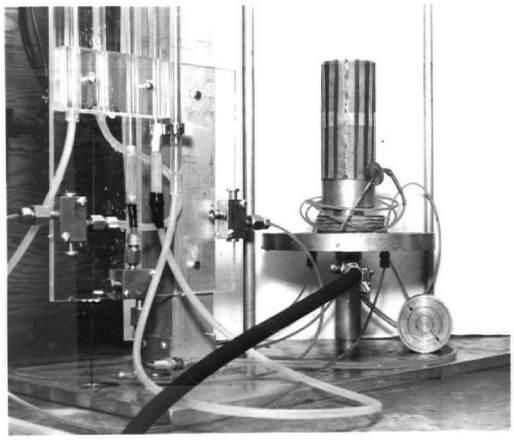

Specimen with
Side Drains
in Position.

SPECIMEN PREPARATION (Cont'd.)

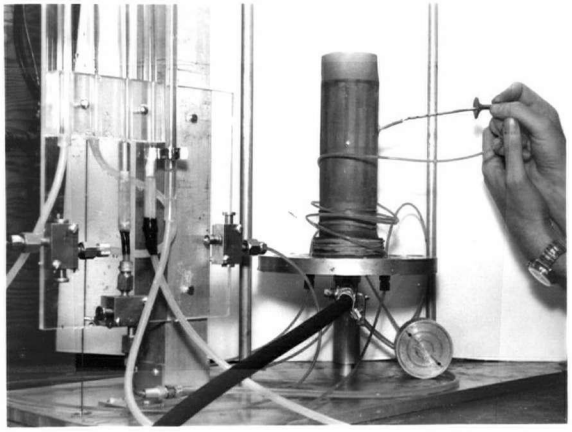

Inserting Probe.

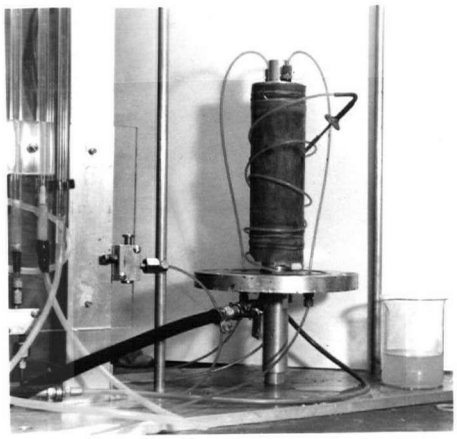

Application of
Twin Membranes
and Seals.

SPECIMEN PREPARATION (Cont'd.)

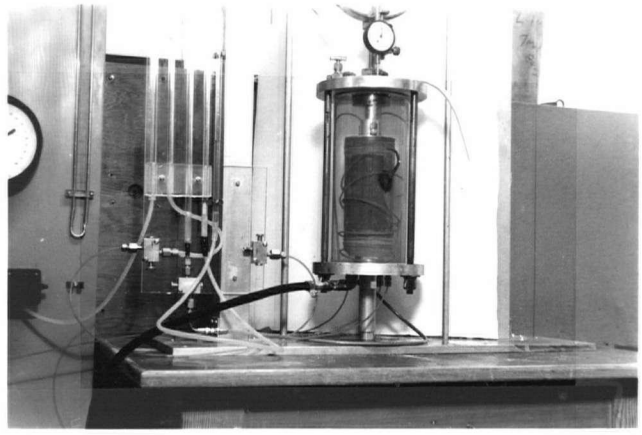

Prepared Specimen.

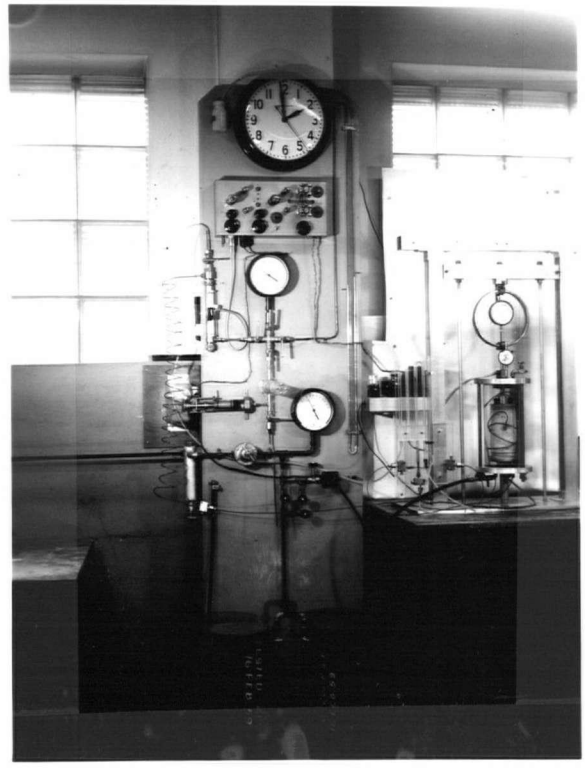

Complete Installation
Showing Triaxial
Machine, Pore—
Pressure Apparatus
and Automatic Control.

Contains: 20 Graphs
and Original Figures (in page order)
2 master illustrations

Graphs 4-1 - 4-5,
4-7 - 4-8,
4-10 - 4-16,
4-18 - 4-19,
4-21 - 4-24
App 1 p. iii + v.

To follow page 51.

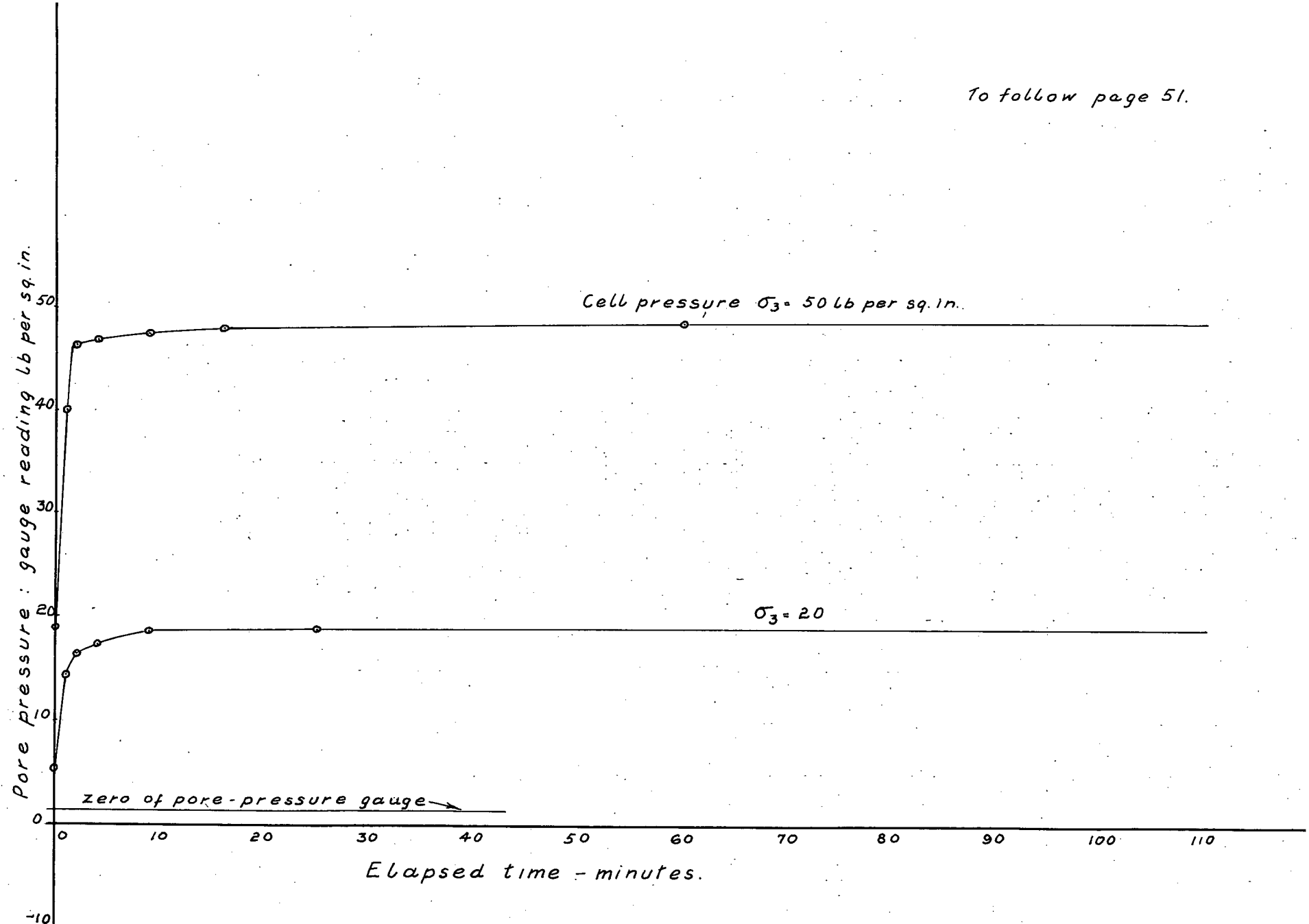

To follow page 54

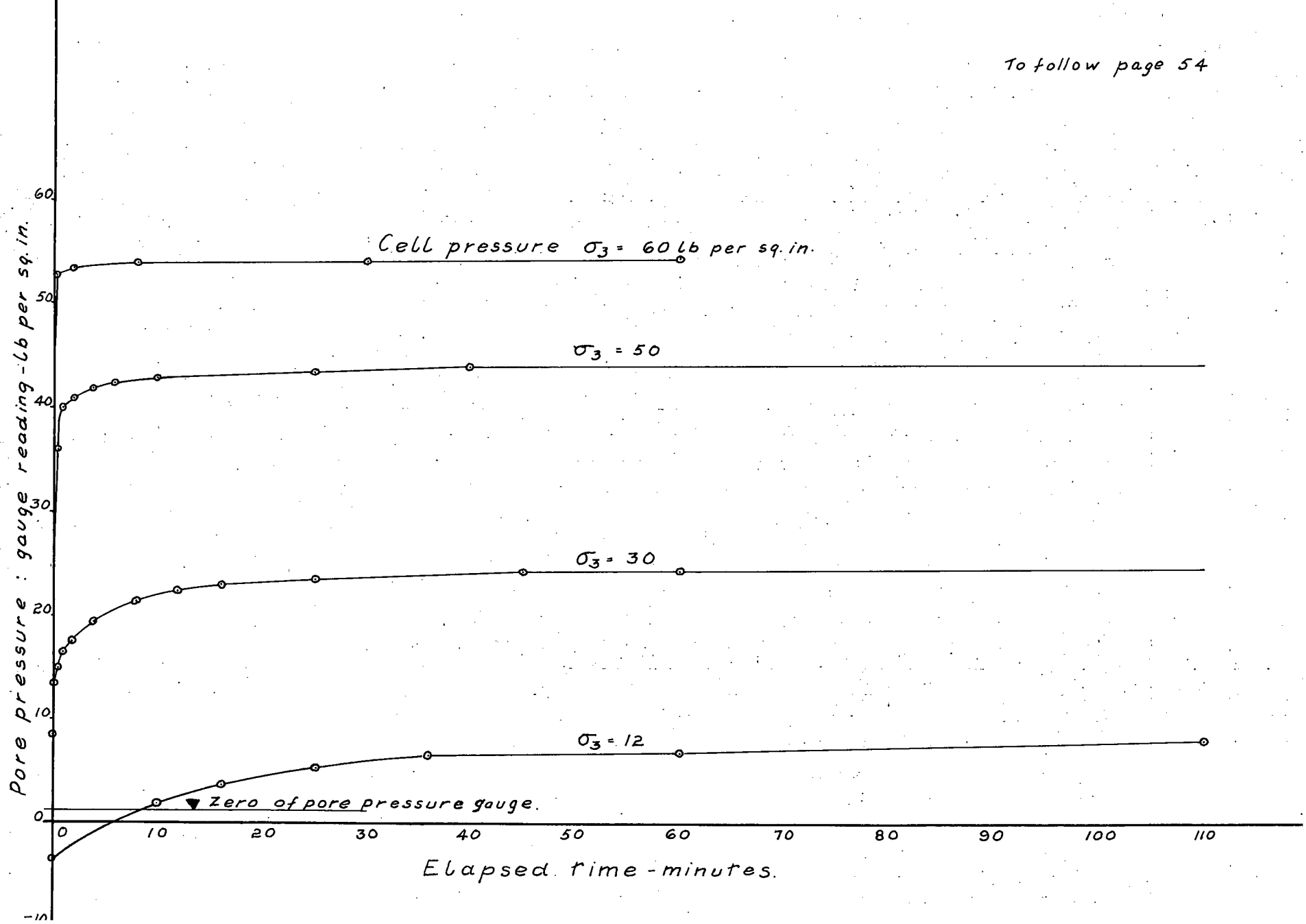

DRAINAGE STAGE - TEST 2.

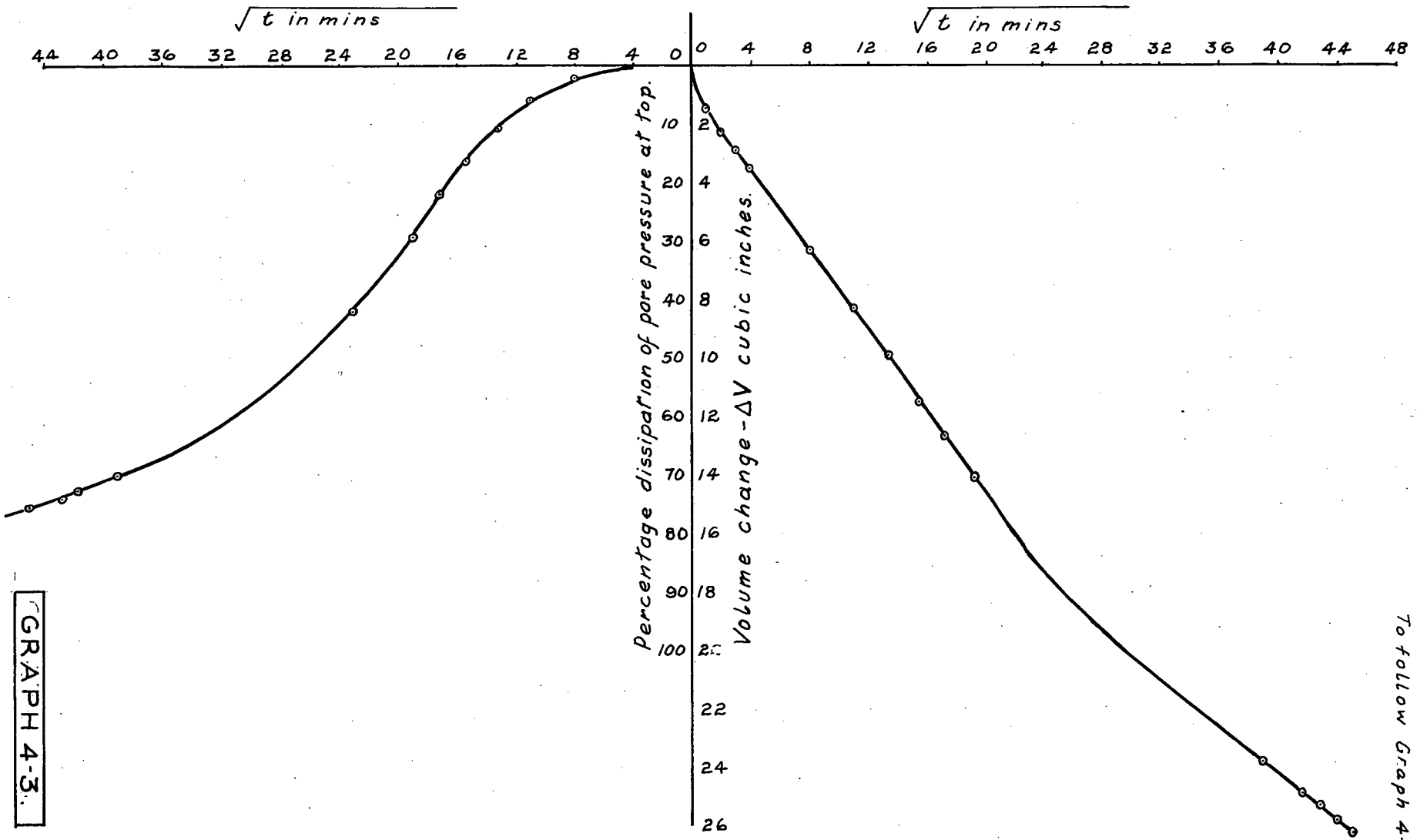

GRAPH 4-3.

To follow Graph 4-2

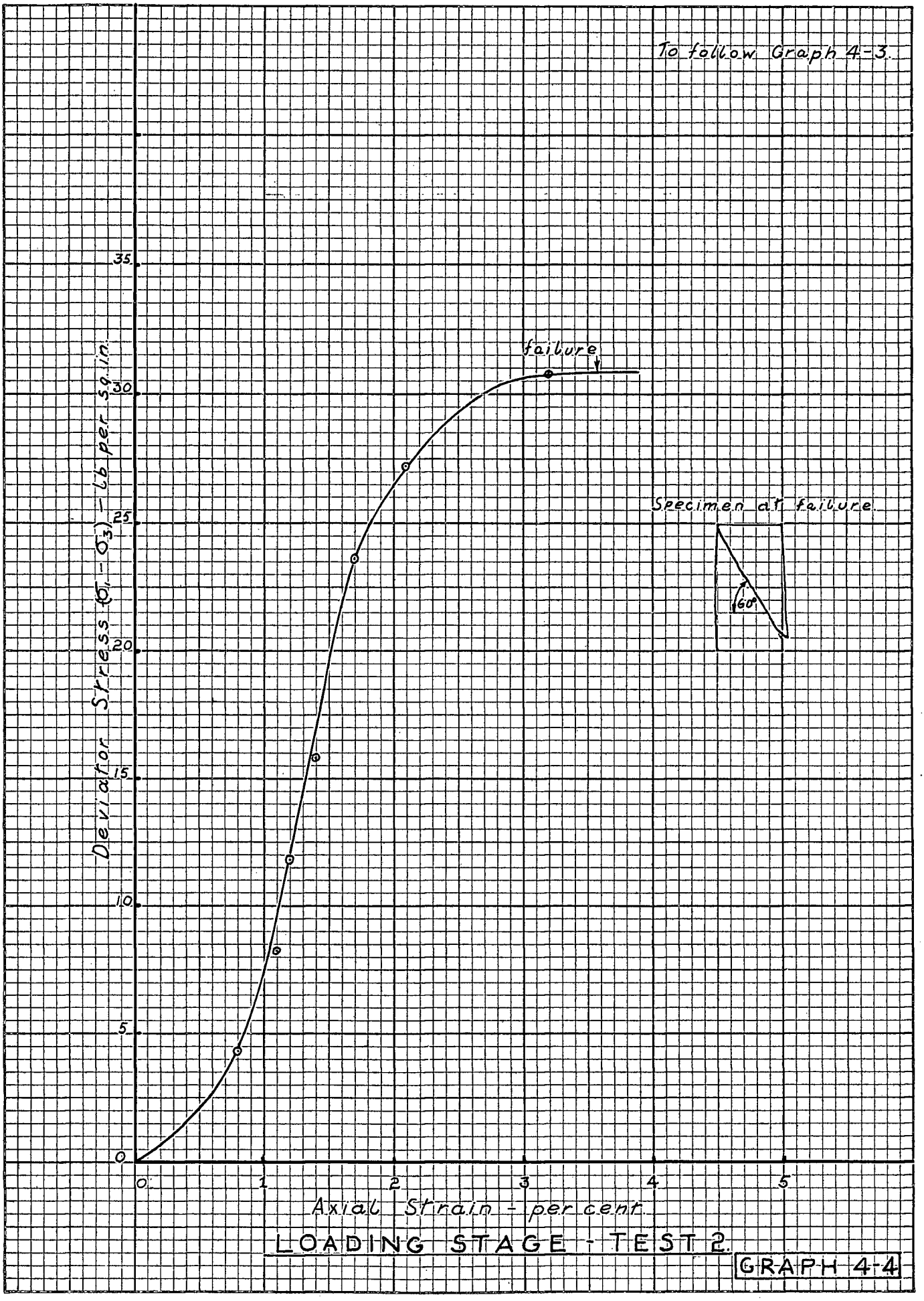

LOADING STAGE - TEST 2.

GRAPH 4-4

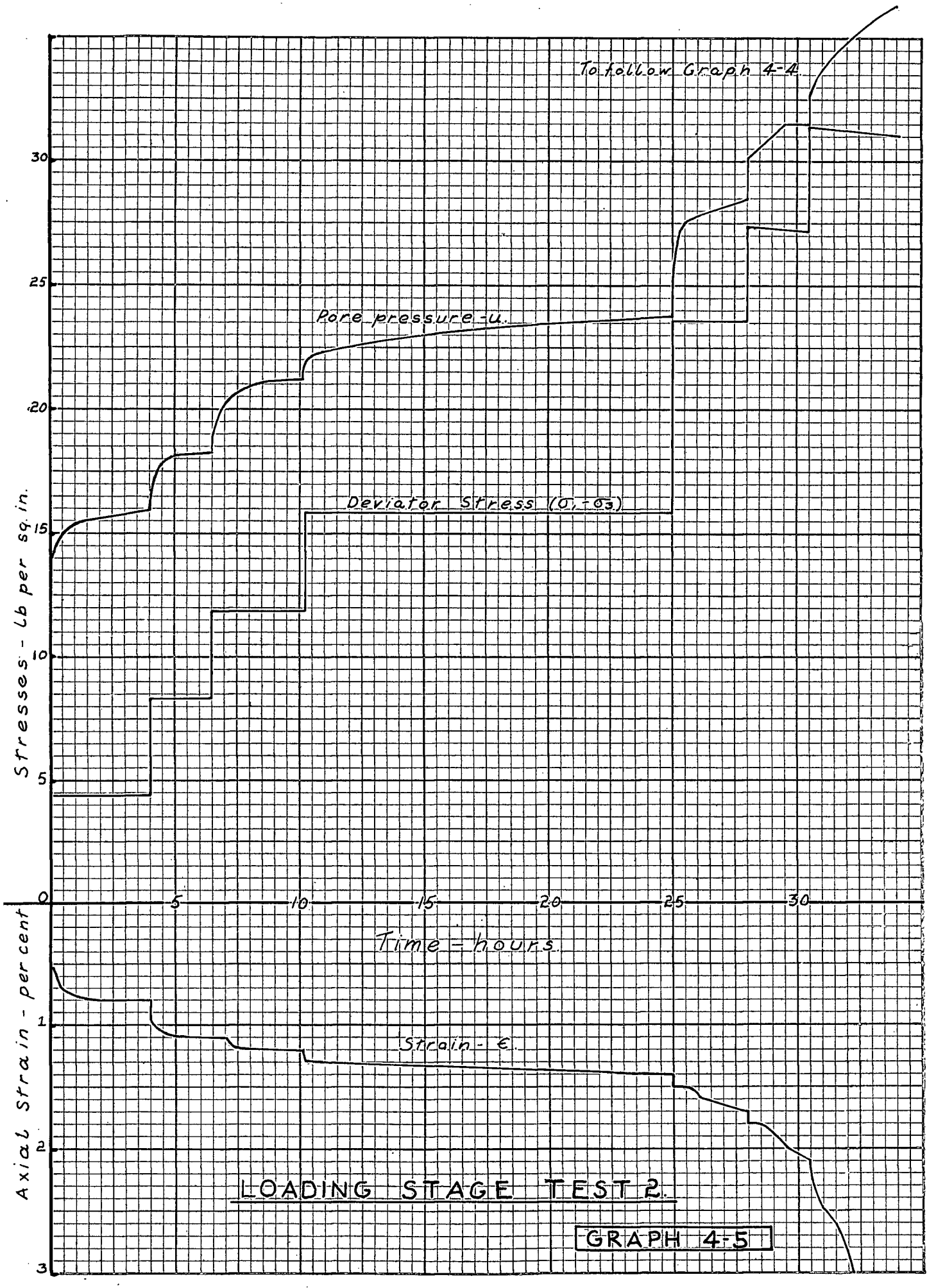

LOADING STAGE TEST 2.

GRAPH 4-5

To follow page 57

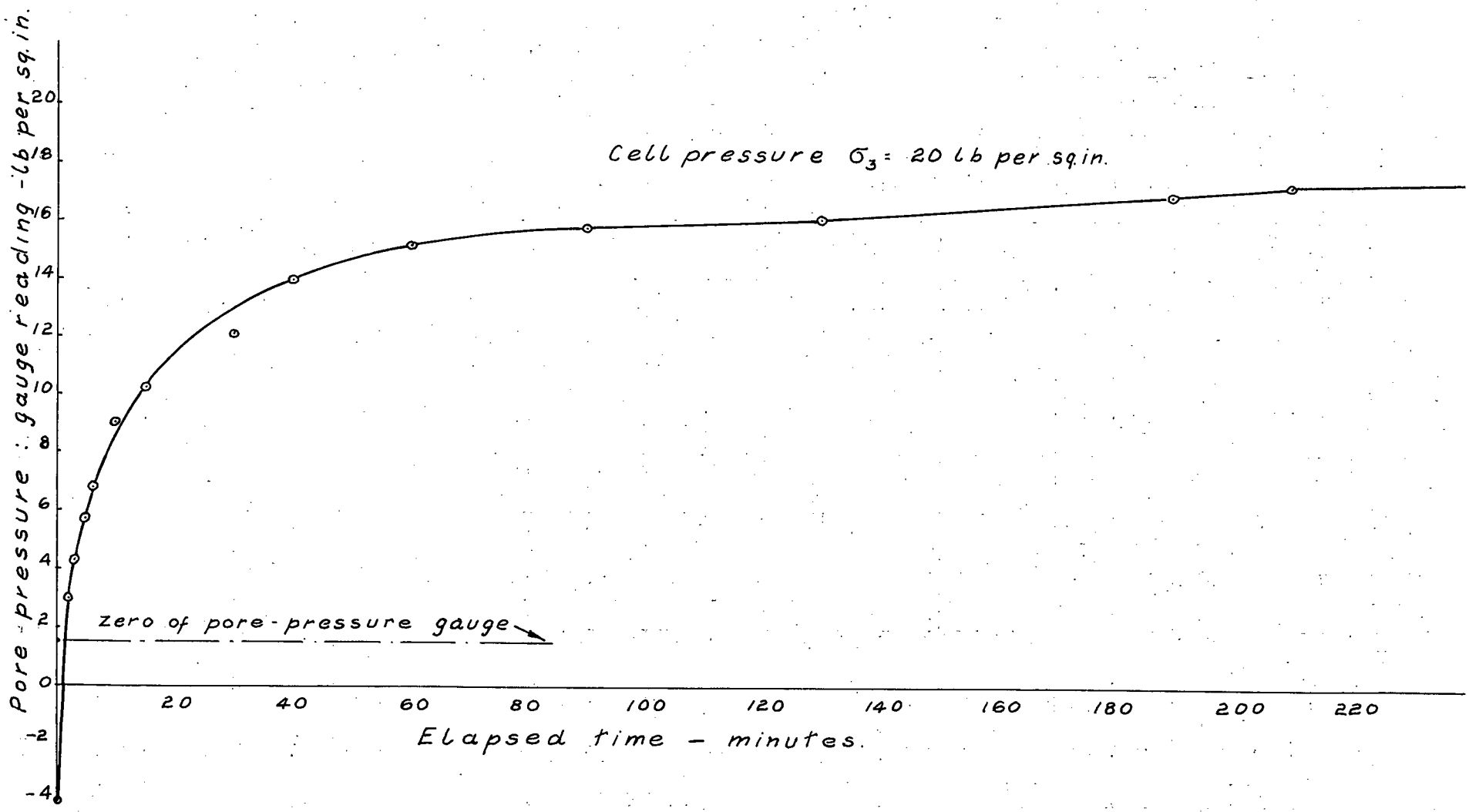

DRAINAGE STAGE - TEST 3.

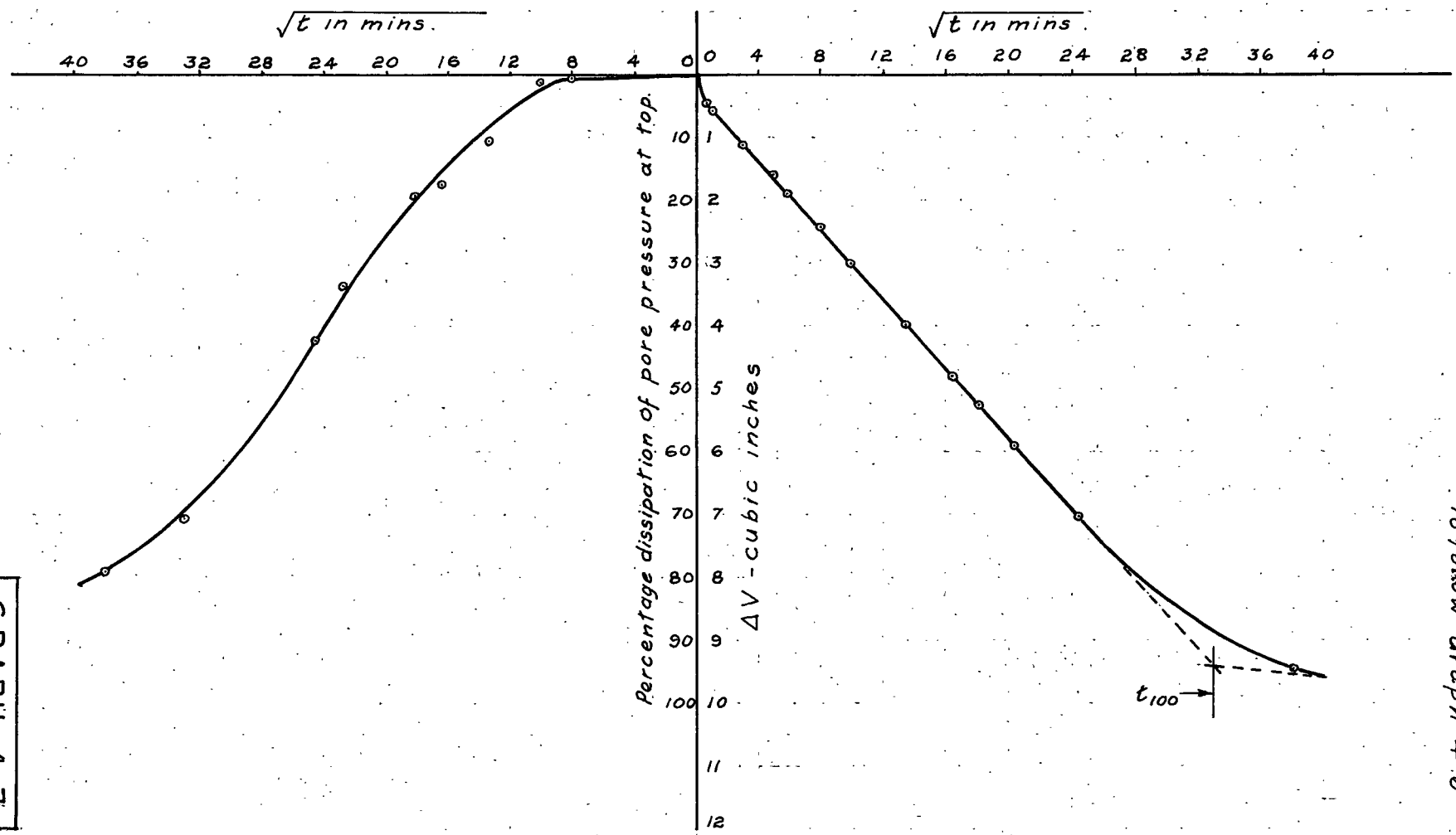

GRAPH 4-7

To follow Graph 4:6

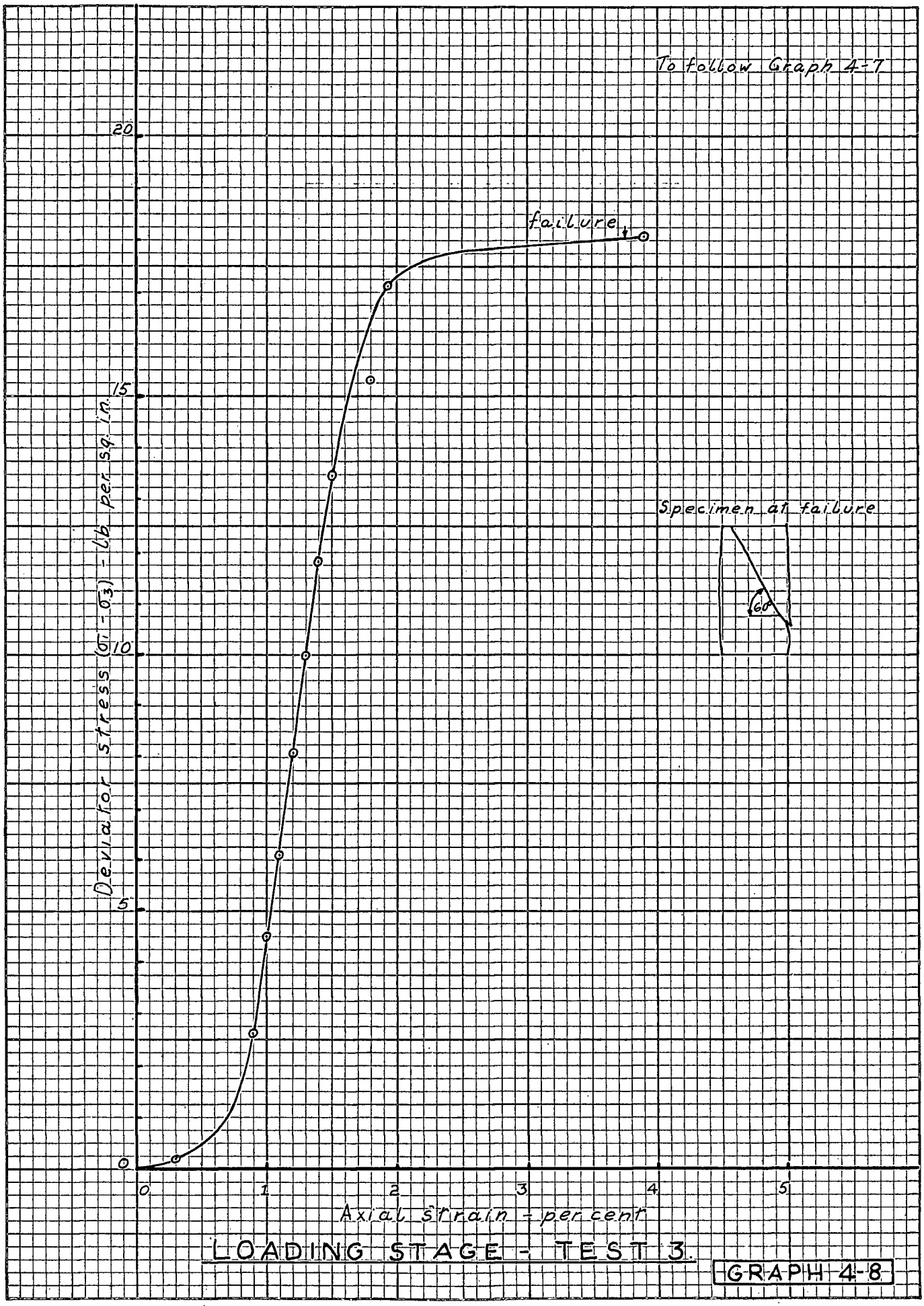

LOADING STAGE - TEST 3.

GRAPH 4-8

To follow page 59

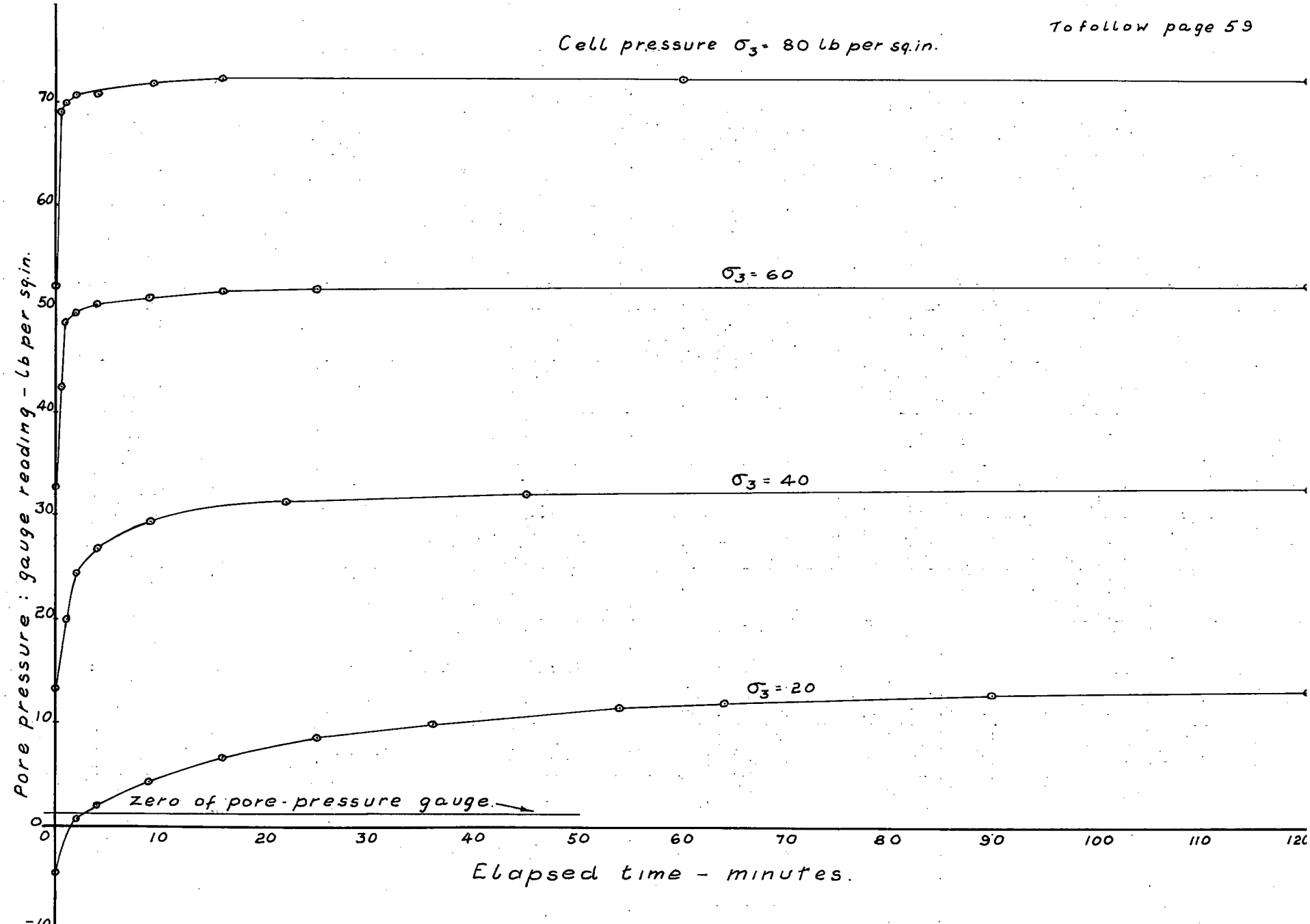

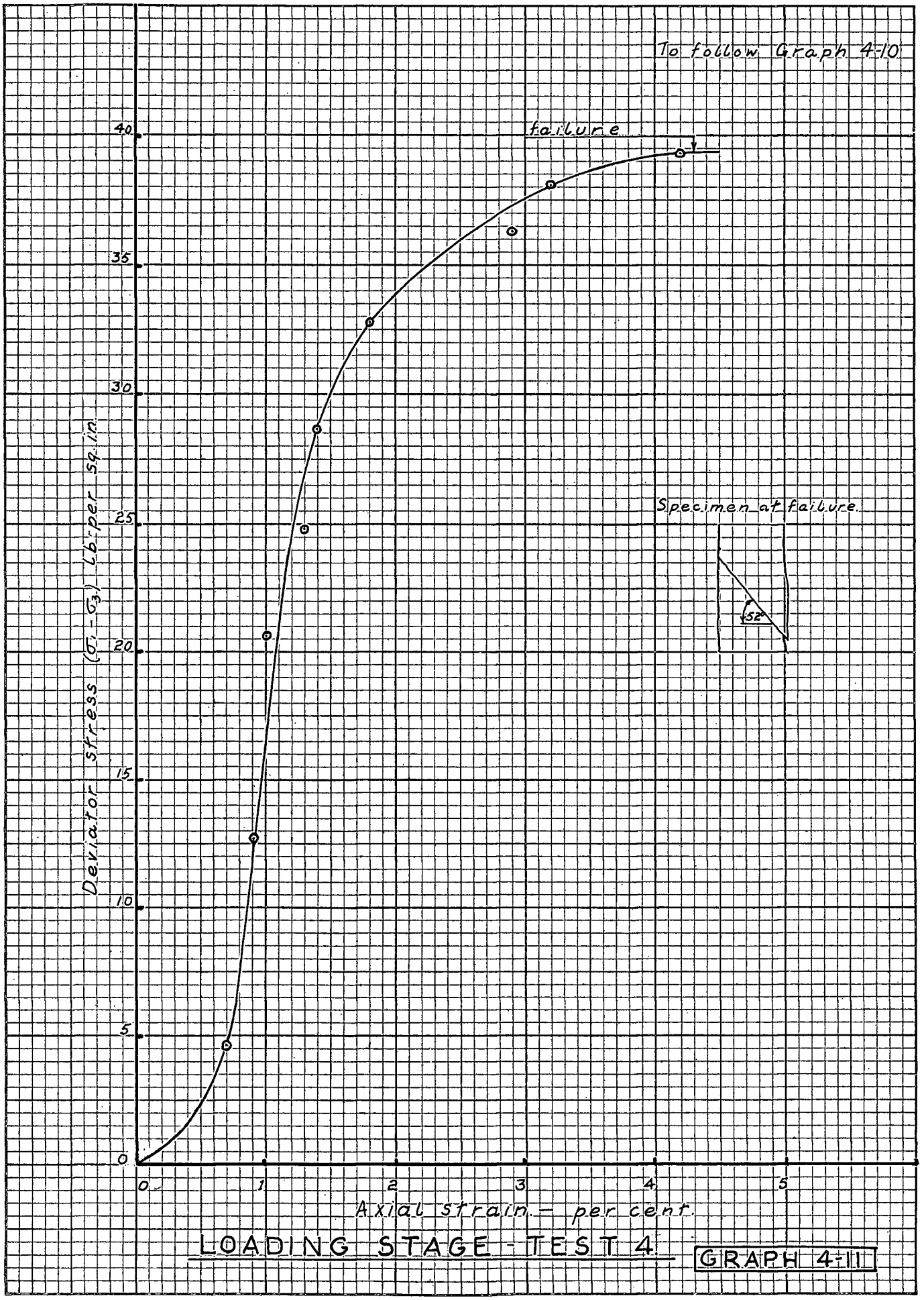

LOADING STAGE - TEST 4

GRAPH 4-11

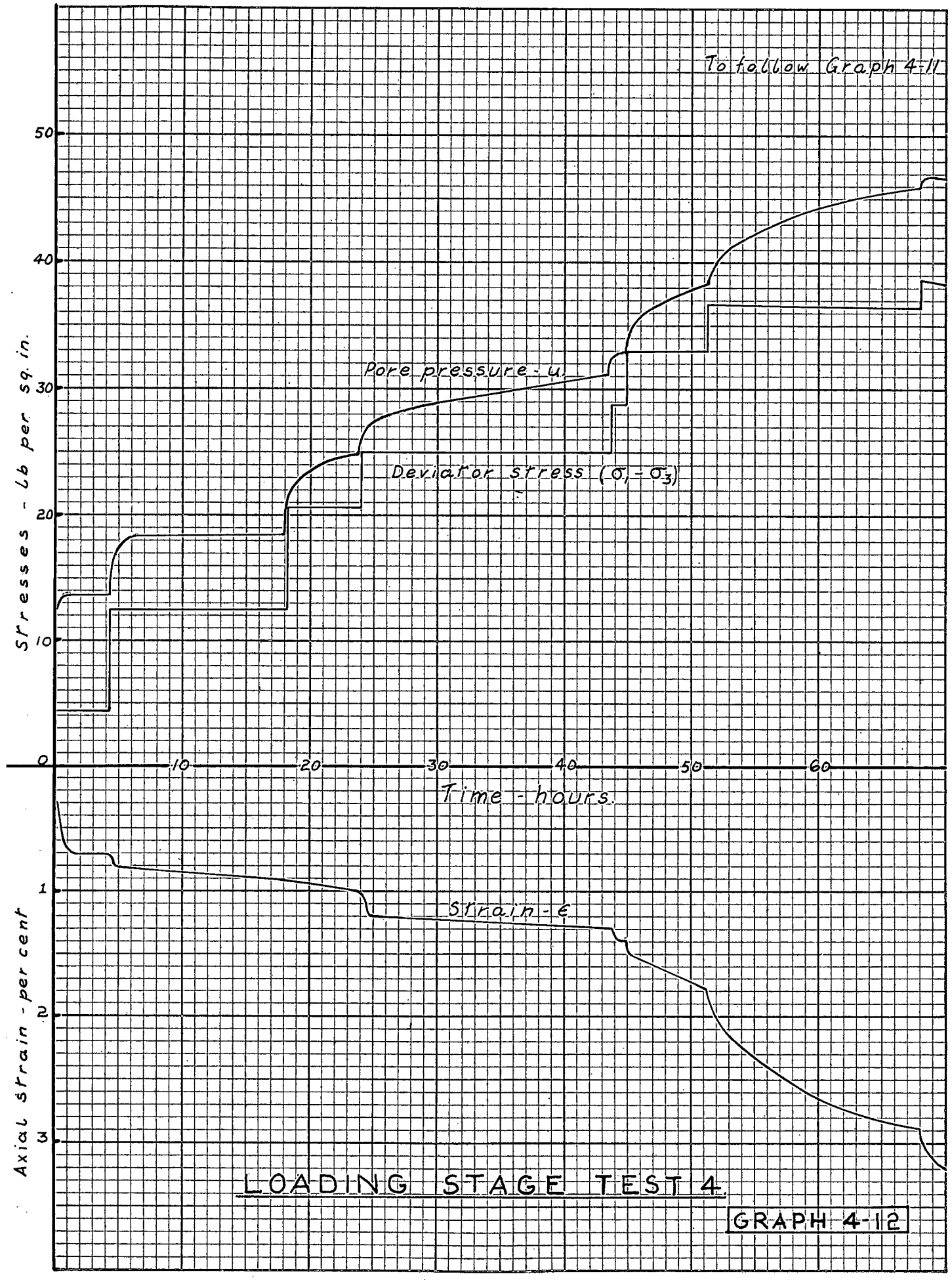

LOADING STAGE TEST 4.

GRAPH 4-12

To follow page 61

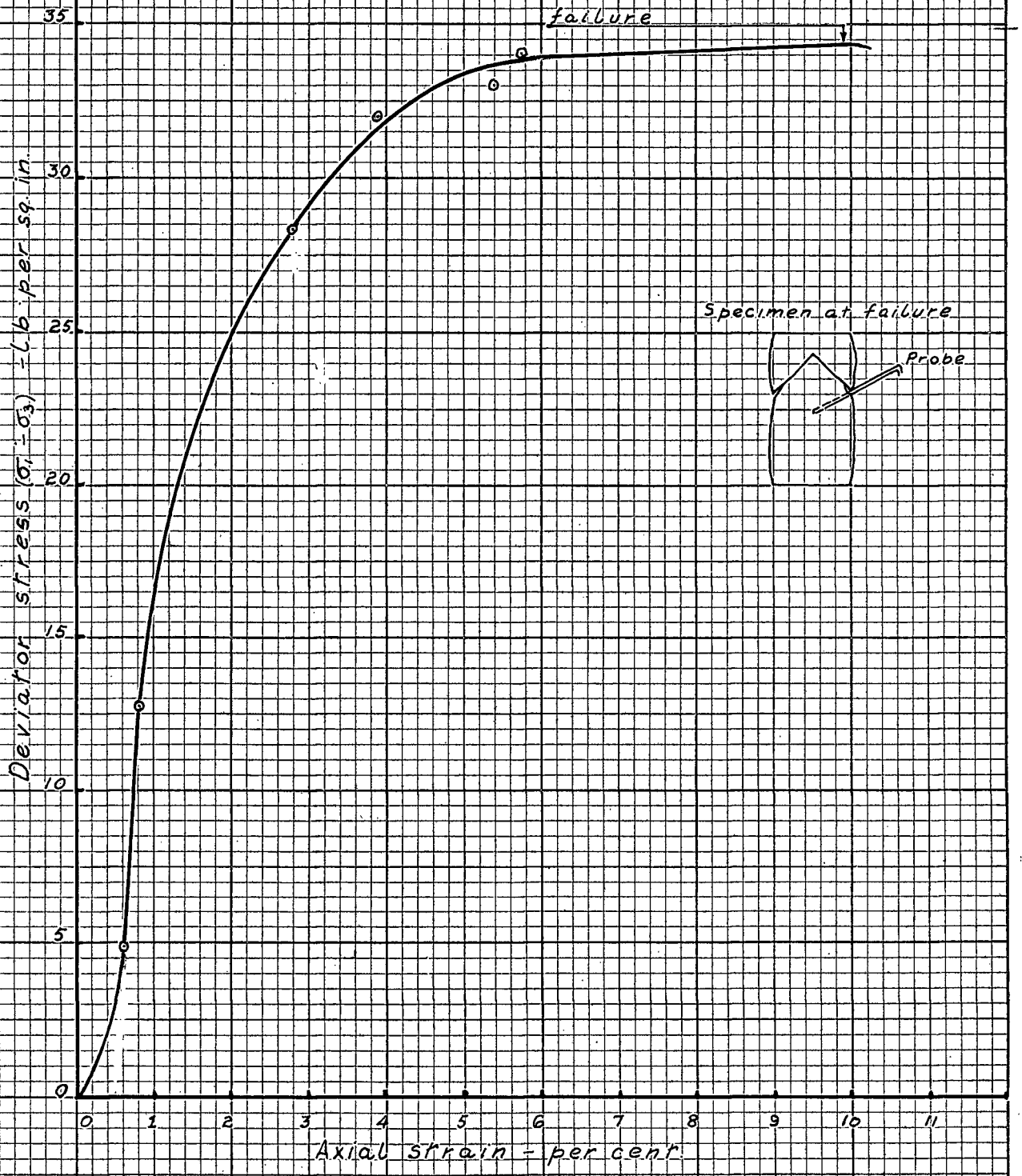

LOADING STAGE - TEST 5.

GRAPH 4-13

To follow page 66

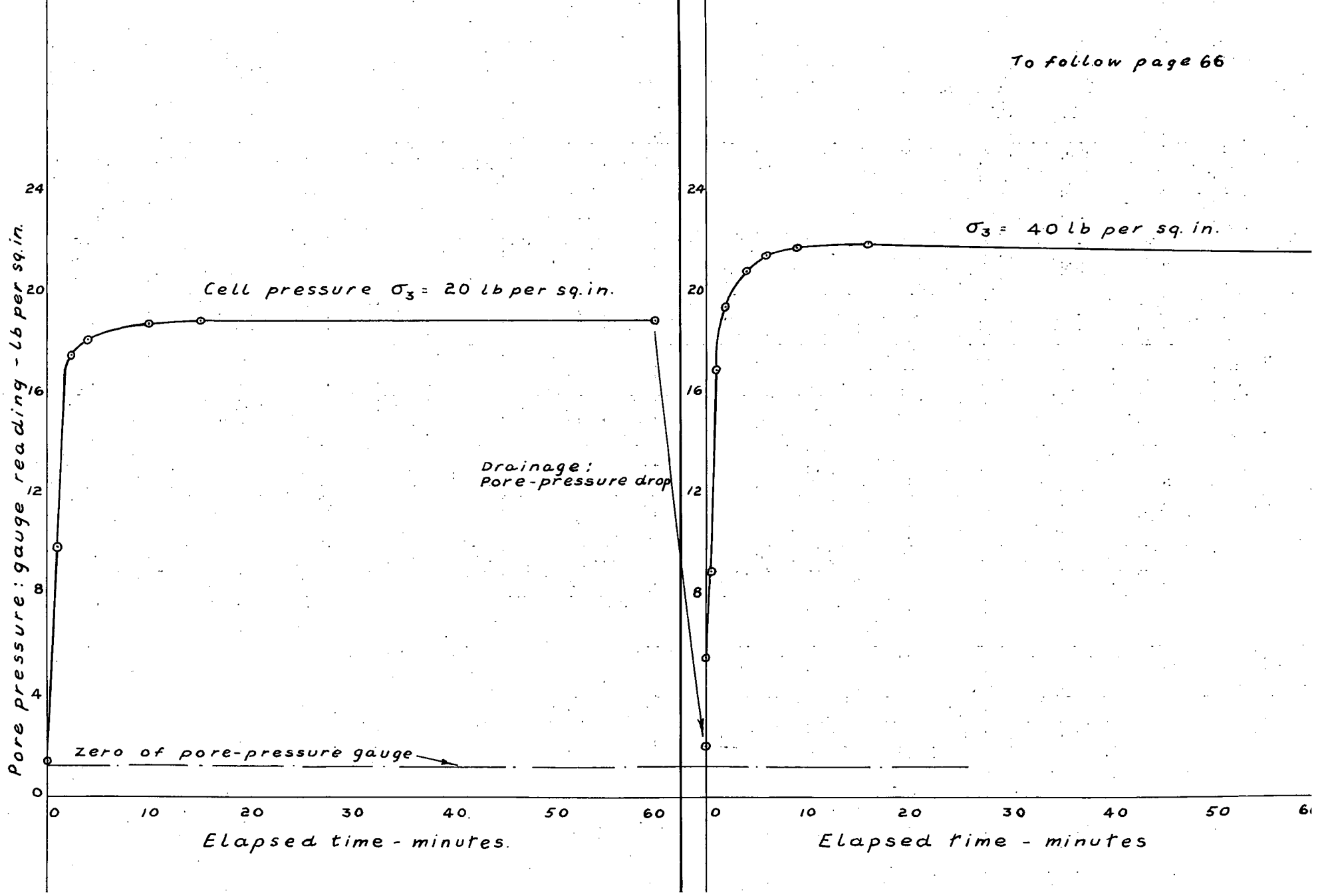

DRAINAGE STAGE - TEST 6.

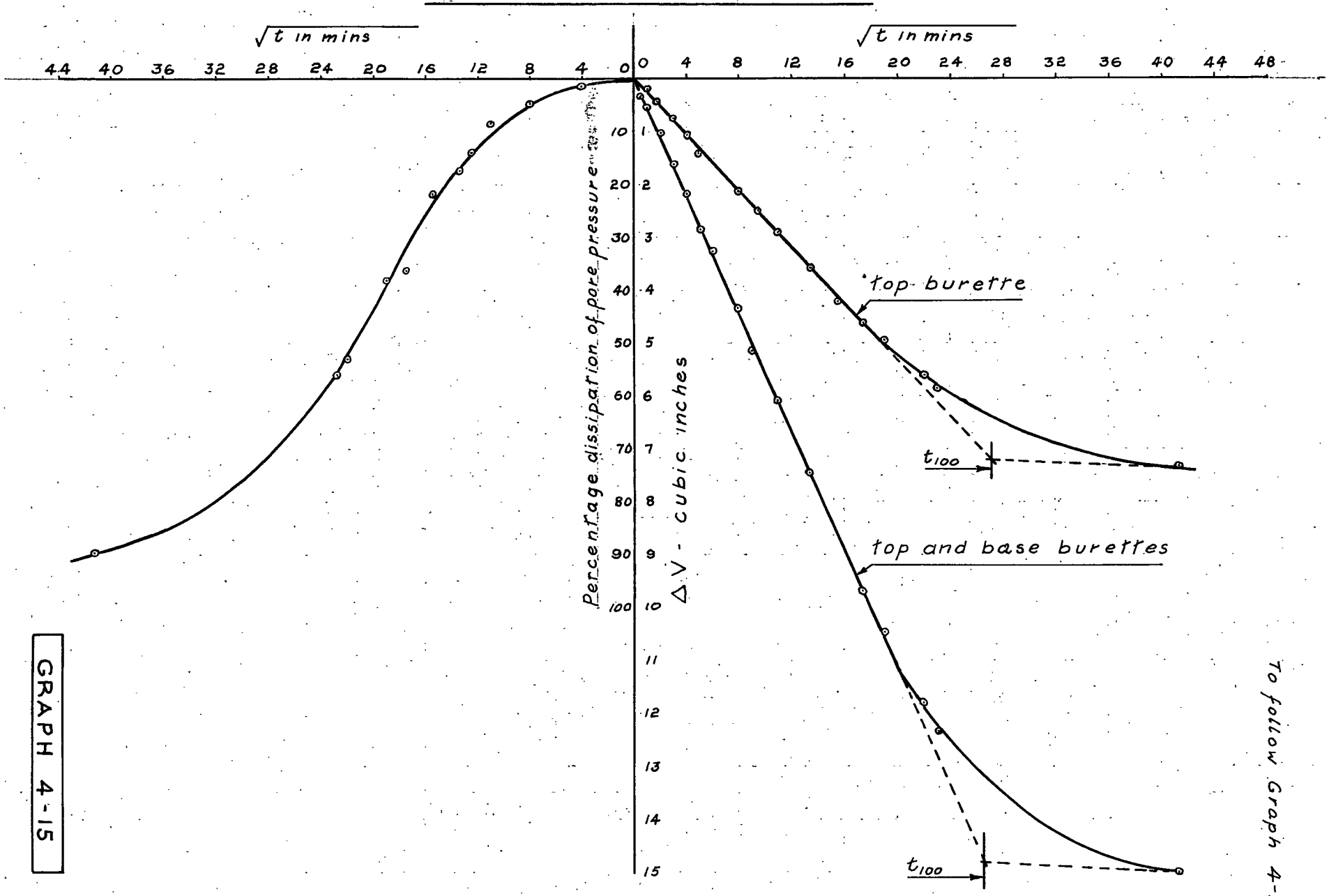

GRAPH 4-15

To follow Graph 4-14

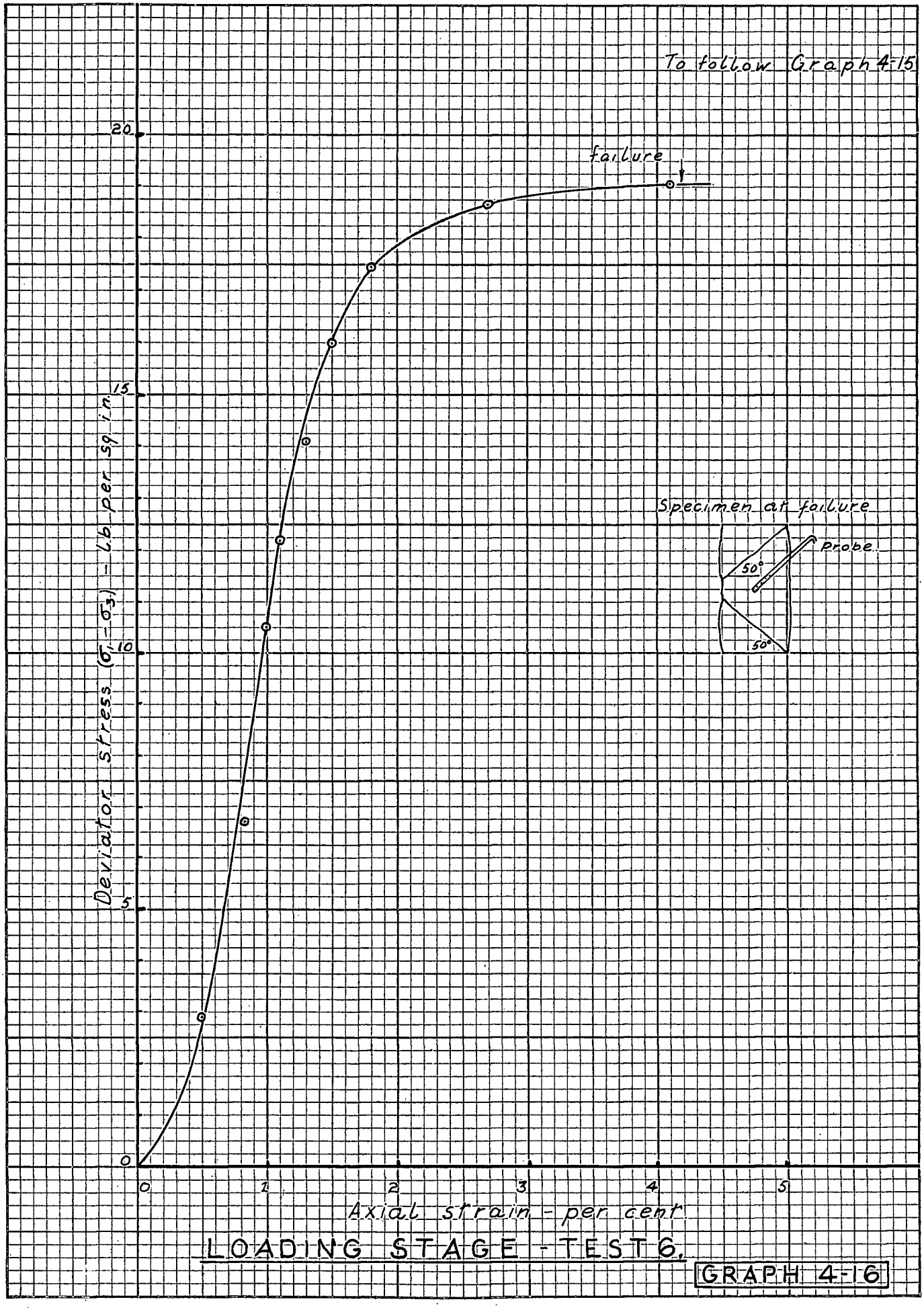

LOADING STAGE - TEST 6.

GRAPH 4-16

To follow page 68.

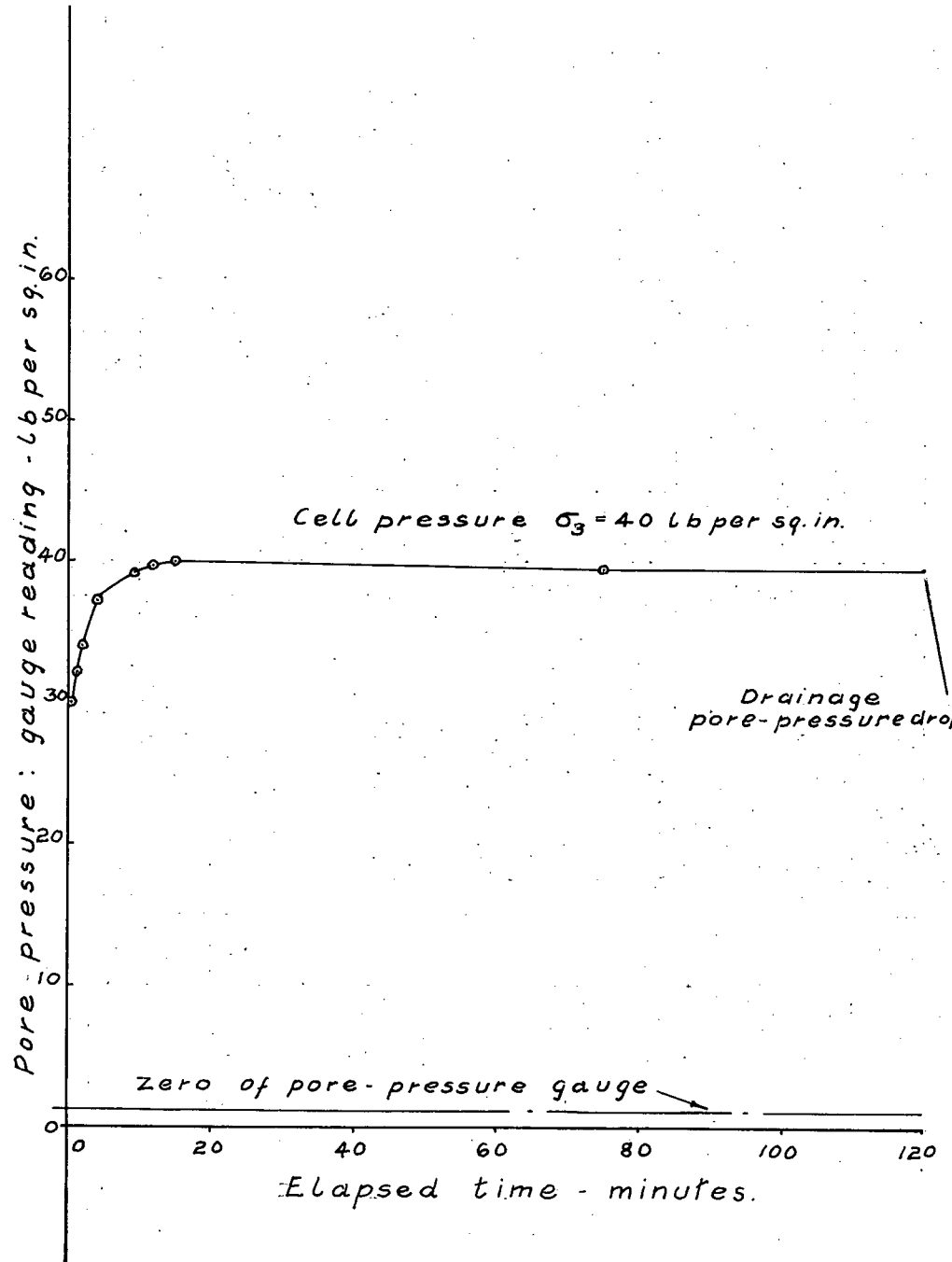

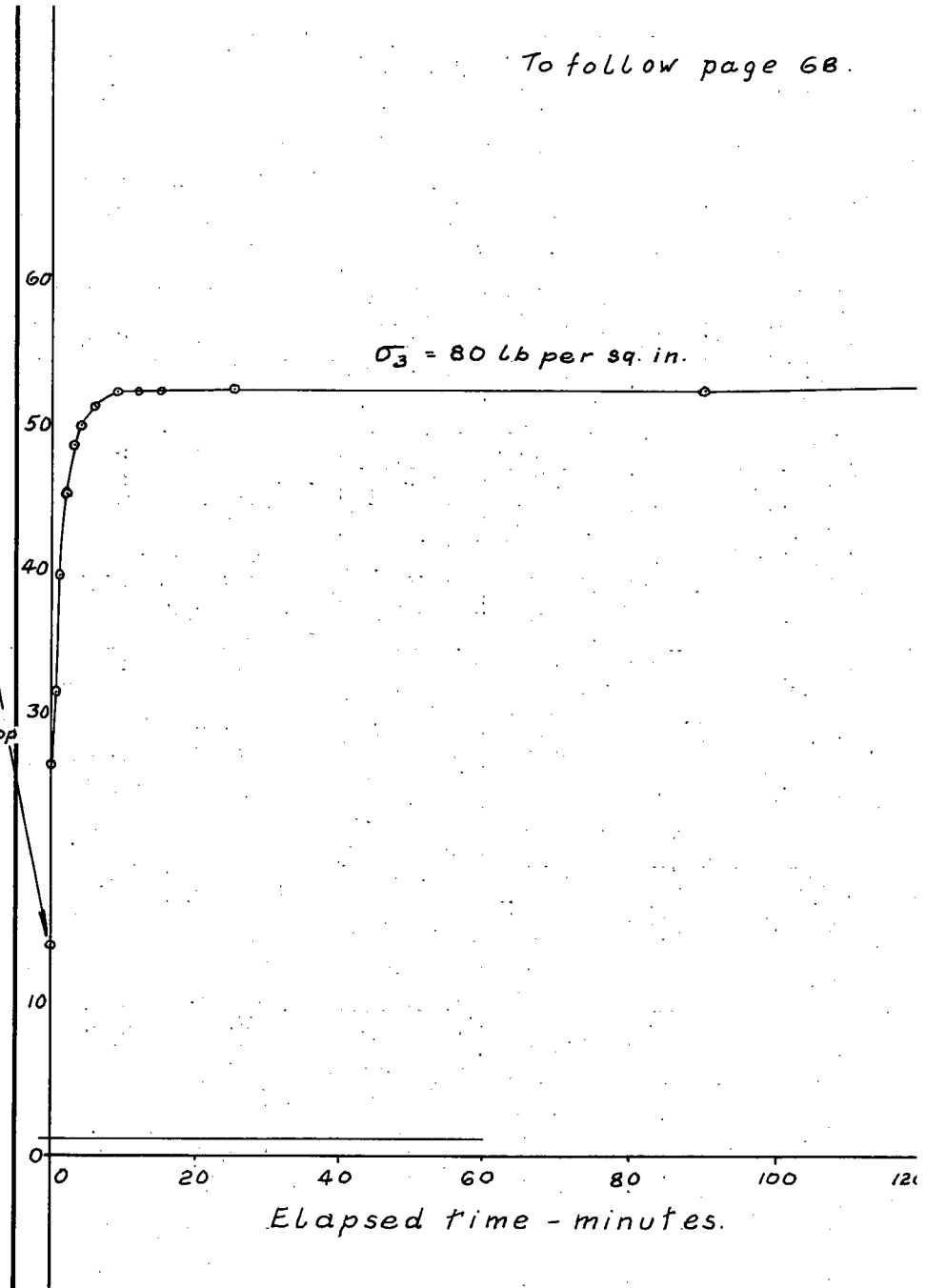

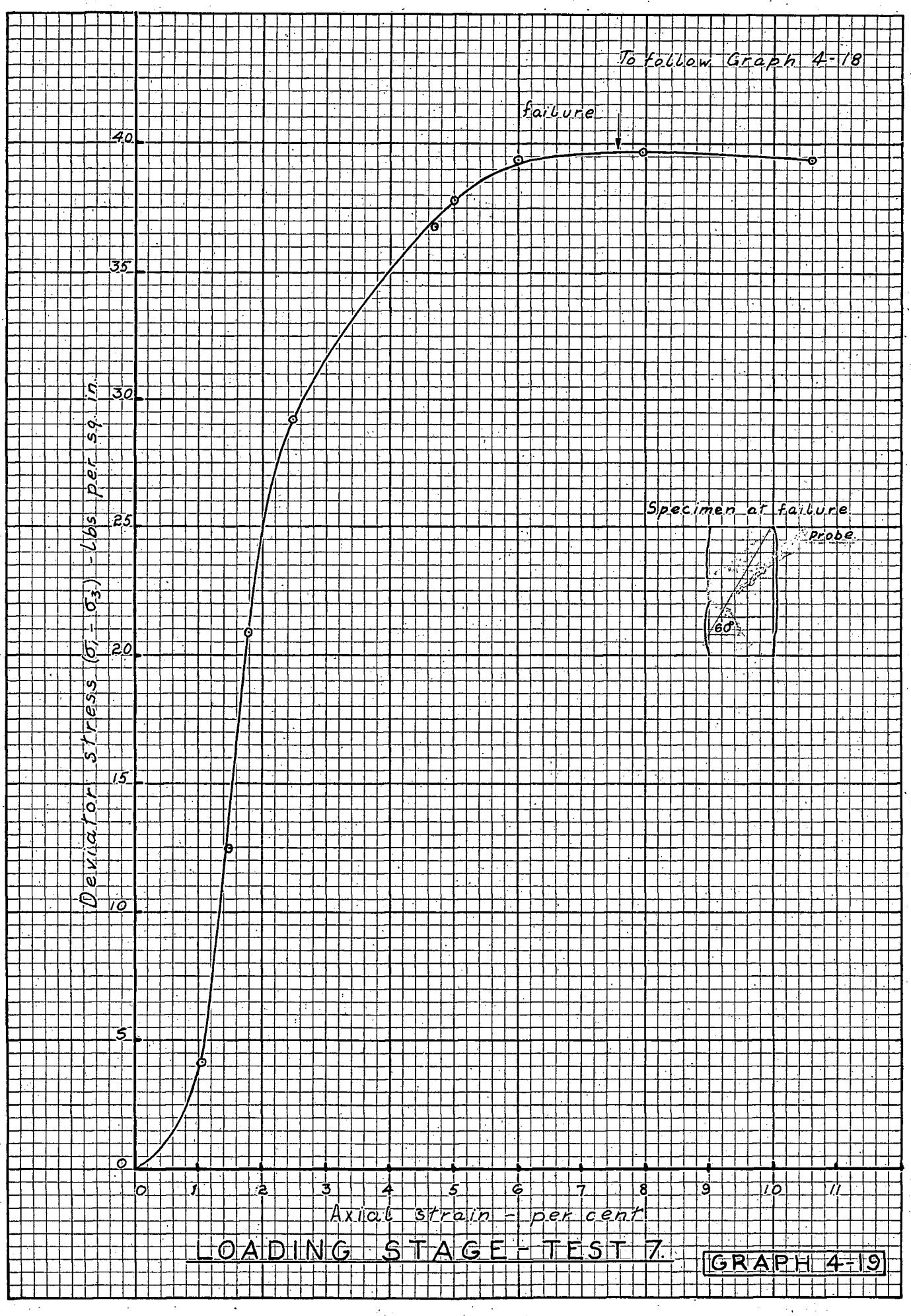

LOADING STAGE - TEST 7.

GRAPH 4-19

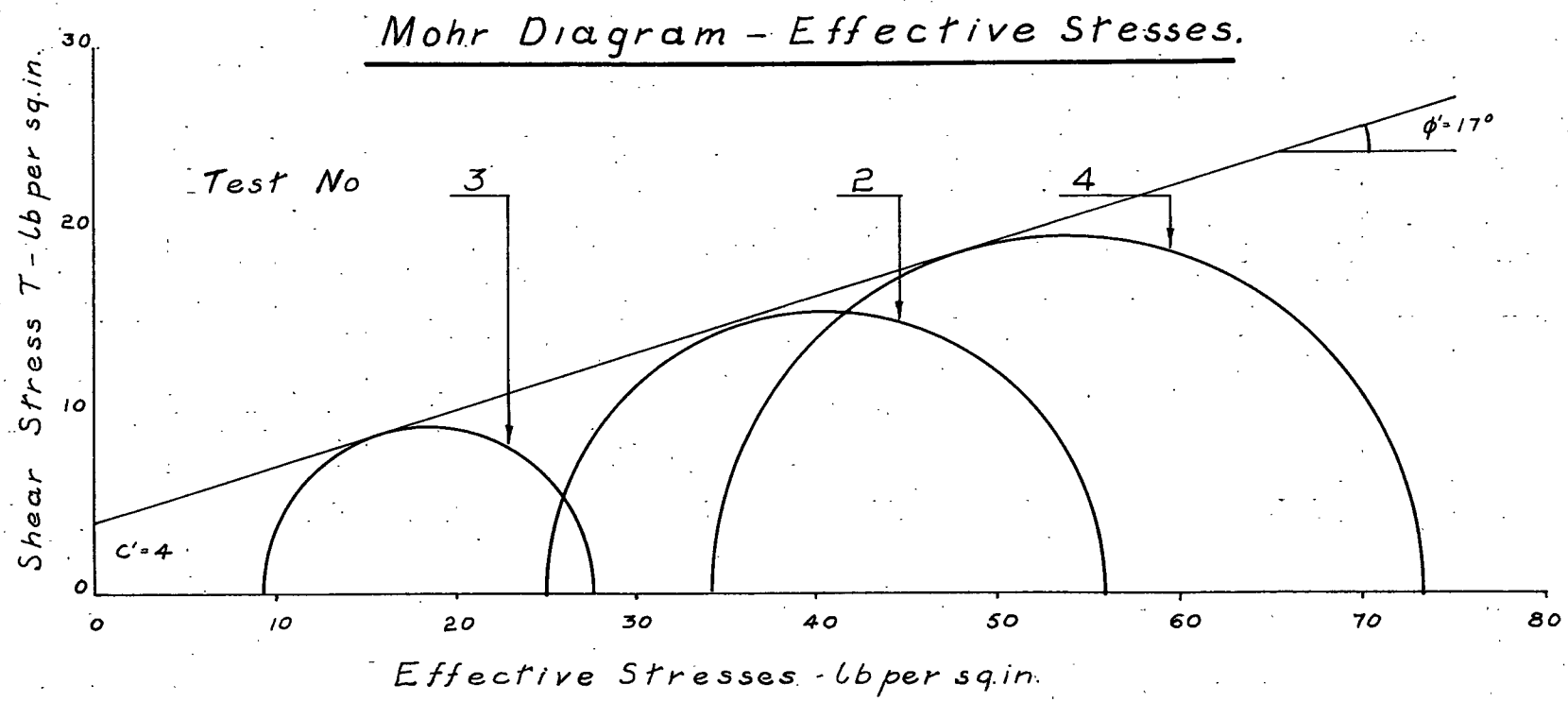

GRAPH 4-21

To follow page 72.

To follow Graph 4-21

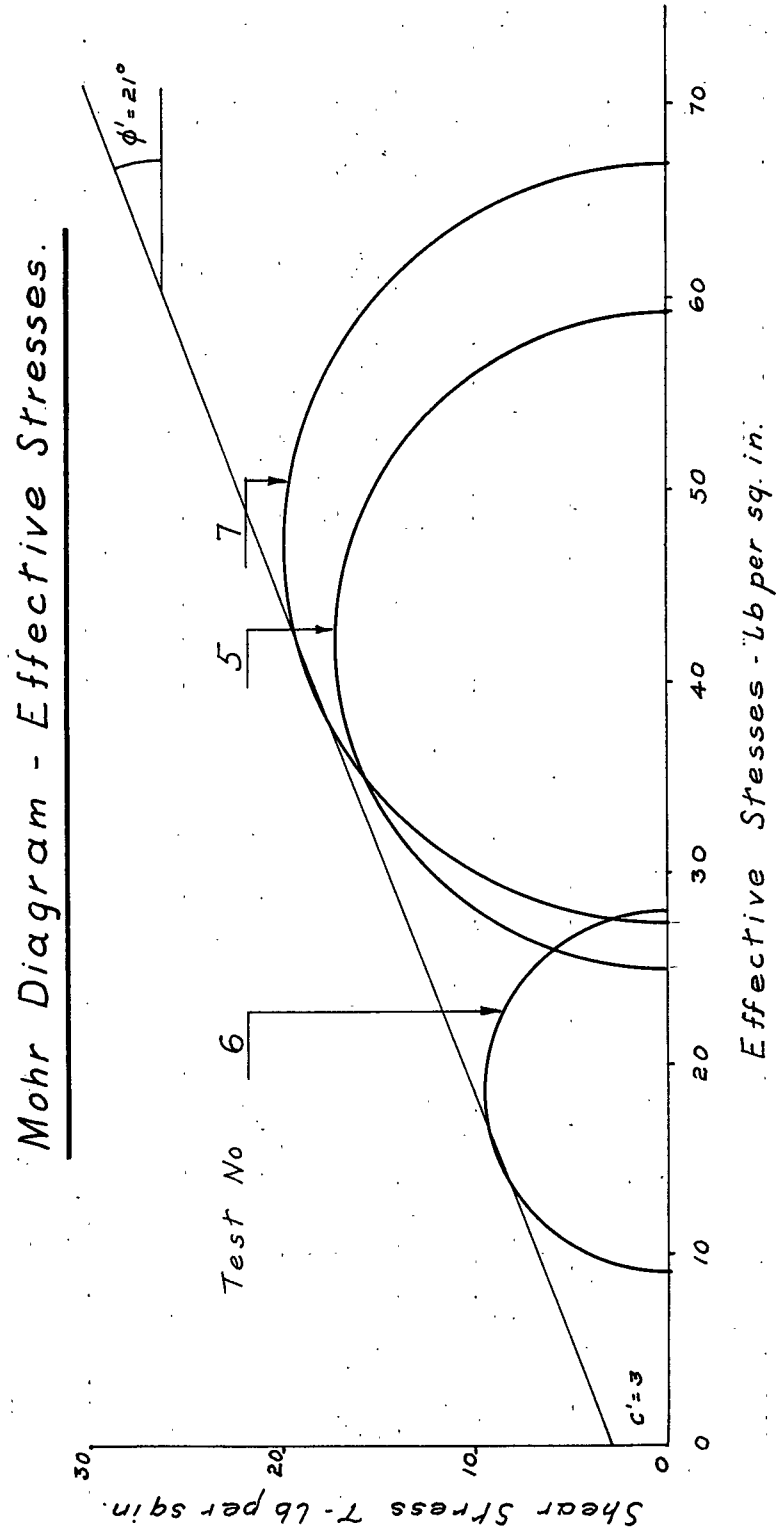

GRAPH 4-22

To follow Graph 4-22.

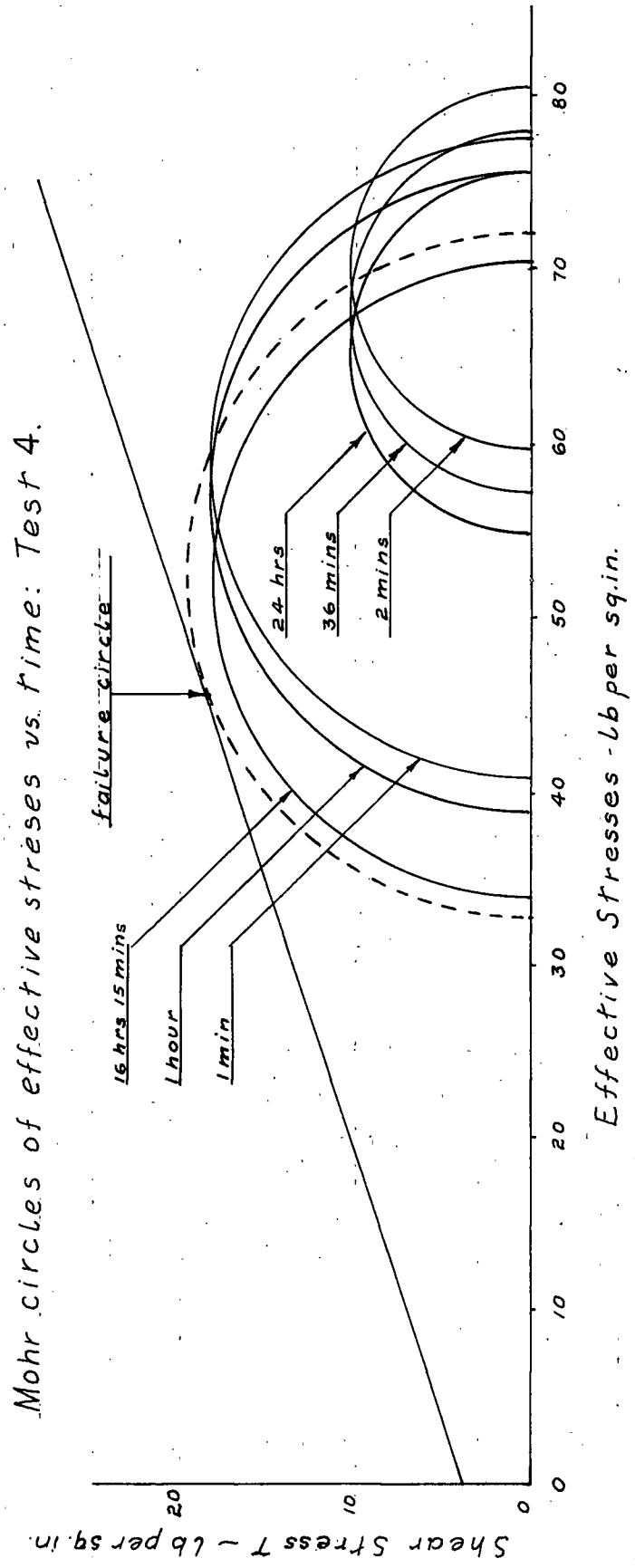

GRAPH 4-23

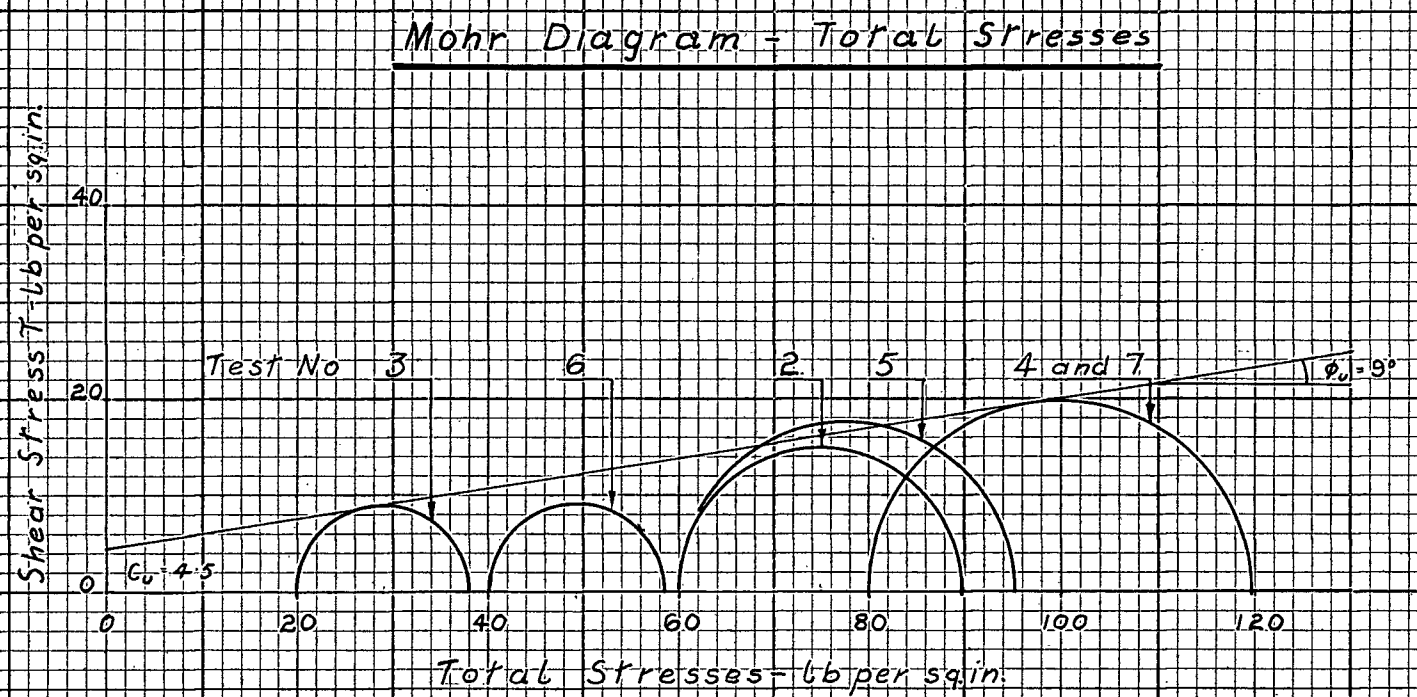

GRAPH 4-24

To follow Graph 4-23

Contains: Figs. 1-18
Graphs 4-9
4-17
4-20
Consol. Test

To follow page 5

Crystalline Components of Clay Minerals.

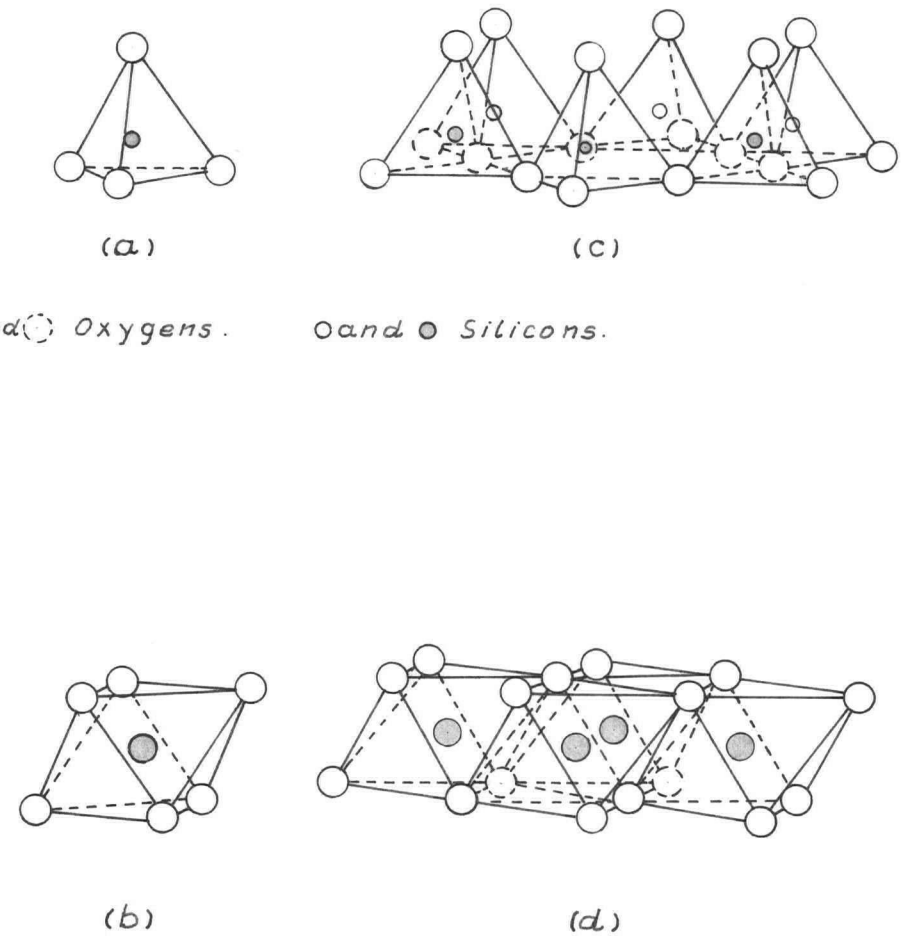

FIG 1. CLAY MINERALS.

(After R.E. Grim. 1959)

To follow page 7.

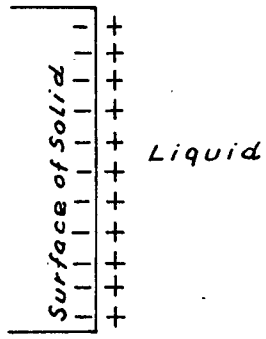

(a) Helmholtz Double Layer

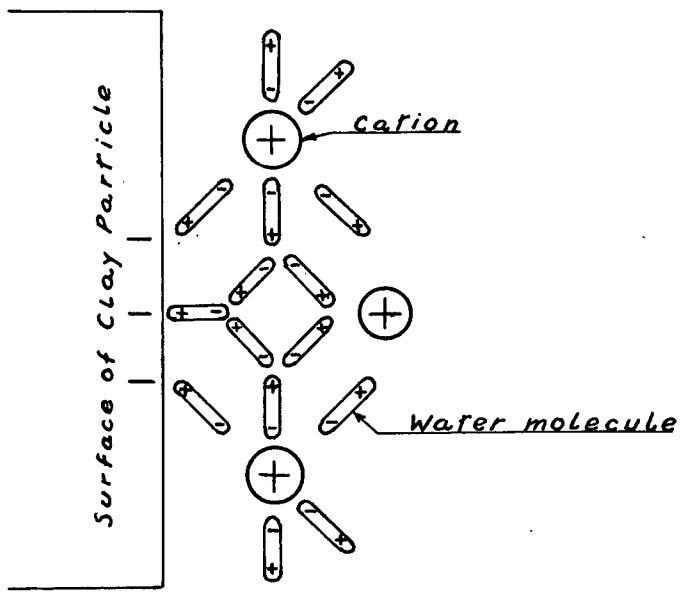

(b) Ion-water complex.

FIG 2. HELMHOLTZ AND DIFFUSE LAYERS

To follow page 7.

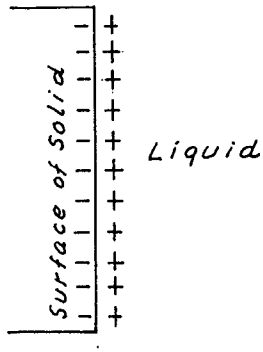

(a) Helmholtz Double Layer.

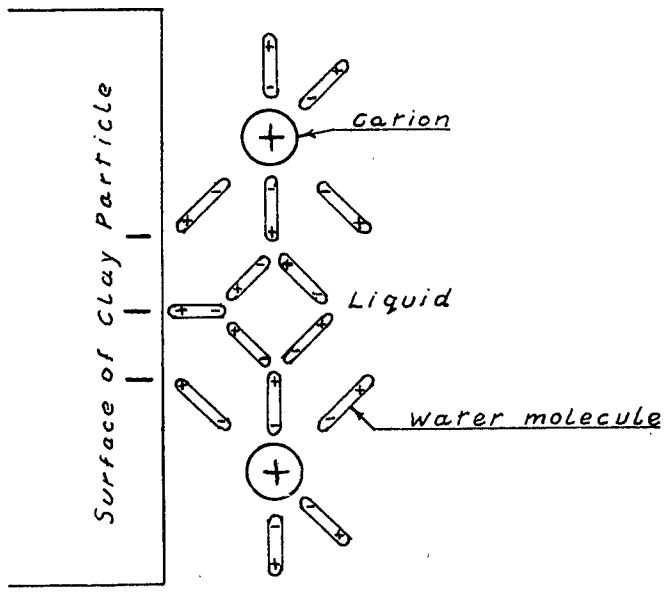

(b) Ion-water complex.

FIG 2. HELMHOLTZ AND DIFFUSE LAYERS.

(Schematic)

To follow page 8

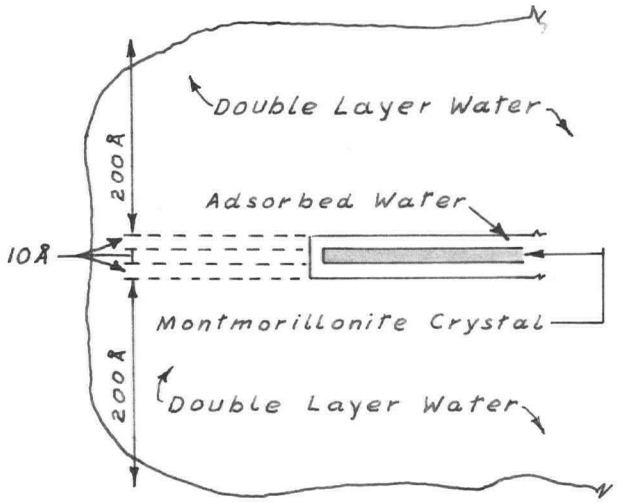

Montmorillonite Sheet

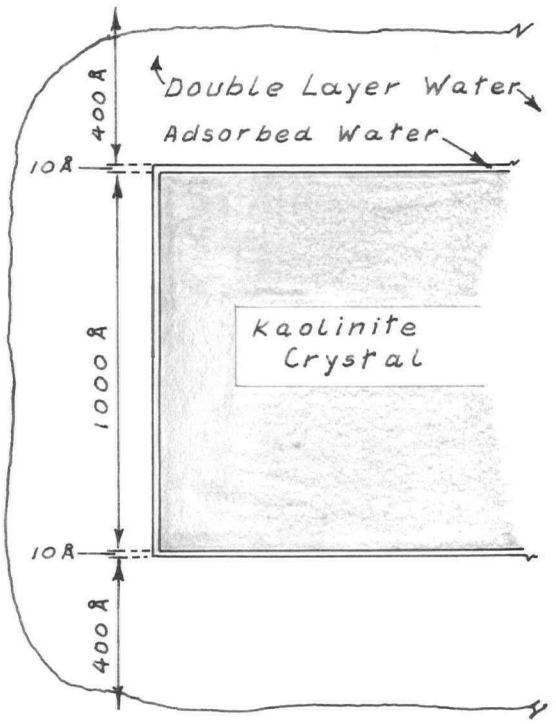

Kaolinite Sheet

FIG 3. CLAY-WATER SYSTEM.

(After T.W. Lambe. 1958)

To follow page 12

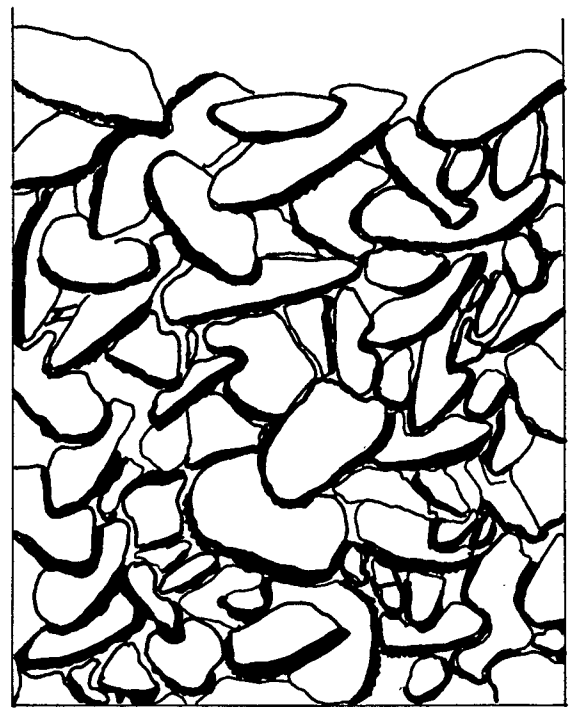

FIG 4. STRUCTURE OF MARINE CLAY.

(After T.K. Tan. 1957.)

To follow page 19

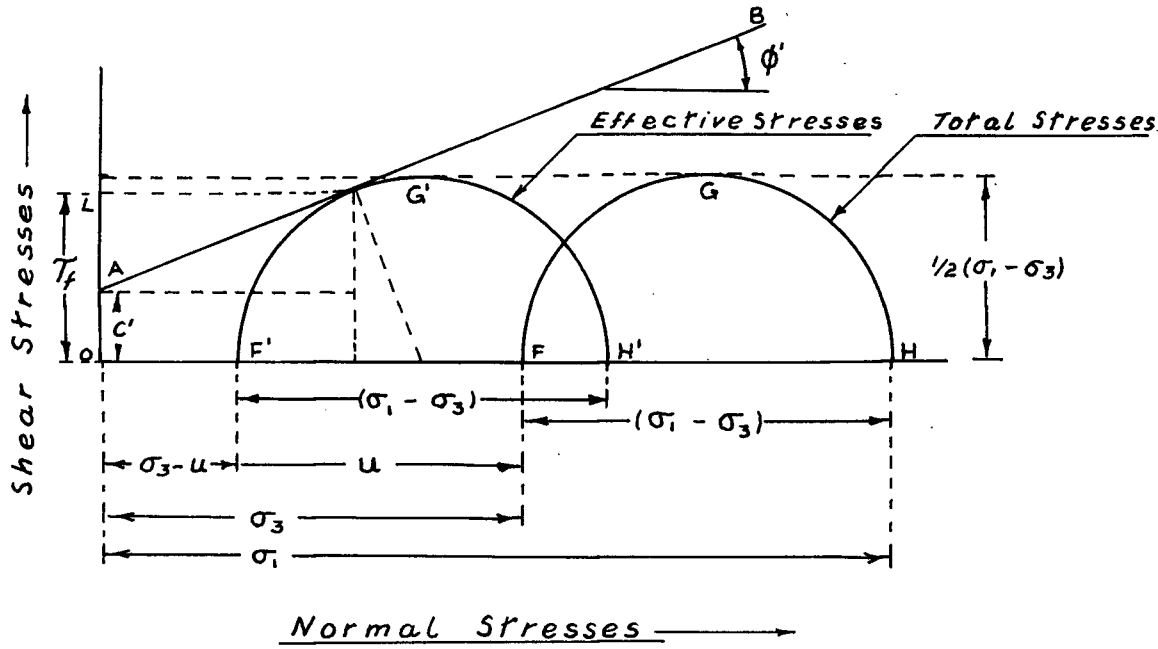

Fig 5. Mohr Diagram : Total and Effective Stresses

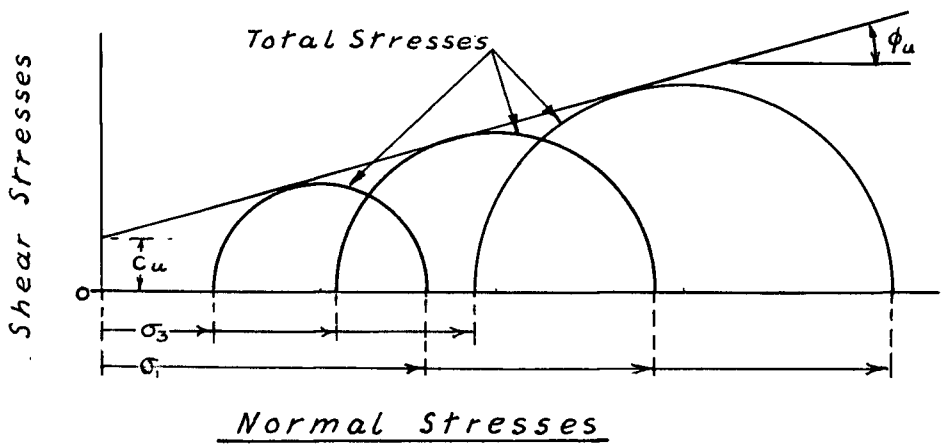

Fig 6. Mohr Diagram : Total Stresses

FIGS. 5 and 6

To follow page 21

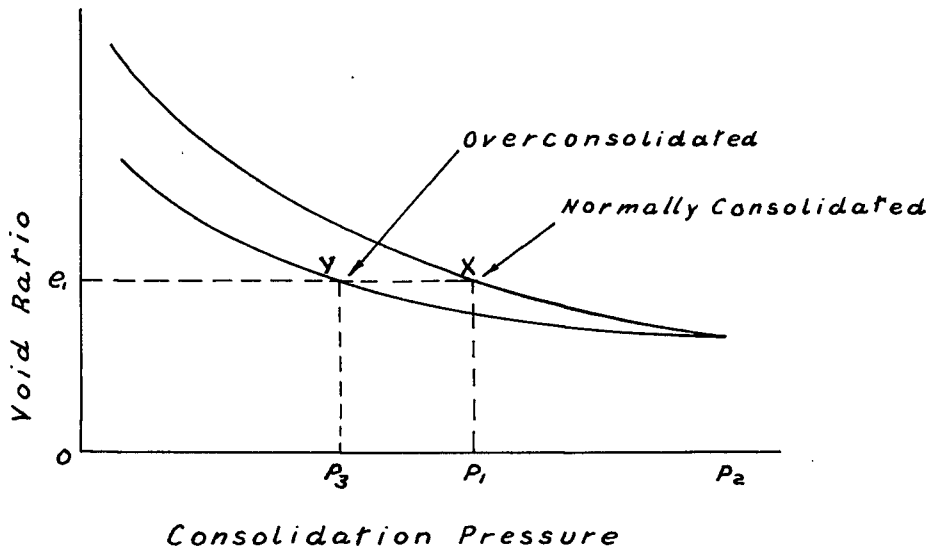

FIG 7. CONSOLIDATION HISTORIES

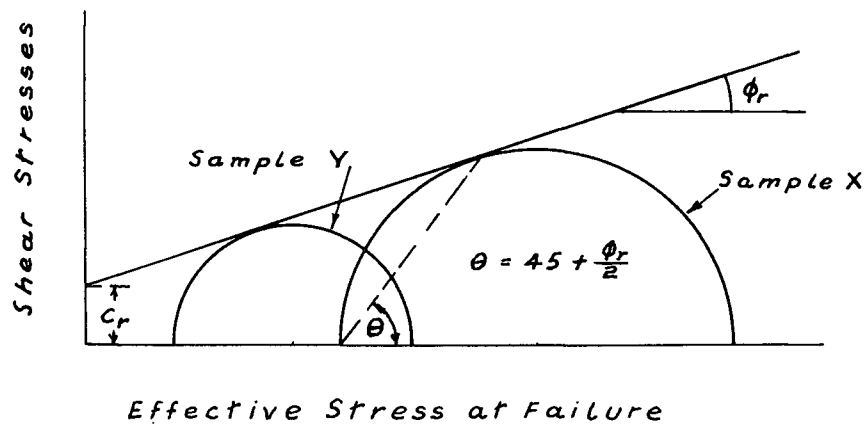

FIG 8. MOHR DIAGRAM : TRUE PARAMETERS

FIGS 7 and 8

To follow page 31

FIG 9. STRESS-CONTROLLED TRIAXIAL MACHINE

FIG 10. TRIAXIAL CELL

To follow page 37.

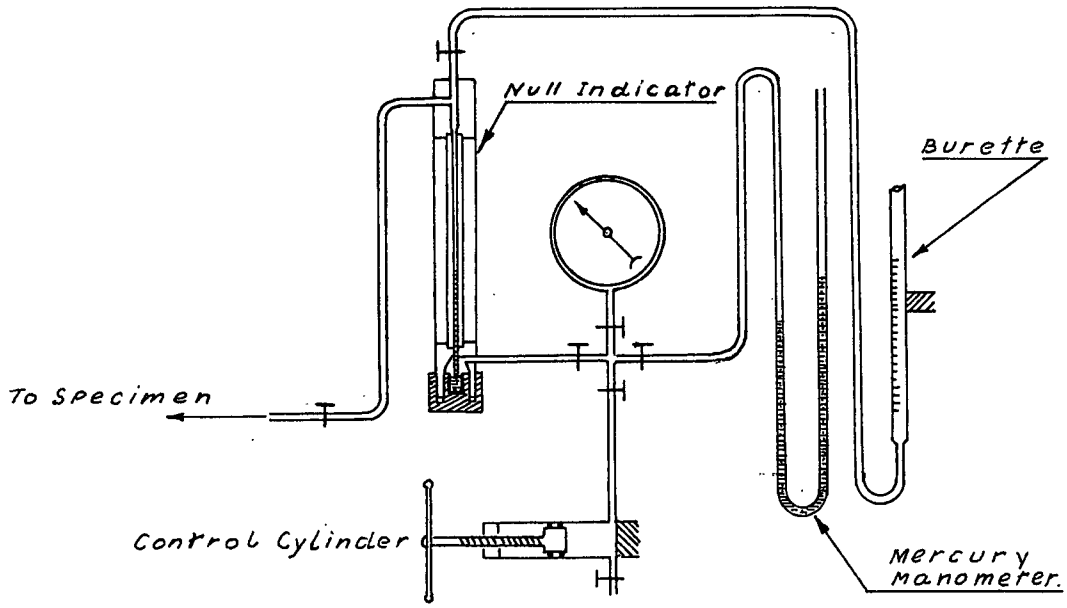

Layout of Apparatus for Measuring Pore Pressure.

FIG 13. PORE-PRESSURE APPARATUS.

To follow page 43

Fig 11. Proving-ring Correction for Cell Pressure

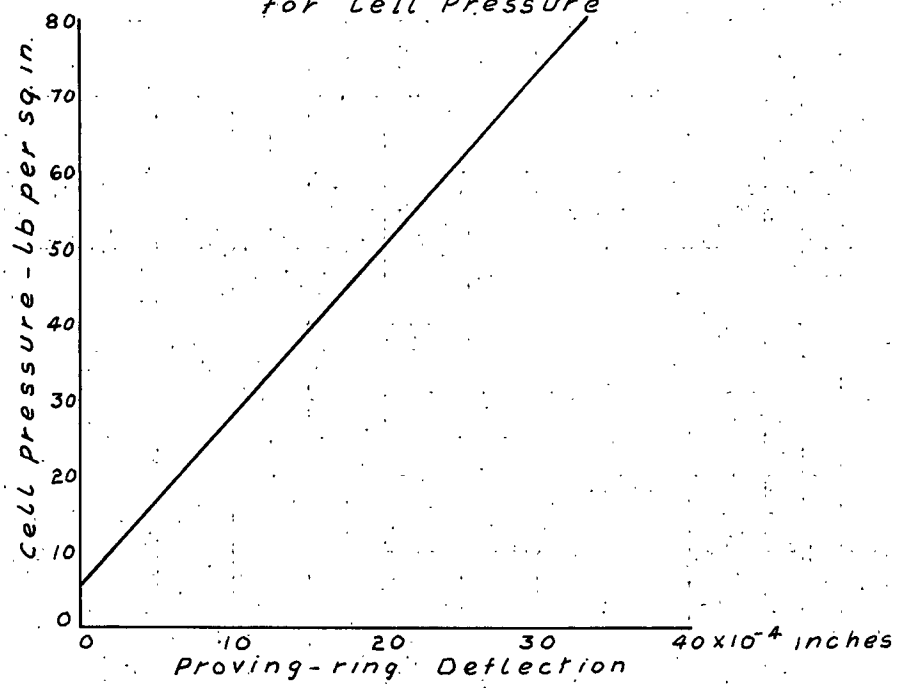

Fig 12. Rubber Membrane Stress vs. Strain Curve.

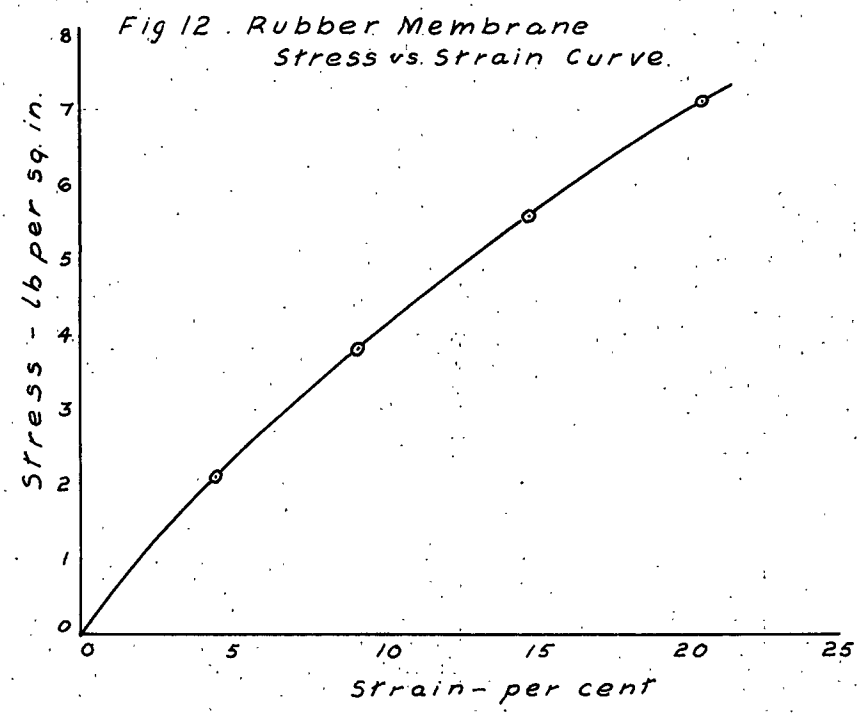

FIGS. 11 and 12.

To follow page 77

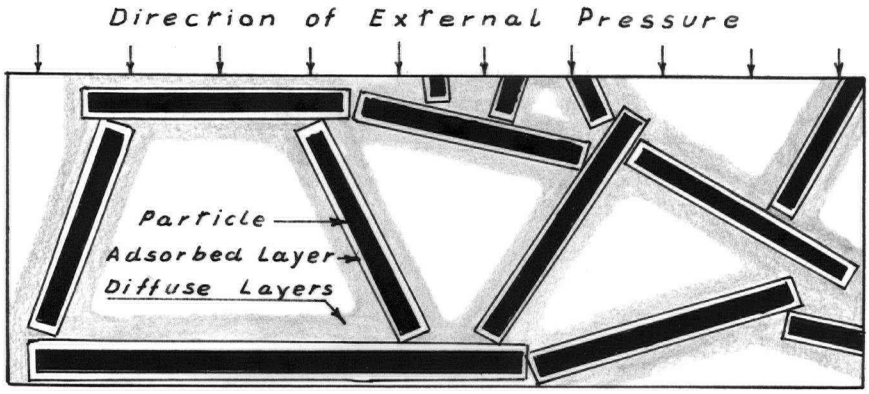

Time t_0 : External Pressure taken partly by Intergranular Stresses.

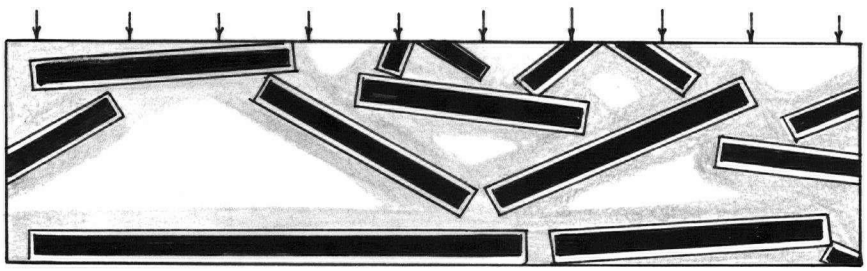

Time t_1 : External Pressure taken entirely by Pore Water.

FIG 14. CLAY- WATER SYSTEM: EFFECTS OF PLASTIC DEFORMATION OF THE ADSORBED LAYERS.

To follow page 86

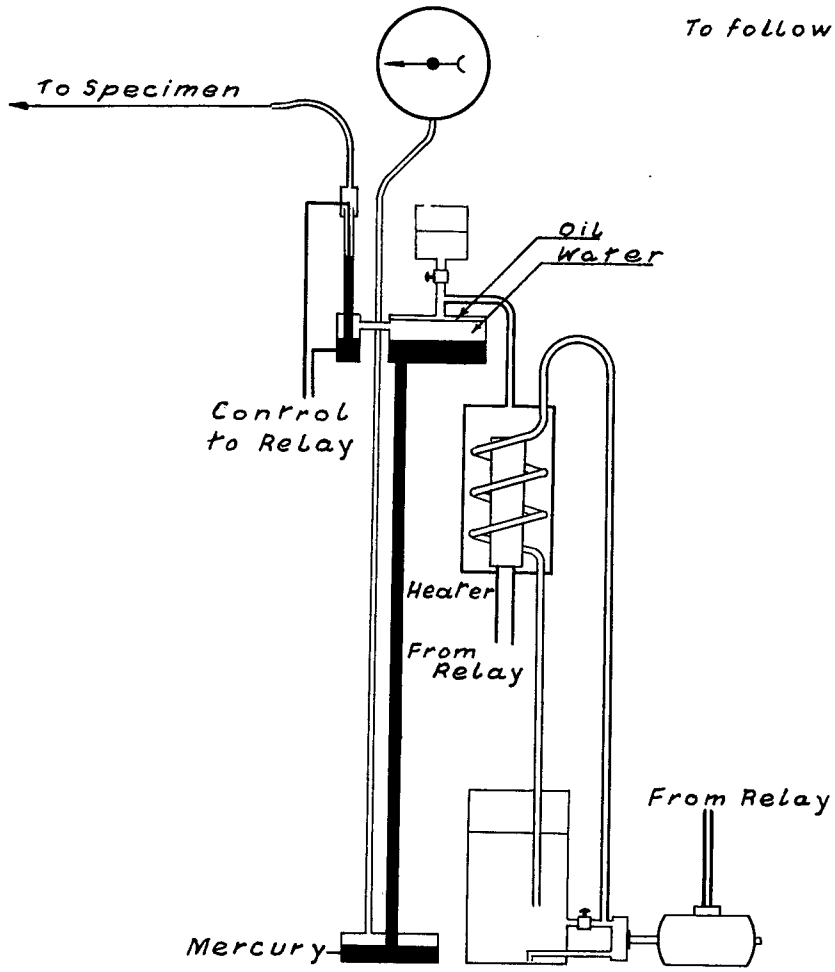

FIG 15. PORE-PRESSURE DEVICE

(After A.D. Penman 1953)

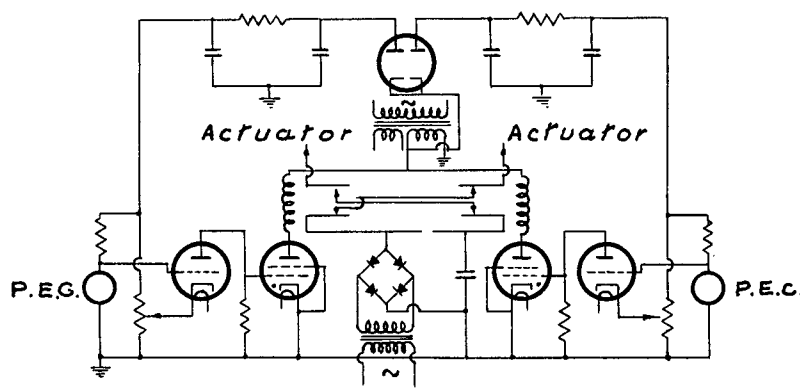

FIG 16. CIRCUIT OF AUTOMATIC CONTROL

(After L.J. Burton 1956)

FIGS 15 and 16.

To follow page 89.

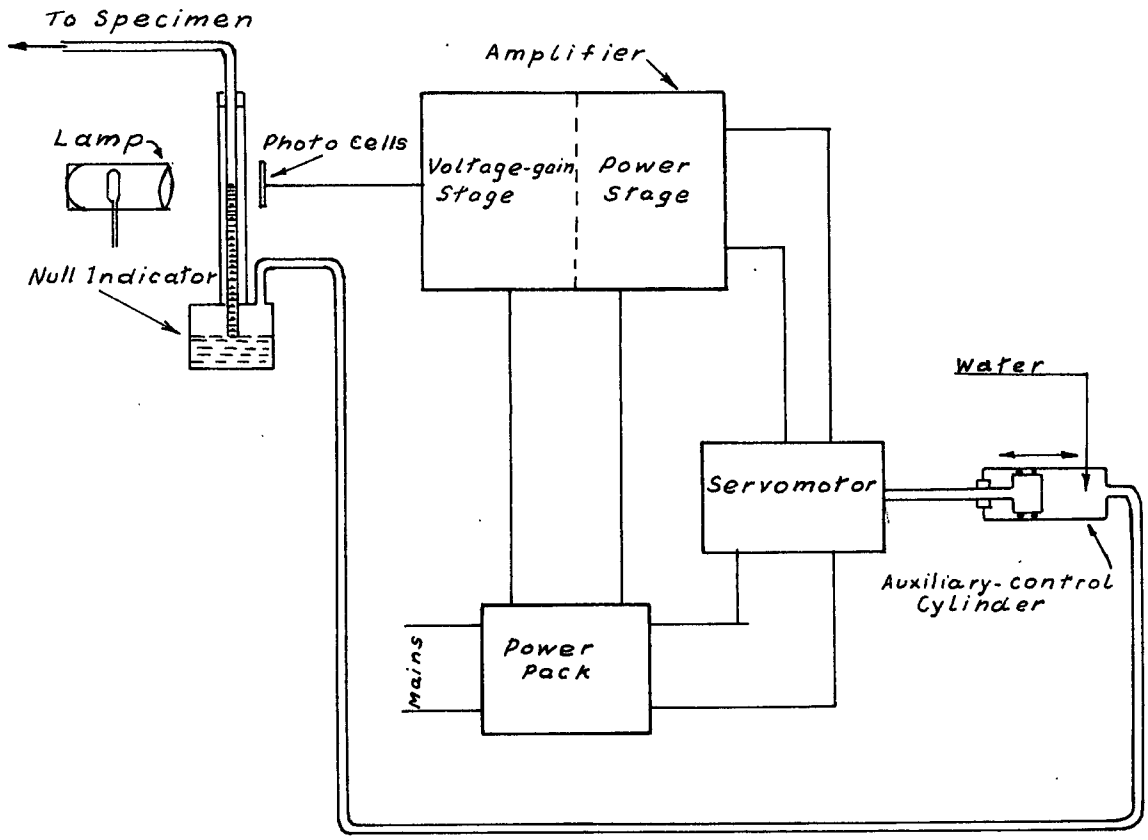

FIG 17. LAYOUT OF AUTOMATIC CONTROL

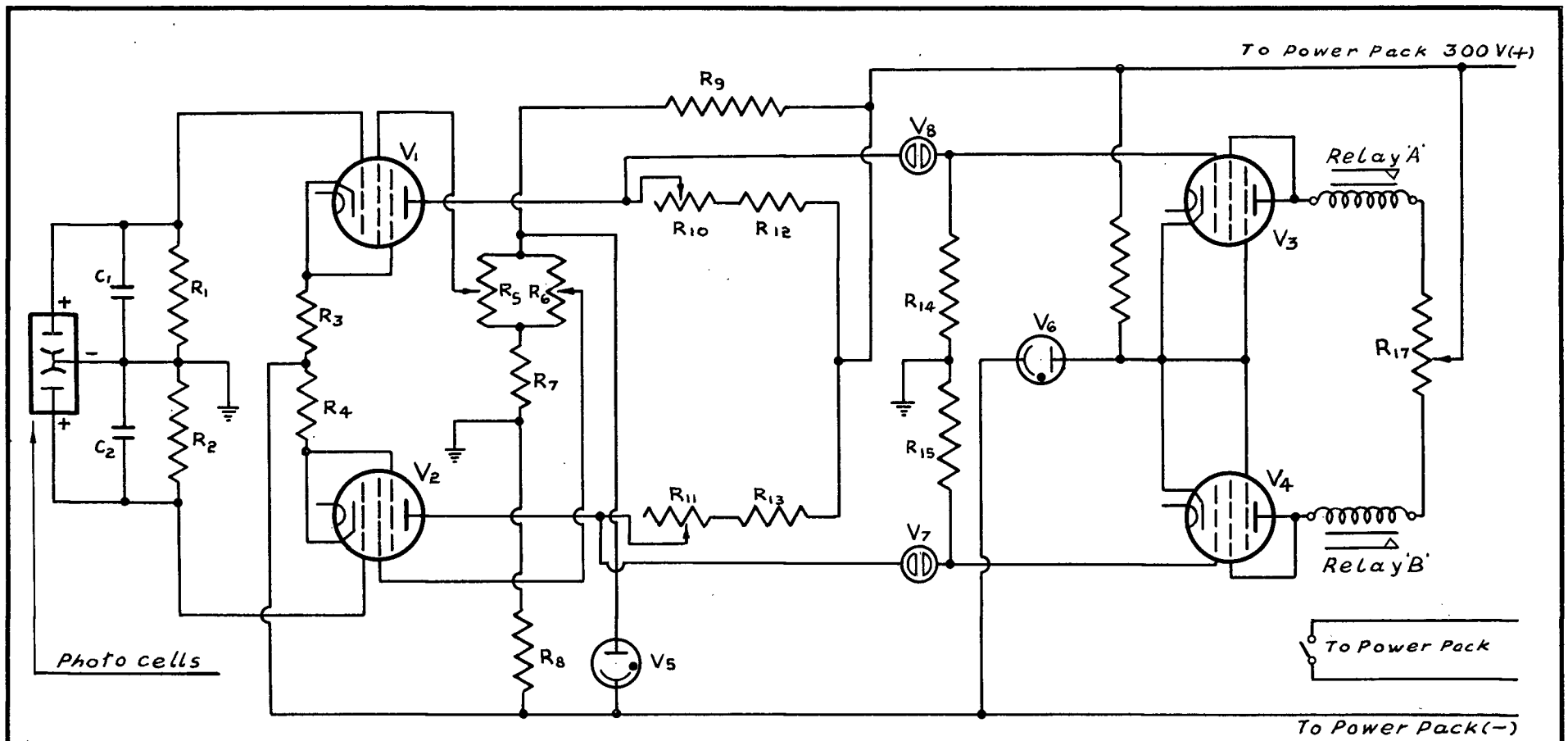

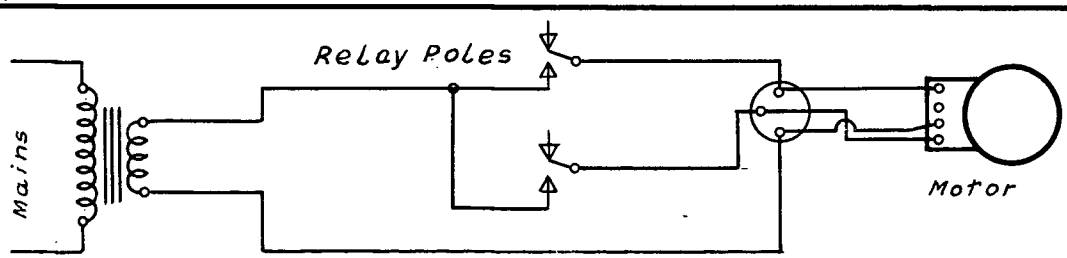

(b) CIRCUIT OF SERVOMOTOR

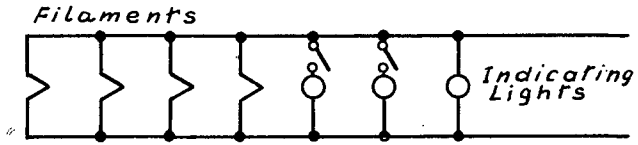

(a) CIRCUIT OF AMPLIFIER

FIG 18. AUTOMATIC CONTROL

To follow page 91.

To follow Graph 4-8

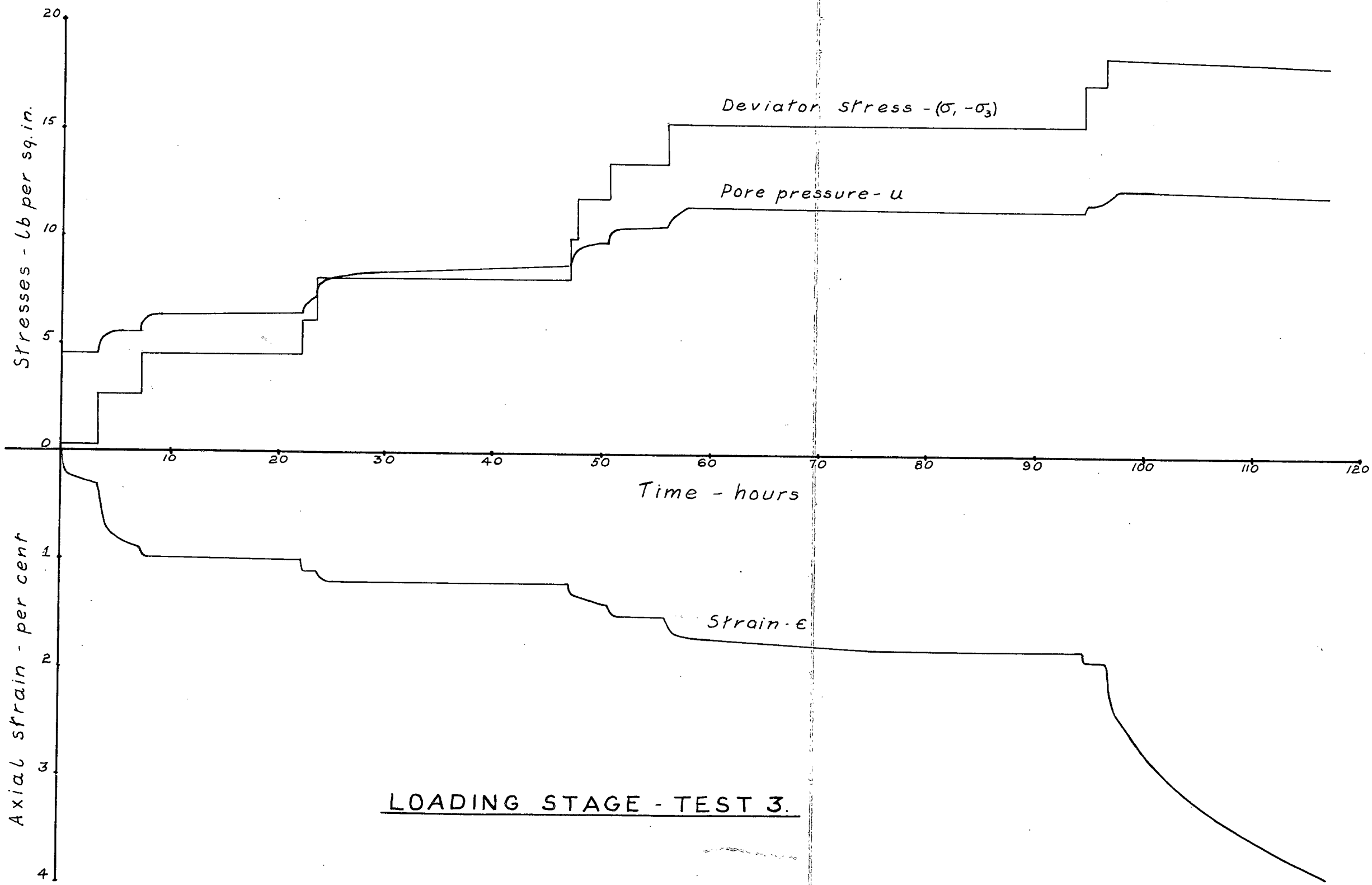

LOADING STAGE - TEST 3.

GRAPH 4-9

To follow Graph 4-16

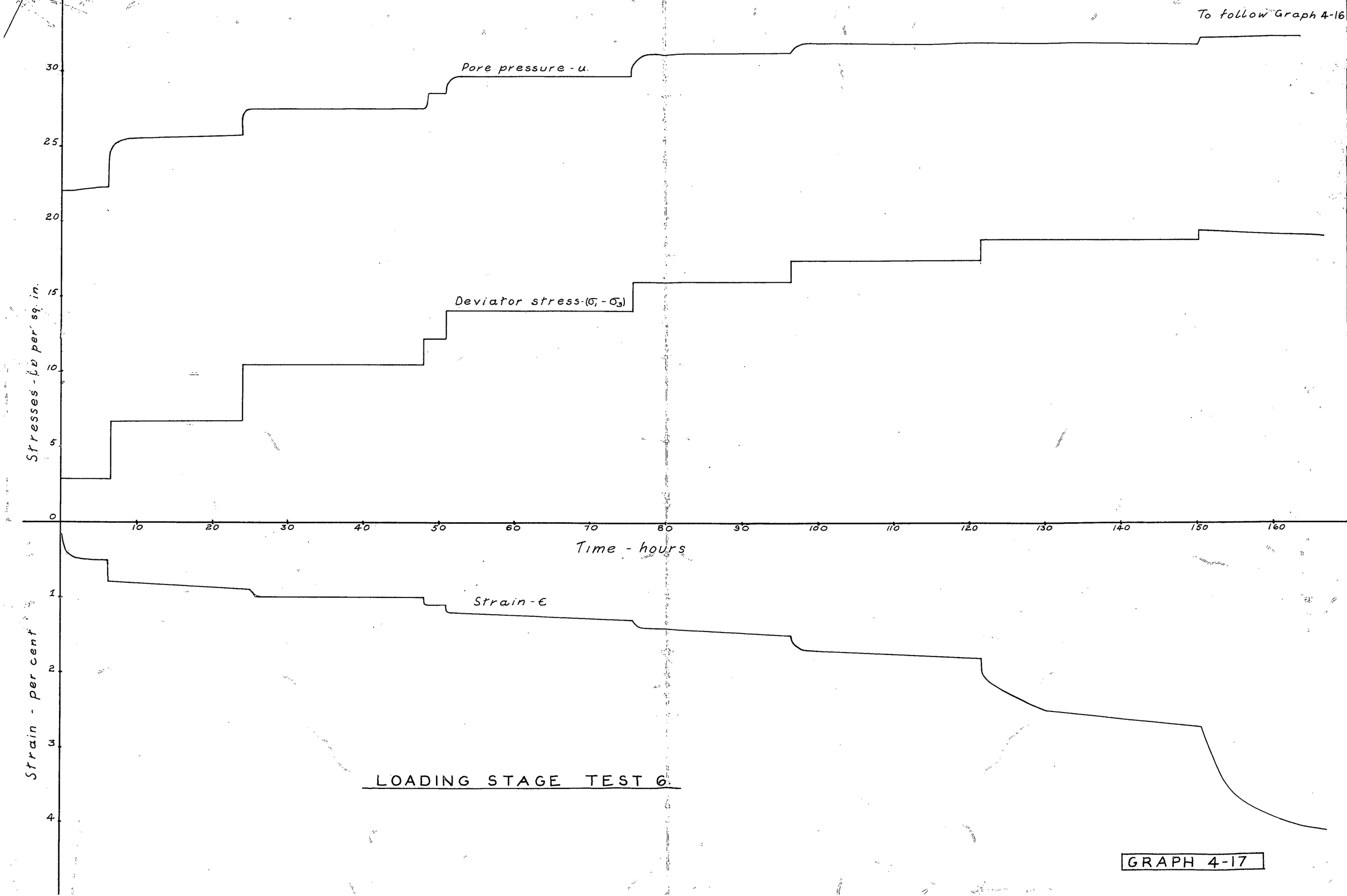

GRAPH 4-17

To follow Graph 4-19

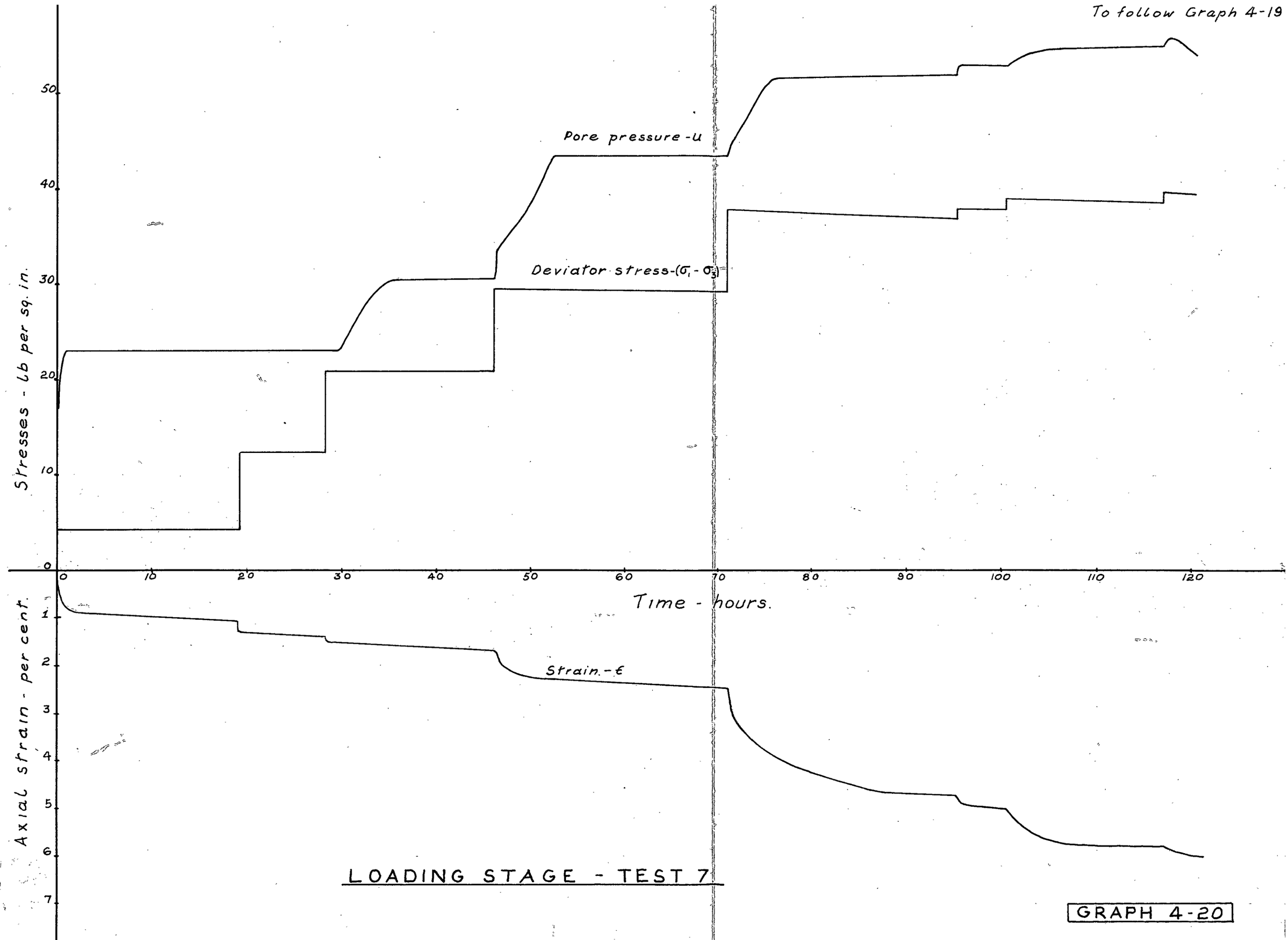

LOADING STAGE - TEST 7

GRAPH 4-20

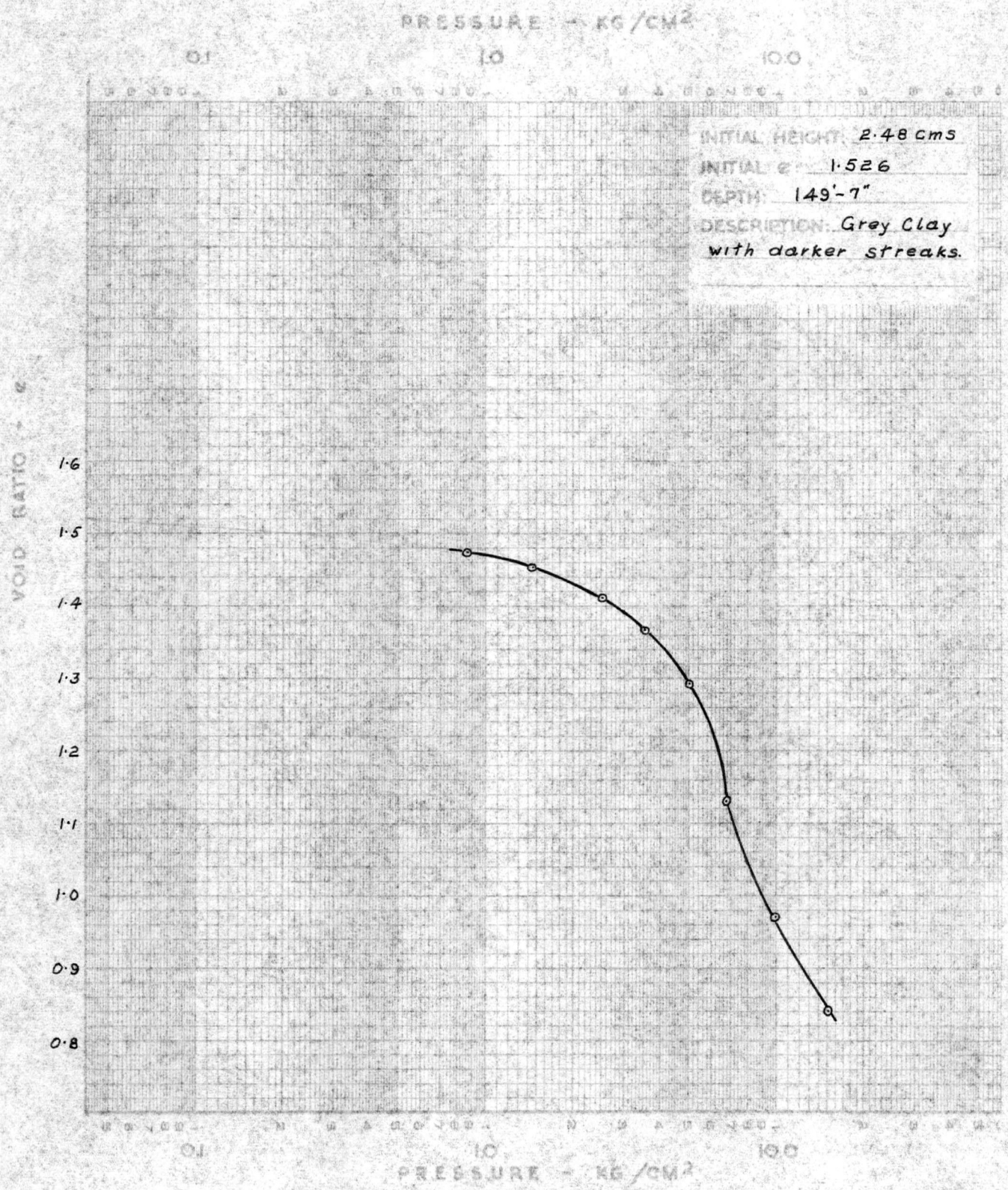

PORT MANN.	CONSOLIDATION TEST	JOB NO. KE3 B7
R.A. SPENCE, P.ENG.	HOLE BS 2F. SAMPLE 43	DATE: 1960 A7 94 P6

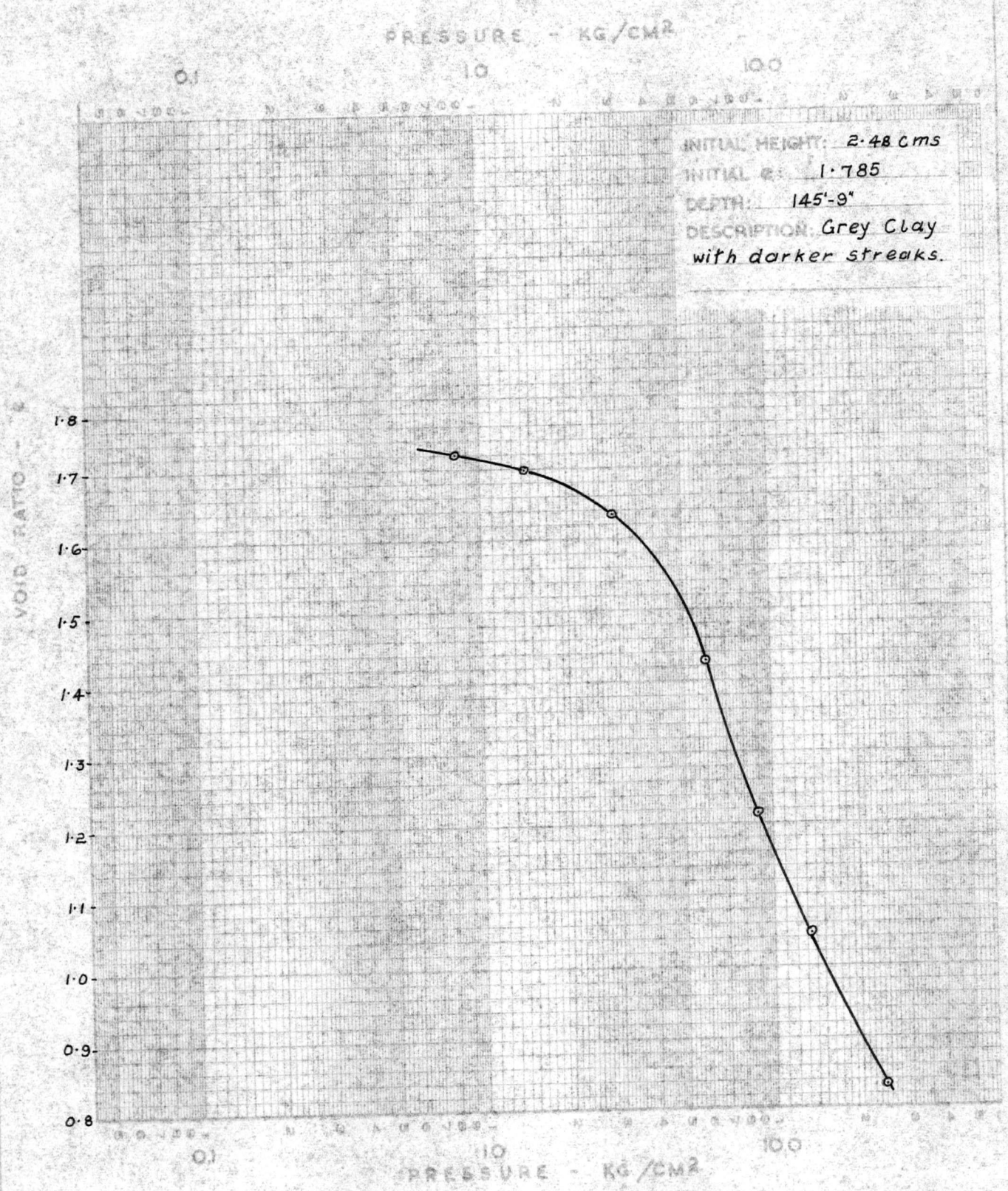

PORT MANN.	CONSOLIDATION TEST	JOB NO.
R.A. SPENCE, P.ENG.	HOLE BN 23F. SAMPLE 37	DATE:

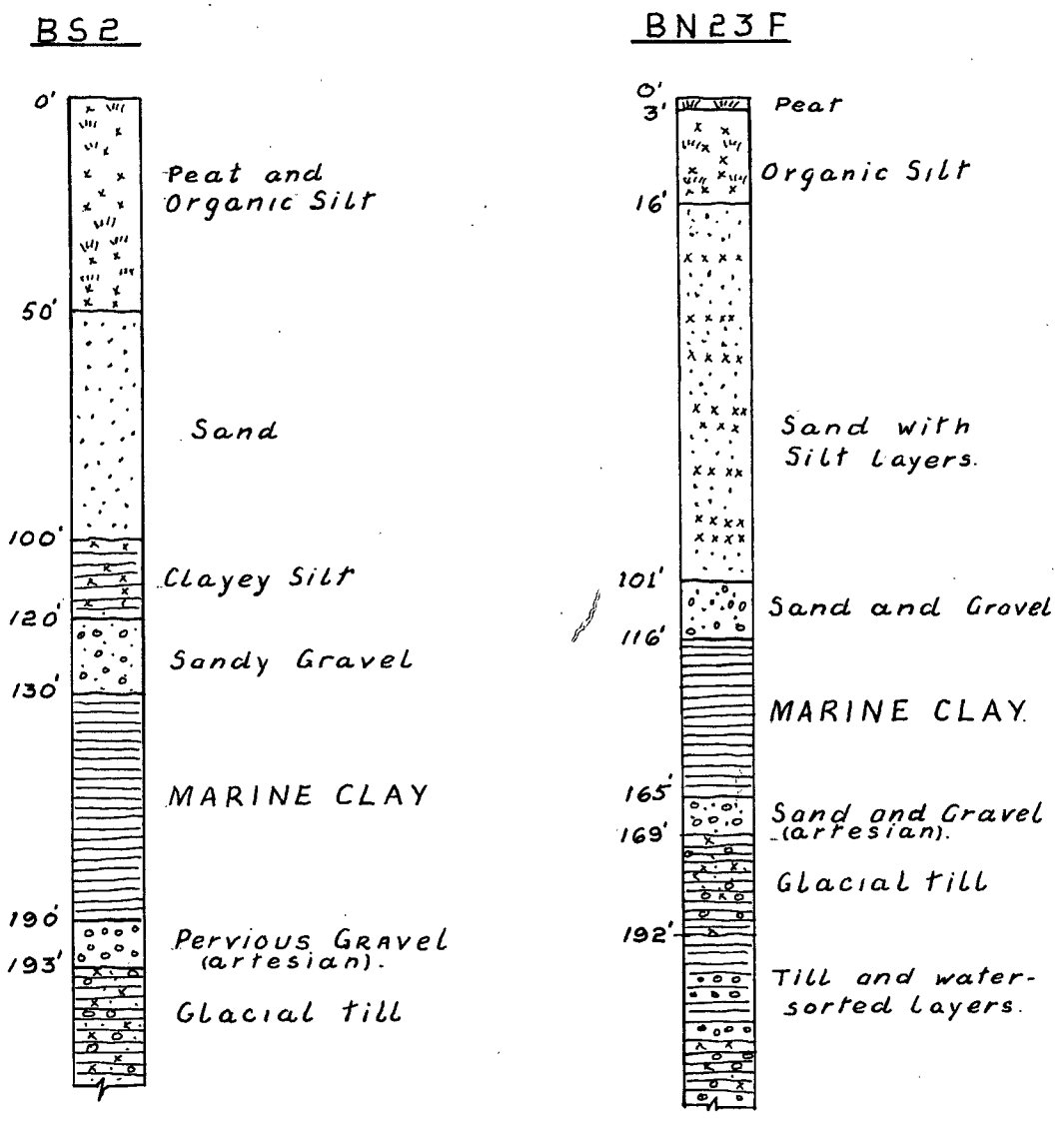

Borehole Logs (idealized).